

Impact of Pedestrian Volumes on the Operational Performance of Modern Roundabouts

by

Alaa Sindi

A thesis
presented to the University of Waterloo
in fulfillment of the
thesis requirement for the degree of
Master of Applied Science
in
Civil Engineering

Waterloo, Ontario, Canada, 2011

©Alaa Sindi 2011

AUTHOR'S DECLARATION

I hereby declare that I am the sole author of this thesis. This is a true copy of the thesis, including any required final revisions, as accepted by my examiners.

I understand that my thesis may be made electronically available to the public.

Abstract

Modern roundabouts are increasingly being considered as a preferred intersection design within urban street networks in North America due, in large part, to the increased safety provided by roundabout. In the last decade, much research has been conducted in North America to quantify the performance of roundabouts in terms of vehicle delay as a function of vehicle traffic volume and roundabout geometry. In most jurisdictions, vehicles entering and existing the roundabout are required by law to yield right-of-way to pedestrians crossing the roundabout approach, and consequently, the presence of substantial pedestrian volumes are expected to degrade operational performance of the roundabout for vehicles. However, very little research has been conducted to estimate the impact that pedestrian volumes have on average vehicle delay. The aim of this research is to study the effects of pedestrian volume, entry traffic volume, and conflicting or circulating volume, on the delays that vehicles experience when traversing the roundabout.

An analytical model is proposed to estimate vehicle delays on the basis of traffic flow and queuing theory. The model is applicable to single lane roundabouts. The model was calibrated and validated using vehicle delays obtained from the micro-simulation software, VISSIM (version 5.2) for a range of different conditions.

The research described in this thesis demonstrates that pedestrian flows cause delays to vehicles traversing the roundabout in four distinct ways. Existing analytical techniques included within most design manuals consider only one of these sources of delays and consequently, conventional models typically under-estimate the impact that pedestrian flows have in terms of increasing delays to vehicles traversing the roundabout.

Acknowledgements

Many thanks go out to Professor Bruce Hellinga, from the University of Waterloo, Department of Civil and Environmental Engineering, for his supervision, advice and guidance throughout, which helped me to conduct and complete this research. Special thanks go out to all professors in The Department of Civil and Environmental Engineering at University of Waterloo and professors in The Civil Engineering Department at King Abdulaziz University for their guidance. I learned from all of my professors a lot. They were generous in giving the knowledge and excellent teachers.

I wish to thank King Abdulaziz University and Saudi Cultural Bureau for their unlimited financial support to complete this research.

A thank goes to all my colleagues, friends, proofreaders, Instructional Technologies and Multimedia Services (ITMS) staff at University of Waterloo and ptv America technical support staff for their support.

This thesis would not have been possible to be completed without my wife Noorah, my daughter Janna, my father, my mother and my family motivations. It is a pleasure to thank them. They make the thesis possible to be completed.

Table of Contents

List of Figures	vii
List of Tables	xi
Chapter 1 : Introduction	1
1.1 Background	1
1.2 Problem definition	7
1.3 Thesis Structure.....	7
Chapter 2 Literature Review.....	8
2.1 Introduction.....	8
2.2 Theoretical (Gap acceptance) models for estimating capacity	8
2.2.1 HCM 2000 model (HCM, 2000)	8
2.2.2 Australian model.....	12
2.2.3 German model	16
2.3 Empirical models for estimating capacity.....	17
2.3.1 Kimber method (Kimber, 1980)	18
2.3.2 German model (Brilon, Wu and Bondzio)	21
2.3.3 FHWA (Robinson et al., 2000).....	22
2.3.4 Swiss model.....	24
2.3.5 French model.....	26
2.4 Comparison of theoretical (gap acceptance) and empirical models	29
2.5 International pedestrian reduction factor models	29
2.5.1 English method (Marlow and Maycock, 1982)	30
2.5.2 French method (Loua, 1992)	33
2.5.3 German method (Brilon et al., 1993)	34
2.6 Simulation models	35
2.7 Other relevant research	37
2.7.1 Analytical Analysis of Pedestrian Effects on Roundabout Exit Capacity (Rodegerdts and Blackwelder, 2005).....	38
2.7.2 Simulation of Pedestrians Crossing a Street (Boenisch and Kretz, 2010).....	39
2.7.3 Effects of pedestrian crossing on roundabout capacity (Duran, 2010)	40
Chapter 3 Methodology.....	41
3.1 Introduction.....	41

3.2 Coding VISSIM.....	42
3.3 Definition of roundabout geometry	43
3.4 VISSIM modelling coding and assumptions	44
3.4.1 Model inputs.....	44
3.4.2 Model output is recorded.....	45
3.5 Experimental Design	46
3.6 Proposed model:.....	46
3.6.1 Source 1: Delay at entry leg	49
3.6.2 Source 2: Delay at exit lane.....	50
3.6.3 Source 3: Delay within circulating roadway due to queue spillback	51
3.6.4 Source 4: Delay due to queue spill back into circulating roadway	52
3.6.5 Proposed Analytical experimental design	53
Chapter 4 : Results and Data Analysis	56
4.1 VISSIM validation.....	56
4.1.1 Vehicle trajectory in VISSIM.....	57
4.1.2 Vehicle delay from field data, VISSIM and HCM	58
4.1.3 Entry capacity from VISSIM, Field data and HCM 2000 model	62
4.2 Calibration of the proposed analytical model.....	66
4.3 Validation of proposed analytical model	68
Chapter 5 : Conclusions and Recommendations.....	76
References	78
Appendix A : Roundabout features, diminutions, and key words	82
Appendix B : Entry capacity and capacity reduction factor from existed analytical models	89
Appendix C : Coding the roundabout in VISSIM 5.2.....	102
Appendix D : Field data collection methodology and coding VISSIM for validation	118

List of Figures

Figure 1: Characteristics of traffic Circle (L'Arc De Triomphe, 2002).....	2
Figure 2: Characteristics of modern roundabout (Three-leg Multi-Lane Roundabout in East Lansing, Michigan, 2011).....	3
Figure 3: Roundabout dimensions (Robinson et al., 2000)	4
Figure 4: Urban double lane roundabout layout (Robinson et al., 2000)	6
Figure 5: Exponential distribution of time headways $P[T \geq t] = e - t\lambda$	9
Figure 6: Entry capacity of roundabout approach using HCM 2000 (Equation 3, and 4).....	11
Figure 7: Vehicle delay based on different entry volumes and capacities for a single lane roundabout (computed using Equations 3 and 5).....	12
Figure 8: Entry capacity using Troutbeck model (Equation 8).....	14
Figure 9: Domain and sub-domain streams	15
Figure 10: Entry capacity calculated values using Brilon and Wu model (Equation 13).....	17
Figure 11: Kimber method geometric parameters (Kimber, 1980).....	19
Figure 12: Kimber method geometric parameters (Kimber, 1980).....	20
Figure 13: Entry capacity calculated values using Kimber model (Equation 15).....	20
Figure 14: Entry capacity using German empirical model (Equation 23).....	22
Figure 15: The entry capacity using FHWA model (Robinson et al., 2000)	23
Figure 16: Entry capacity using Swiss model (Equation 24).....	24
Figure 17: Vehicle volumes and the length ℓ	25
Figure 18: The relation between distance ℓ and parameter α (Mauro, 2010)	26
Figure 19: French model traffic volume and geometric parameters (Mauro, 2010)	28
Figure 20: Entry capacity using French model (Equation 26)	29
Figure 21: The impact of pedestrians on entry capacity for different pedestrian volume	32
Figure 22: The impact of pedestrians on entry capacity for different entry capacity models.....	32
Figure 23: Comparing the capacity reduction factor for different methods	34
Figure 24: The RMSE values for different models based on observed and estimated entry leg delay based on the data collected by Nikolic and Pringle (2010)	36
Figure 25: Deflection point in the circulatory road way as shown in VISSIM micro-simulation	37
Figure 26: Sources of delay caused by conflicts with pedestrian streams.....	42

Figure 27: Roundabout configuration used for model	47
Figure 28: Definition of parameters used in proposed model.....	48
Figure 29: Treating the circulating roadway as a shared lane.....	51
Figure 30: Queue spill back impacting entry capacity of next upstream leg	52
Figure 31: Vehicle trajectory for left movement.....	58
Figure 32: Average vehicle delay from different sites	62
Figure 33: Average vehicle delay over the maximum queue length ratio	62
Figure 34: VISSIM, field data, and HCM 2000 entry capacity results for one-lane roundabouts	65
Figure 35: Examining the entry capacity of both lanes in VISSIM and field data for two-lane roundabouts	66
Figure 36: Examining the entry capacity of critical lane in VISSIM, and HCM 2000 for two lane roundabout.....	66
Figure 37: Vehicle delay based on different capacity reduction factor models	70
Figure 38: Regression lines for different capacity reduction factor models	70
Figure 39: Comparison of estimated delays obtained from the proposed and HCM analytical models with the delays obtained from VISSIM.....	72
Figure 40: Comparison of estimated delays obtained from the proposed and HCM analytical models with the delays obtained from VISSIM by entry leg.....	74
Figure 41: Comparison of estimated delays obtained from the proposed and HCM analytical models with the delays obtained from VISSIM for OD 4-1	75
Figure 42: Roundabout features (Robinson et al., 2000).....	83
Figure 43: Roundabout dimensions (Robinson et al., 2000)	84
Figure 44: Approach numbering for one lane roundabout	85
Figure 45: Inner and Outer lanes in Two-lane roundabout (Robinson et al., 2000).....	86
Figure 46: HCM entry capacity model.....	92
Figure 47: German (Gap Acceptance) entry capacity model.....	93
Figure 48: German (empirical) entry capacity model	94
Figure 49: FHWA entry capacity model	95
Figure 50: Australian entry capacity model.....	96
Figure 51: Kimber entry capacity model.....	97
Figure 52: English entry capacity and capacity reduction factor model.....	98
Figure 53: English capacity reduction factor and German entry capacity models.....	99

Figure 54: German capacity reduction factor model.....	100
Figure 55: French capacity reduction factor model.....	101
Figure 56: Driving behavior parameter sets for following vehicles in VISSIM (VISSIM 5.20 User Manual 2009).....	102
Figure 57: Driving behavior parameter sets for lane change in VISSIM (VISSIM 5.20 User Manual 2009)	103
Figure 58: Roundabout back ground	105
Figure 59: Scaling the roundabout	106
Figure 60: The coded links in VISSIM	107
Figure 61: The coded connectors in VISSIM	107
Figure 62: The coded links and connector location in one-lane roundabout in VISSIM	108
Figure 63: The coded links and connector location in two-lane roundabout in VISSIM	109
Figure 64: The coded links and connector location in two-lane roundabout in VISSIM	109
Figure 65: The link and connector lengths	110
Figure 66: All route decision for two-lane roundabout and for each lane (How to Navigate Modern Roundabouts, 2011)	111
Figure 67: Route decision for one-lane roundabout in VISSIM	111
Figure 68: The coded conflict areas for pedestrians and vehicles for one-lane roundabout in VISSIM	112
Figure 69: The coded conflicting areas for two-lane roundabout, and for pedestrians in VISSIM ...	113
Figure 70: The coded reduced speed area marked in green in VISSIM	115
Figure 71: The coded desired speed decision marked in green in VISSIM.....	115
Figure 72: The delay measure start and end	116
Figure 73: Pedestrian volume generated in the major approach in VISSIM	117
Figure 74: A truck in a roundabout approach	119
Figure 75: A truck at the yield line or roundabout entry	120
Figure 76: Google satellite picture for Sawmill Rd. / Arthur St. S (HW 85)	121
Figure 77: Roundabout in the University Ave W/ Ira Needles as video recorded	122
Figure 78: Google satellite picture for University Ave W/ Ira Needles roundabout.....	122
Figure 79: Roundabout in the Erb St. W/ Ira Needles as video recorded.....	127
Figure 80: Google satellite picture for Erb St. W/ Ira Needles	128

Figure 81: The flare length for Erb St. W/ Ira Needles and Sawmill Rd. / Arthur St. S roundabouts as coded in VISSIM 128

Figure 82: Roundabout in the Sawmill Rd. / Arthur St. S (HW 85) as video recorded 131

Figure 83: Google satellite picture for Sawmill Rd. / Arthur St. S (HW 85) 132

List of Tables

Table 1: Comparison between the old traffic circle and the modern roundabout (Jacquemart, 1998)..	1
Table 2: Comparison between roundabout types and roundabout design elements (Robinson et al., 2000)	5
Table 3: The upper and lower bounds of critical gap and follow-up time for modern roundabouts (Rodegerdts et al., 2007)	10
Table 4: Headway between Vehicles in the Circulating volume (Δ) (Troutbeck, 1989).....	16
Table 5: Percentage of vehicles following a leading circulating vehicle (θ)	16
Table 6: The range of the geometric parameters used in the Kimber method (Kimber, 1980)	19
Table 7: Parameter values for Equation 22 (Brilon and Stuwe, 1990).....	21
Table 8: Parameters for Equation 23 (Brilon et al., 1997).....	22
Table 9: The geometric parameters used to establish the FHWA model based on the Kimber method and the German formula (Robinson et al., 2000).....	23
Table 10: Geometric element range for French model (Mauro 2010)	28
Table 11: The geometry of one-lane and two-lane roundabout	43
Table 12: Characteristics of single lane roundabout use for case study	54
Table 13: Sources of delays associated with each O-D pair	55
Table 14: Data collected from the three roundabouts in the region of Waterloo	59
Table 15: Summary of the average vehicle delay and maximum queue length observed from different sites.....	60
Table 16: Summary of the average vehicle delay and maximum queue length from different sites using HCM 2000 model	60
Table 17: Average vehicle delay and maximum queue length generated from VISSIM code for University Avenue with Ira Needles site.....	60
Table 18: Average vehicle delay and maximum queue length generated from VISSIM for Erb Street with Ira Needles site.....	61
Table 19: Average vehicle delay and maximum queue length generated from VISSIM for Arthur Street and Sawmill Road site (HWY 85).....	61
Table 20: The roundabout geometry for one- and two-lane roundabouts found from research and coded in VISSIM (Bared and Edara, 2005).....	63

Table 21: The entry capacity for one and two-lane roundabout based on the geometry in Table 20 (Bared and Edara, 2005).....	64
Table 22: Parameters in Proposed Model.....	67
Table 23: RMSE values for different entry capacity and capacity reduction factor models based on VISSIM delay results	69
Table 24: Regression results	71
Table 25: Key words used in the research and their description.....	87
Table 26 : Comparing entry capacity and capacity reduction factor results from references to the calculated using the equations	90
Table 27: The geometry of one lane roundabout	104
Table 28: The geometry of two lane roundabout	104
Table 29: Conflict area parameters	112
Table 30: Data collection recording condition.....	118
Table 31: Field speed data in kilometers per hour (Anglastro, 2010)	123
Table 32: Vehicle volume at University Ave W/ Ira Needles	125
Table 33: Vehicle volume at Erb St. W/ Ira Needles	130
Table 34: Vehicle volume at Sawmill Rd. / Arthur St. S (HW 85).....	134

Chapter 1: Introduction

1.1 Background

In Canada and the U.S., the use of the first traffic circles began in 1904 but by the 1950s the use of traffic circles had fallen out of favour and many existing traffic circles were reconstructed as signalized intersections. A resurgence of this form of unsignalized intersection design, labeled the “modern” roundabout began to be used in the early 1990s (Weber, 2010).

Traffic circles differ from modern roundabouts in several important ways (Table 1). The traffic circle has a bigger inscribed diameter and the right-of-way is to the vehicles approaching the roundabout (Figure 1). On the other hand, the modern roundabout has a smaller diameter and the right-of-way is to the circulating vehicles. The traffic circle has operational and safety problems (Jacquemart, 1998).

Table 1: Comparison between the old traffic circle and the modern roundabout (Jacquemart, 1998)

Comparison Feature	Traffic Circle	Roundabout
Right-of-way	To the entering vehicles	To the circulating vehicles
Entry curve	Tangential to the circulating road (high speed entry)	Sharp entry curves (slow entry speed)
Pedestrians	Can cross into central island	Cross one or two-lanes per one direction and not allowed to cross into central island
The control system	Traffic signals	Yield signs
Parking	Allowed in the central island	No parking is allowed



Figure 1: Characteristics of traffic Circle (L'Arc De Triomphe, 2002)

The modern roundabout (Figure 2) is an unsignalized intersection design that accommodates vehicles, pedestrians, cyclists, and motorcycles through the use of special geometry and operational driving rules. These rules are as follows:

- 1- Approaching vehicles should reduce their speed to enter the roundabout and chose the appropriate lane based on the desired movement (i.e. in two lane roundabout the right lane is used to turn right and go straight, and the left lane is used to turn left, perform a U-turn and to go straight).
- 2- Approaching vehicles must give the right of way to pedestrians crossing the roundabout approach leg and then must give right of way to vehicles within the roundabout on the circulating roadway.
- 3- Vehicles must enter and traverse the roundabout at a low speed due to the restricted geometry.
- 4- Vehicles leaving the roundabout must give right of way to pedestrians crossing the exit lane.

Unlike at intersections controlled by traffic signals or stop signs vehicles entering the roundabout are not required to stop before entering the roundabout. Instead, vehicles traversing the roundabout only experience delays when they must stop to seek gaps in the pedestrian or circulating traffic streams.



Figure 2: Characteristics of modern roundabout (Three-leg Multi-Lane Roundabout in East Lansing, Michigan, 2011)

The unique characteristics of modern roundabouts result in several advantages over other forms of intersection control (Jacquemart, 1998). Studies have shown that roundabouts improve vehicle and pedestrian safety, reduce vehicle delays, and reduce fuel consumption and vehicle tailpipe emissions. As a result of these advantages, a large number of roundabouts have been recently planned and/or constructed. There are now more than 1200 modern roundabouts in Canada and many are under construction (The City of Waterloo, 2011). The Regional Municipality of Waterloo currently has 15 modern roundabouts (Region of Waterloo, 2011) and more are under construction (Waterloo Region approves two new roundabouts, 2011).

In many jurisdictions, including Waterloo Region, pedestrian crossings are provided at the entrance and the exit of the roundabout (Figure 3). The crossing line (zebra line) is located at a distance of between one and two car lengths away from the roundabout yield line at the entrance and the exit. This distance allows entering vehicles to interact only with conflicting or circulating vehicles. Pedestrians crossing at this location have right of way over cars entering and exiting the roundabout. This distance also gives the exiting vehicle a safe space to stop if required while interacting with pedestrians in the exit lane until the vehicle finds an appropriate gap between pedestrians to exit the roundabout. Roundabouts have a refuge island for pedestrians to cross from one side to the other.

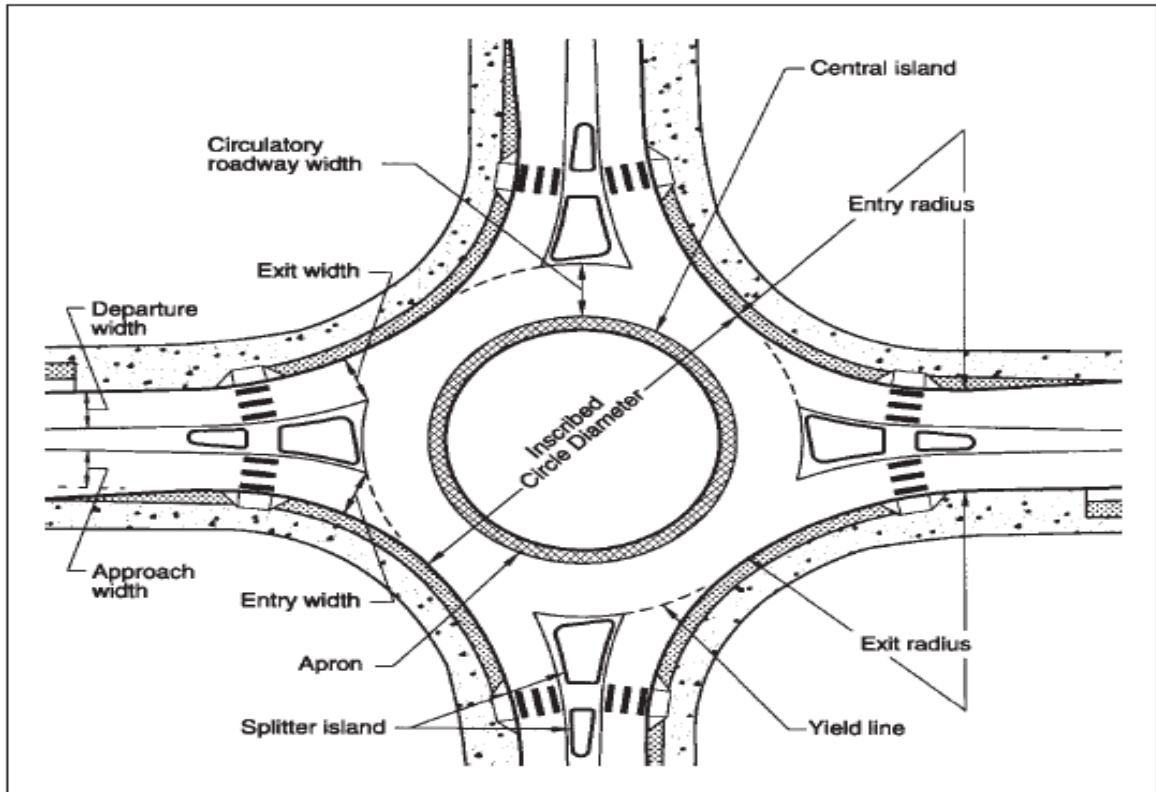


Figure 3: Roundabout dimensions (Robinson et al., 2000)

The operation speed for the modern roundabout is low. The circulating speed is around 30 km/h, and the approach speed is around 50 km/h (Robinson et al., 2000). In modern roundabouts, vehicles are not allowed to change lanes in the circulating lanes.

There exist a number of types of modern roundabouts (Table 2) for which the inscribed circular diameter is the dominant geometric feature that characterizes the type of roundabout.

Mini-roundabouts

Based on Robinson et al. (2000) mini-roundabouts are roundabouts used in urban areas under low operating speeds. Because of the roundabout's small geometry, it is usually used when there is not enough land. There is no difference in capacity between this roundabout and the urban compact roundabout.

Urban Compact roundabout

Based on Robinson et al. (2000) the urban compact roundabout is a single lane roundabout with entry from all the four directions. The design requirements for pedestrians' safety are satisfied by this roundabout. The operating speed is considerably low.

**Table 2: Comparison between roundabout types and roundabout design elements
(Robinson et al., 2000)**

Roundabout types \ Roundabout design elements	Mini-Roundabout	Urban Compact	Urban Single-lane	Urban Double-lane	Rural Single-lane	Rural Double-lane
Recommended maximum entry design speed (km/h)	25	25	35	40	40	50
Maximum number of entry lanes per approach	1	1	1	2	1	2
Typical inscribed circle diameter (m)	13-25	25-30	30-40	45-55	35-40	55- 60

Urban single lane roundabout

Based on Robinson et al. (2000) the urban single roundabout is a roundabout in the urban area with one circulating lane and one entry lane at all approaches. The design requirements for pedestrians’ safety are met by this roundabout. Its inscribed circle diameter is larger than the urban compact roundabout. Its operating speed is higher than the urban compact roundabout. The entry and circulating speed is low. Pedestrians and cyclists can use this facility safely due to its low operating speed.

Urban double lane roundabout

Based on Robinson et al. (2000) the urban double lane roundabout is a roundabout in an urban area with two circulating wide lanes and two entry lanes, or one-lane flared to two-lanes at the entry. The roundabout operating speed is slightly higher than the urban single lane roundabout.

Because of the considerably low speed of this roundabout, this roundabout is considered a safe traffic system for pedestrians and cyclists (See Table 2 for more details; see Figure 4 for urban double lane roundabout layout).

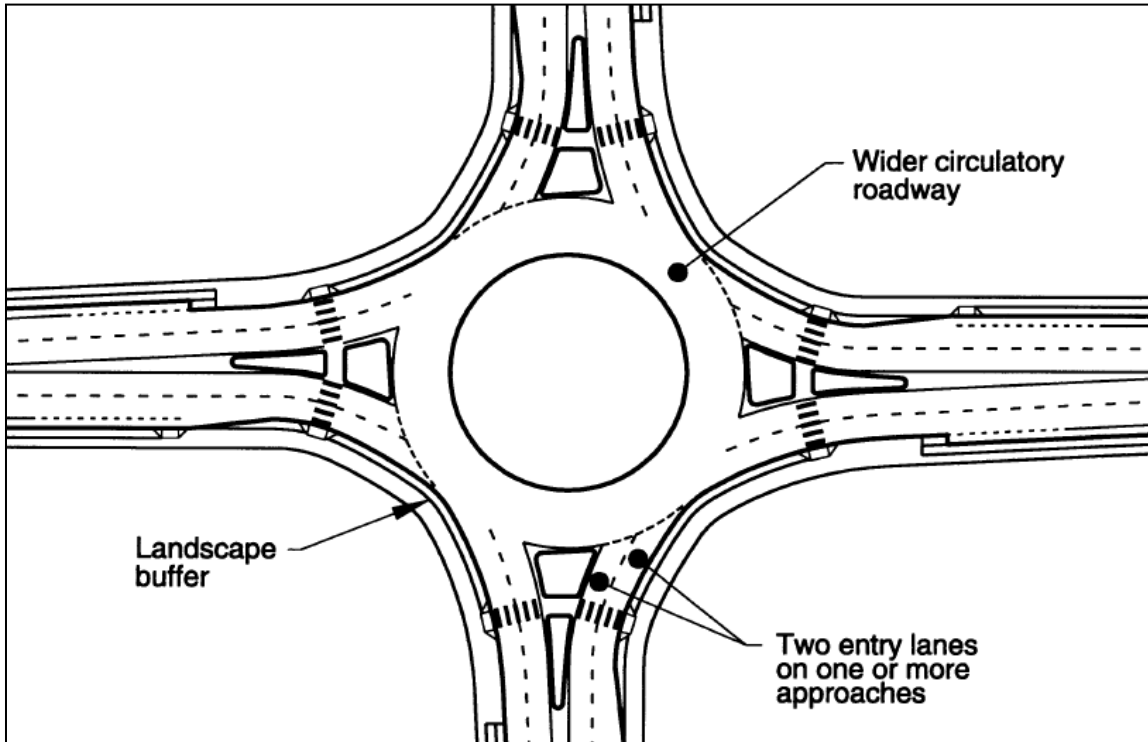


**Figure 4: Urban double lane roundabout layout
(Robinson et al., 2000)**

Rural single lane roundabout

Based on Robinson et al. (2000) this is a roundabout in a rural area with one circulating and entry lane. Its inscribed diameter is higher than the urban roundabout, and its operating speed also higher. Pedestrian volumes are expected to be low, and traffic control devices should be installed in this roundabout. The pedestrians' splitter islands are extended to upstream of the approaches.

Rural double lane roundabout

Based on Robinson et al. (2000) this is a roundabout in a rural area with two-lanes circulating and with a two-lane or one-lane entry, and flared at the roundabout entry to two-lanes. It has a large inscribed diameter and its operating speed is high. The number of pedestrians using this facility is assumed to be low. This roundabout is supported with traffic control devices. The pedestrians' splitter islands are extended to upstream of the approaches. See Appendix A for more details about modern features and diminutions.

Many municipalities of Ontario are planning to replace regular intersections with roundabouts (e.g., Ottawa Street and Homer Watson Boulevard, Waterloo, Ontario, Canada). The modern roundabout proves to be a safe and efficient traffic system.

Compared to a regular intersection, a roundabout is much safer (Waterloo Region approves two new roundabouts, 2011). The severity of the crashes and conflicting points are less in roundabout than signalized intersection and that makes it more effective (Robinson et al., 2000). However, it has been shown that a signalized intersection provides slightly better operational performance than a roundabout when the roundabout is operating at its capacity. The roundabout performs better in term of vehicle delay than signalized intersection when operating under capacity (Hallmark et al., 2009). Modern roundabouts do not require a large amount of land (although typically more than a signalized intersection). In addition, they do not have operating costs, for electricity and programming traffic signals. Recent research (Alisoglu, 2010) suggests that a roundabout saves around \$90,000 (net present value) compared to a signalized intersection assuming a service life of 29 years and considering annual maintenance and the construction cost.

1.2 Problem definition

Much research has been conducted in Canada studying the modern roundabout from a safety and operational perspective (e.g. Robinson et al., 2000; Hallmark et al., 2009). Modern roundabouts are considered a good solution to address safety and operational issues (Waterloo Region approves two new roundabouts, 2011). Many transportation agencies plan roundabouts instead of other traffic systems; however, most of the previous studies focus on the effects of entering vehicle volume, conflicting vehicle volume, and the geometry of the roundabout, namely, the number of lanes and the Inscribed Circle Diameter (ICD) on the entering vehicle capacity. Only a few international studies have examined the effects of pedestrian flows on the delays to vehicles traversing the roundabout. The models that have been developed from these studies use different assumptions and different entry capacity models and consequently it is not clear how applicable these models are to Canadian roundabouts. The goal of this research is to quantify the impact that pedestrian volumes have on the operational characteristics of roundabouts (as measured in terms of vehicle delays).

1.3 Thesis Structure

The next chapter provides a review of the relevant literature pertaining to the effect that pedestrians have on the operational performance of roundabouts.

Chapter 3 presents the proposed analytical model for estimating vehicle delay as a function of pedestrian and vehicle volumes. Chapter 4 describes the calibration and validation of the proposed model using the VISSIM simulation model. Chapter 5 provides the conclusions and recommendations.

Chapter 2 Literature Review

2.1 Introduction

The roundabout entry capacity is a key feature in analyzing roundabout performance. Based on Weber (2010) there are three different categories of models used to analyze roundabout entry capacity.

- 1- Gap acceptance based models (e.g., HCM 2000, Synchro, SIDRA).
- 2- Empirical models (e.g., U.K. model, RODEL, ARCADY).
- 3- Simulation models (e.g., micro-simulation software [VISSIM, PARAMICS, AIMSUN]).

The literature review in this Chapter focuses on the following four areas:

1. Theoretical models that estimate roundabout performance;
2. Empirical models for estimating roundabout performance;
3. Macro- and micro-simulation software that could be used to model roundabout performance including the effects of pedestrians; and
4. Roundabout entry capacity data described in the literature.

2.2 Theoretical (Gap acceptance) models for estimating capacity

Three different gap acceptance based models – the Australian, German, and HCM 2000 are reviewed in this section.

2.2.1 HCM 2000 model (HCM, 2000)

The gap acceptance model was originally proposed to explain behavior, and estimate capacity, at two-way stop controlled intersections. The basic concept of the model is that entering vehicle must find a suitable gap in the conflicting (circulating) traffic stream. This gap is measured as time headway. Two parameters are used to define the required gaps, t_c and t_f . If an entering vehicle finds a gap between a pair of circulating vehicles accepts this gap and goes between the circulating vehicles, then this is known as the critical gap t_c or the minimum gap. If the second entering vehicle finds a gap between the same pair of circulating vehicles, then this is called the follow-up time t_f . In other words, the minimum time headway required for at least one vehicle on the approach to make its manoeuvre is t_c . The minimum time headway required for two vehicles to make their manoeuvres is $t_c + t_f$. The minimum time headway required for N vehicles to complete their manoeuvres is $t_c + Nt_f$.

The supply of the time headways within the conflicting traffic stream is determined by the distribution of vehicle arrivals on the circulating roadway at the roundabout entry location. The gap acceptance model assumes the vehicles arrive according to a Poisson distribution with an average arrival rate of λ . If the arrivals follow a Poisson distribution, then vehicle headways follow an exponential distribution (see Figure 5) and the probability of a headway being larger than some value t is given by.

$$P[T \geq t] = e^{-t\lambda} \quad \text{Equation (1)}$$

Where:

- λ = Average arrival rate for the conflicting traffic stream (veh/h)
- t = Time headway (h)

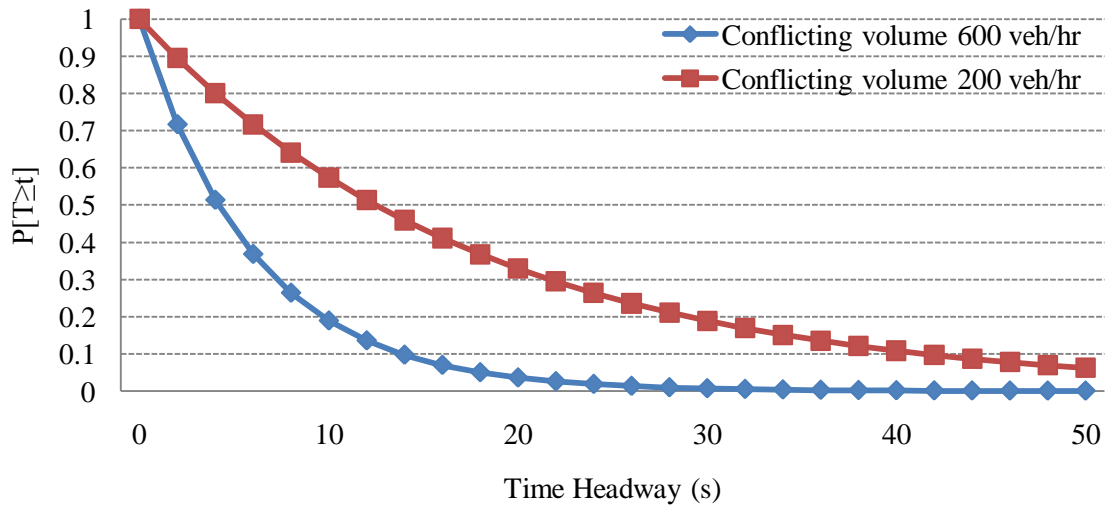


Figure 5: Exponential distribution of time headways $P[T \geq t] = e^{-t\lambda}$

Equation 1 which describes the availability of time gaps in the conflicting traffic stream, can be combined with t_c and t_f to estimate entry leg capacity. This is achieved through the following steps: 1) finding the probability of one vehicle accepting the gap in the circulating road; 2) followed by the probability of a number of vehicles accepting the gap; 3) multiplying each of the probabilities by the number of vehicles accepting the gap; 4) multiplying this number by the arrival rate; and 5) summing up all the products in the previous step.

As the required time headway become larger, the probability of observing a time headway of that length or longer within the conflicting traffic stream decreases.

This is evident in Figure 5. The probability of observing a headway that is longer than one second is much larger than the probability of observing a headway that is more than 10 seconds. Moreover, the probability of observing a time headway of at least t seconds decreases as the arrival rate of the conflicting traffic stream increases (Figure 5).

An equation (Equation 2 and Figure 6) has been developed that captures this effect (HCM, 2000). The model can be calibrated based on the critical gap and follow-up time values which are related to driver behavior and roundabout geometry. Table 3 provides the upper and lower bounds of the critical gap and the follow-up time for U.S. drivers.

$$C_a = \frac{V_c e^{-V_c t_c / 3600}}{1 - e^{-V_c t_f / 3600}} \quad \text{Equation (2)}$$

Where:

- C_a = Approach capacity (veh/h)
- V_c = Conflicting (circulating) traffic volume (veh/h)
- t_c = Critical gap (s)
- t_f = Follow-up time (s)

Table 3: The upper and lower bounds of critical gap and follow-up time for modern roundabouts (Rodegerdts et al., 2007)

	Critical Gap (seconds)	Follow-up Time (seconds)
Upper bound	4.1	2.6
Lower bound	4.6	3.1

Rodegerdts et al. (2007) calibrated values for t_c and t_f for one and two lane roundabouts in the USA and by substituting these values into Equation 2 determined the following simplified capacity models.

Entry capacity for one-lane roundabout

$$C_a = 1130 e^{-0.0010 V_c} \quad \text{Equation (3)}$$

Entry capacity for two-lane roundabout

$$C_a = 1130 e^{-0.0007 V_c} \quad \text{Equation (4)}$$

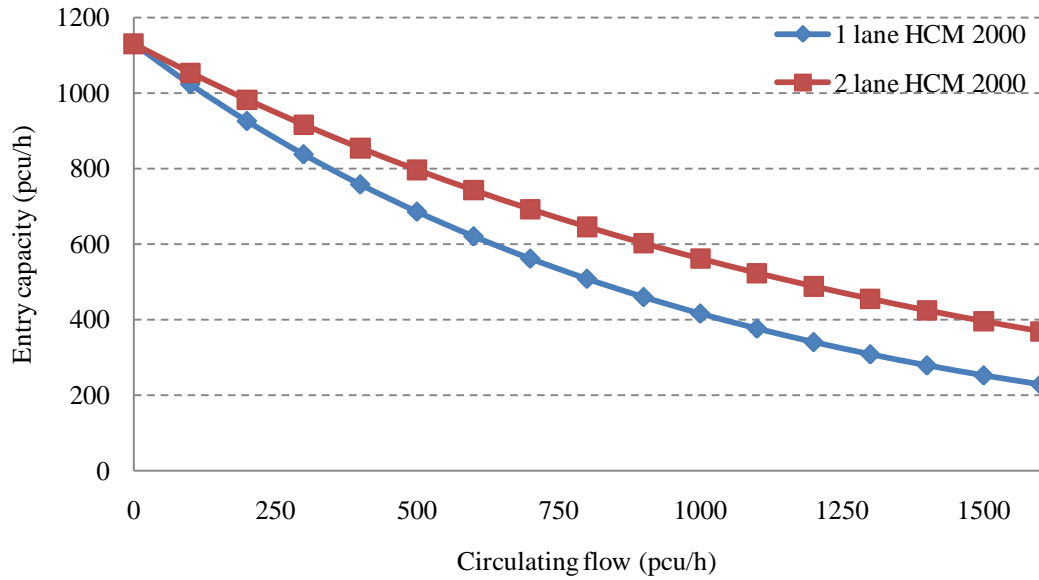


Figure 6: Entry capacity of roundabout approach using HCM 2000 (Equation 3, and 4)

Average vehicle delay can be estimated on the basis of the demand of vehicles attempting to enter the roundabout via the entry leg and the capacity estimated using one of the above models.

Delay models were originally developed for signalized intersections. The models treat the intersection as a queuing system in which arrivals follow a Poisson distribution, the service rate is uniform (deterministic) and arrivals are served in order of arrival (i.e. First-In-First-Out).

The resulting expression proposed by the HCM is provided in Equation 5.

$$d = \frac{3600}{C_{m,x}} + 900 T \left[\frac{V_x}{C_{m,x}} - 1 + \sqrt{\left(\frac{V_x}{C_{m,x}} - 1\right)^2 + \frac{\left(\frac{3600}{C_{m,x}}\right)\left(\frac{V_x}{C_{m,x}}\right)}{450 T}} \right] \quad \text{Equation (5)}$$

Where:

- d = Average vehicle delay in an approach (s/veh)
- V_x = Entering volume (veh/h)
- $C_{m,x}$ = Entry capacity (veh/h)
- T = Analysis time period (h) ($T = 0.25$ for a 15 minute period)

Figure 7 illustrates the resulting relation for a range of capacity and entry volumes. Delay increases non-linearly with increases in volume to capacity ratio. The strength of the HCM model for estimating roundabout capacity and average vehicle delay is it is consistent with the HCM analysis method applied to two-way stop controlled and signalized intersections.

However, the model is calibrated for a narrow range of geometric characteristics and therefore the model cannot be used to evaluate the input of different geometries. Furthermore, the method assumes that pedestrians are considered as vehicles circulating the roundabout. This consideration did not take in to account that pedestrians crossing the zebra line have an impact on entering and exiting vehicles. In addition, entering vehicles must stop for pedestrians up stream of the yield line then yield to circulating vehicles.

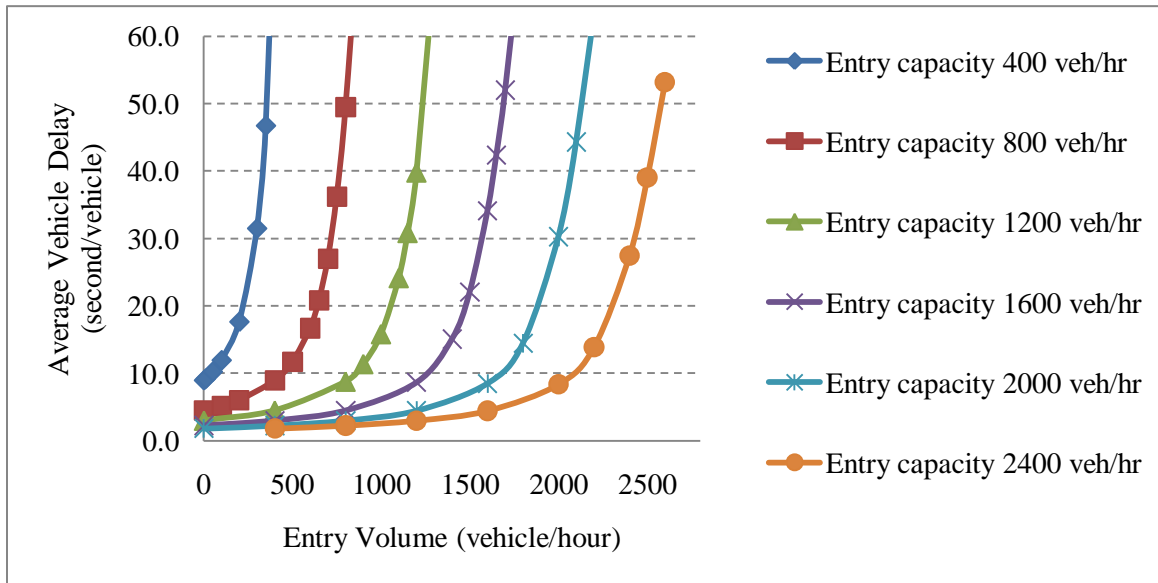


Figure 7: Vehicle delay based on different entry volumes and capacities for a single lane roundabout (computed using Equations 3 and 5)

2.2.2 Australian model

The Australian model is different from the HCM 2000 model primarily in the assumptions it makes about the distribution of arrivals on the circulating roadway. The model (Equation 6) was first proposed by Tanner (Tanner, 1962). He assumed random (Poisson) vehicle arrivals and departures. The vehicles on the entry leg are assumed to wait Δ time (the minimum headway a vehicle can accept) after the vehicle on the circulating roadway passed before attempting to enter the roundabout. The minimum gap for the first vehicle to use a time headway is T , and the time it takes for each additional vehicle using the same gap is T_o .

$$q_e = \frac{q_c (1 - \Delta q_c) e^{q_c(T-\Delta)}}{1 - e^{-q_c T_o}} \quad \text{Equation (6)}$$

- q_e = Entry capacity (veh/h)
- q_c = Circulating flow (veh/h)
- T = Critical gap (s)
- T_o = Follow-up time (s)
- Δ = Minimum headway a vehicle can accept (s)

Similar to the HCM 2000 model Tanner assumed both the major and the minor stream follow an exponential distribution. Troutbeck modified Tanner's model by assuming the vehicle arrivals on the circulating roadway follow Cowan's M3distribution (Mauro, 2010). Cowan's M3distribution (Cowan 1975) is a cumulative distribution function and is defined as follows:

$$F(t) = 1 - \alpha e^{-(t-\Delta)} \quad \text{Equation (7)}$$

- Δ = Minimum headway (s)
- α = Proportion of vehicles with headway greater than Δ

Troutbeck's model for capacity is:

$$Q_e = \frac{3600 (1-\theta) q_c e^{-\lambda(T-\Delta)}}{1 - e^{-\lambda T_o}} \quad \text{Equation (8)}$$

- Q_e = Entering capacity (veh/h)
- q_c = Conflicting flow (veh/h)
- θ = Percentage of vehicles following a leading circulating vehicle
- Δ = Minimum headway in the circulating volume is equal to 1 sec for multi lane roundabouts and 2 seconds for one-lane roundabouts (s)
- T = Critical gap (s)
- T_o = Follow-up time (s)

$$\lambda = \text{decay parameter} = \frac{(1-\theta)q_c}{1-\Delta q_c} \quad \text{Equation (9)}$$

Troutbeck studied the headway and follow-up time in single and multi lane roundabouts and developed regression models to estimate T and T_o as a function of the roundabout geometry and circulating flow. Equation 10 is used to estimate the follow gap time T_o for roundabouts with a single lane entry and for the lane on two lane entry having the highest entry volume (domain lane see Figure 9) (Troutbeck, 1989).

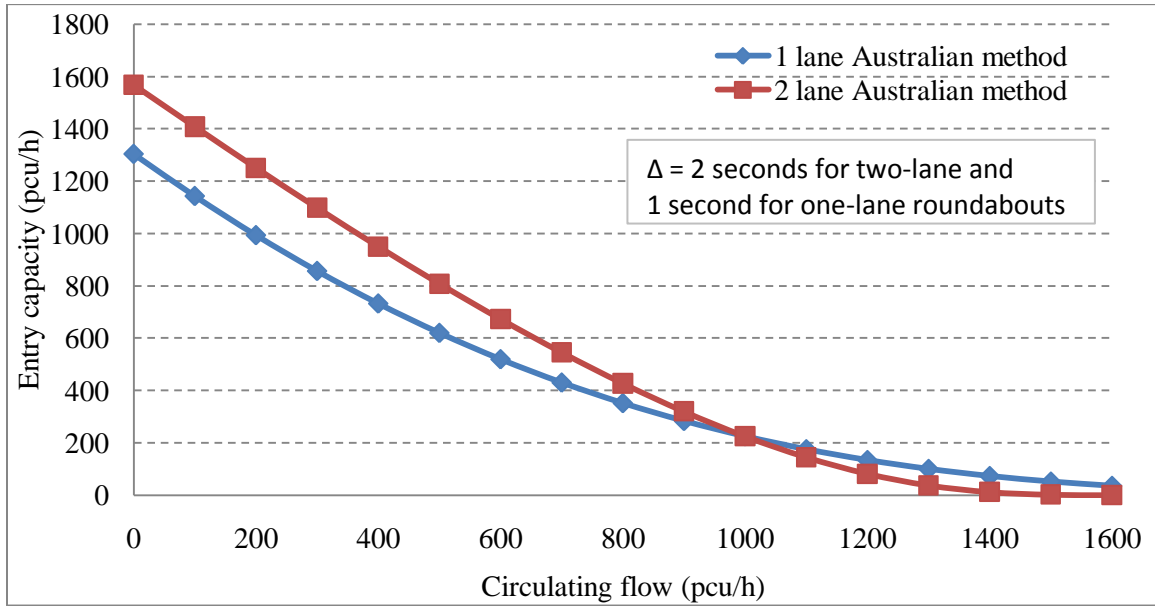


Figure 8: Entry capacity using Troutbeck model (Equation 8)

$$T_{0dom} = 3.37 - 0.000394 Q_c - 0.0208 D_i + 0.0000889 D_i^2 - 0.395 n_e + 0.388 n_c \quad \text{Equation (10)}$$

T_{0dom} = Follow-up time in the domain lane (s)

Q_c = Conflicting flow (veh/h)

D_i = Inscribed diameter, the largest diameter that can be drawn inside the roundabout (m)

n_e = Number of entry lanes

n_c = Number of circulating lanes

Equation 11 is used to estimate T_o for the lane in a two lane entry having the lowest entry volume (sub-domain lane) (Troutbeck, 1989).

$$T_{0sub} = 2.149 + 0.5135 T_{0dom} \frac{Q_{dom}}{Q_{sub}} - 0.8735 \frac{Q_{dom}}{Q_{sub}} \quad \text{Equation (11)}$$

- T_{0sub} = Follow-up time in the sub domain lane (s)
- T_{0dom} = Follow-up time in the domain lane (s)
- Q_{dom} = Vehicle flow in the domain lane (veh/h)
- Q_{sub} = Vehicle flow in the sub domain lane (veh/h)

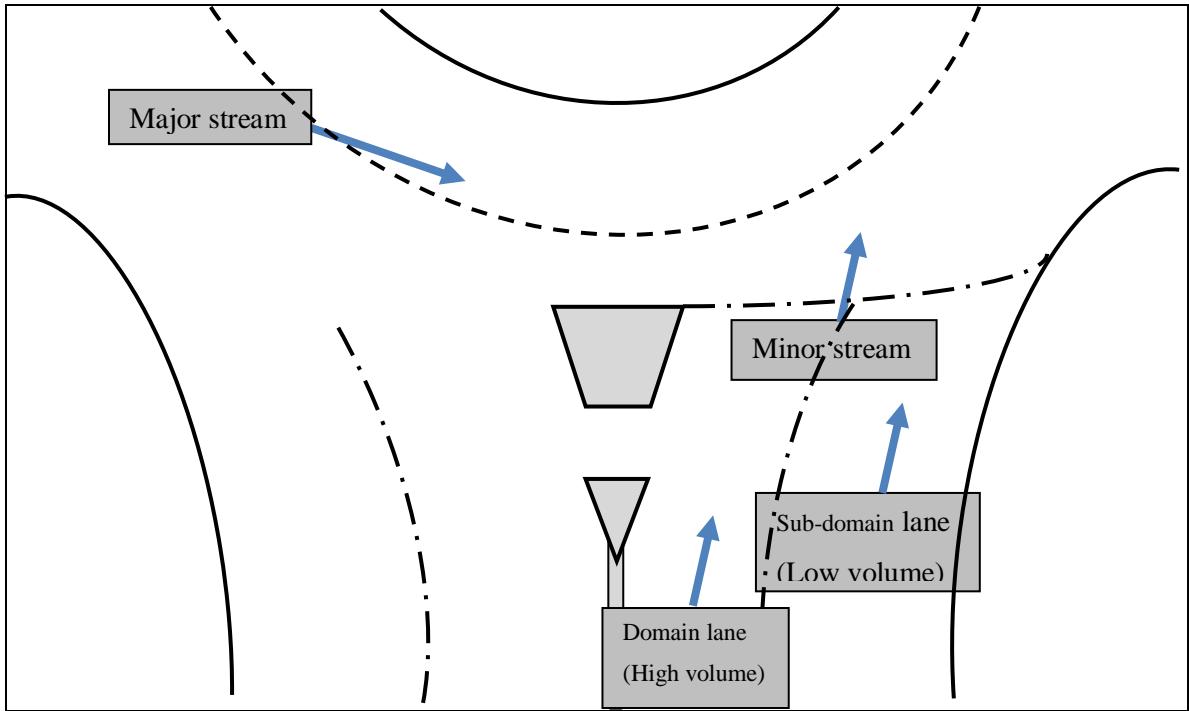


Figure 9: Domain and sub-domain streams

The critical gap T is related to the follow-up time T_o , the conflicting flow, the number of circulating lanes, and the number of entry lanes. The increase in the conflicting flow, the number of circulating lanes and the entry lanes leads to a decrease in the ratio of the critical gap over the follow-up time.

$$\frac{T}{T_o} = 3.6135 - 0.0003137 Q_c - 0.3390 n_e - 0.2775 n_c \quad \text{Equation (12)}$$

- T = Critical headway (s)
- T_o = Follow-up time (s)
- n_e = Number of entry lanes
- n_c = Number of circulating lanes

Table 4 and Table 5 contain minimum headway and percentage of vehicles following a leading circulating vehicle, respectively.

Table 4: Headway between Vehicles in the Circulating volume (Δ) (Troutbeck, 1989)

Circulating Volume	Circulating Roadway Width			
	Less than 10 m		Greater than or equal to 10 m	
	Number of lanes	Headway between vehicles (s)	Number of lanes	Headway between vehicles (s)
<1000 (veh/h)	1	2	2	1
>1000 (veh/h)	1 (or2)	2 (or1)	2	1

Table 5: Percentage of vehicles following a leading circulating vehicle (θ) (Troutbeck, 1989)

Number of circulating lanes	One	More than one-lane
Headway between vehicles , (s)	2	1
Conflicting volume (veh/h)		
0	0.25	0.25
300	0.375	0.313
600	0.5	0.375
900	0.625	0.438
1200	0.75	0.5
1500	0.875	0.563
1800	1	0.625
2000	-	0.667
2200	-	0.708
2400	-	0.75
2600	-	0.792

2.2.3 German model

Similar to the Australian model the German models originate from Tanner's work. However, this model was enhanced by Brilon and Wu (Brilon et al., 1997) as in Equation 13 and Figure 10.

$$Q_e = \left(1 - \frac{\Delta Q_c}{n_c}\right)^{n_c} \left(\frac{n_e}{T_o}\right) e^{-Q_c(t_o - \Delta)} \quad \text{Equation (13)}$$

- Q_e = Entry capacity (veh/h)
- Q_c = Circulating flow (veh/h)
- n_e = Number of entry lanes
- n_c = Number of circulating lanes

$$t_o = T - \frac{T_o}{2} \text{ (s)} \tag{Equation (14)}$$

- T = Critical gap (s)
- T_o = Follow-up time (s)
- Δ = Minimum headway in the circulating lanes (s)

2.3 Empirical models for estimating capacity

Empirical models are essentially regression models that have been calibrated to field data and use geometric properties of the roundabouts as independent variables. The reviewed empirical models are the Kimber method, FHWA method, Switzerland model, German model, and France model.

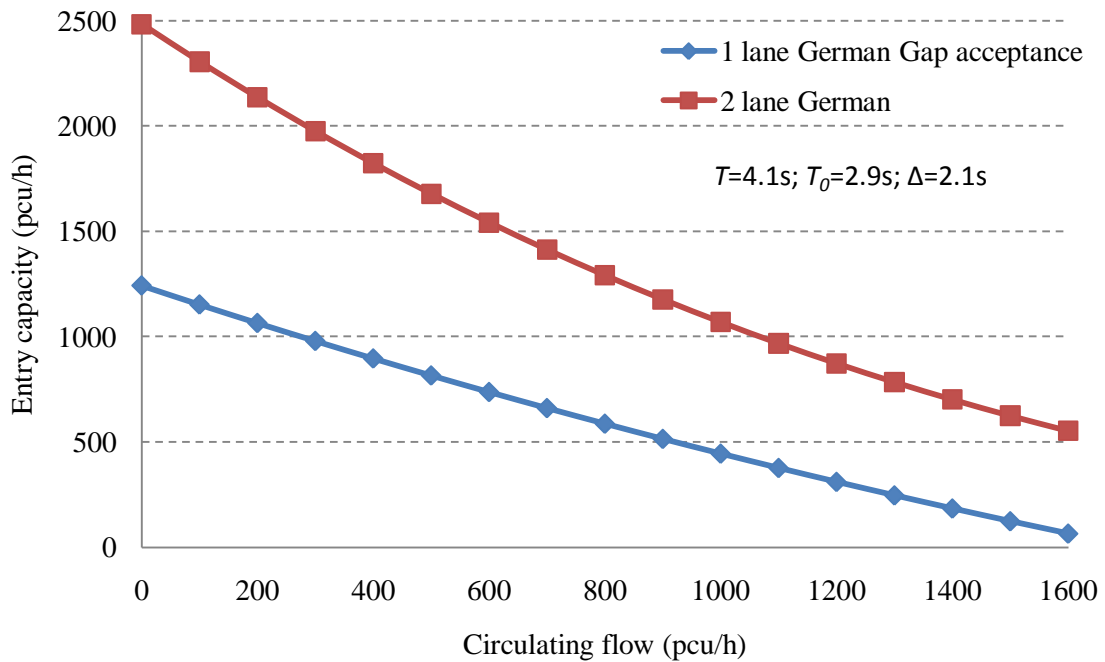


Figure 10: Entry capacity calculated values using Brilon and Wu model (Equation 13)

2.3.1 Kimber method (Kimber, 1980)

The Kimber method was developed on the basis of detailed geometric and traffic data collected from 86 sites in the UK (Kimber, 1980). A linear regression model (Equation 15) was calibrated to these data to estimate entry leg capacity. The model $R^2=0.73$ and its standard error is 200 pcph.

$$Q_e = \begin{cases} Q_e = F - f_c Q_c & f_c Q_c \leq F \\ 0 & otherwise \end{cases} \quad \text{Equation (15)}$$

Q_e = Entry capacity (veh/h)

Q_c = Circulating flow (veh/h)

F, f_c = Regression coefficients

$$K = 1 - 0.00347 (\theta - 30) - 0.978 \left(\frac{1}{r} - 0.05 \right) \quad \text{Equation (16)}$$

$$F = 303 x_2 \quad \text{Equation (17)}$$

$$f_c = 0.210 t_D (1 + 0.2 x_2) \quad \text{Equation (18)}$$

$$t_D = 1 + [0.5/(1 + \exp((D - 60)/10))] \quad \text{Equation (19)}$$

$$x_2 = v + \frac{e-v}{1+2S} \quad \text{Equation (20)}$$

$$S = 1.6 \frac{(e-v)}{I'} \quad \text{Equation (21)}$$

The parameters used in the above equations are illustrated in Figures 11 and 12. The entry width and the flare are mainly related to the increase of the roundabout capacity. The inscribed circle diameter is related to the slope of linear regression lines; the higher the diameter, the lower the slope. The increase of the inscribed circle diameter is more than 70 m, accompanied with a slight increase of the roundabout capacity. Entry angle and radius have small effect on roundabout capacity. The other geometric parameters have no effect on the roundabout capacity except the circulating road width (Kimber, 1980). The ranges of values of the parameters included within Kimber's empirical data are provided in Table 6. The application of Equation 15 for two roundabout geometries is illustrated in Figure 13.

Table 6: The range of the geometric parameters used in the Kimber method (Kimber, 1980)

Variable	Range
e	3.6 – 16.5 (m)
v	1.9 – 12.5 (m)
e'	3.6 - 15.0 (m)
v'	2.9 – 12.5 (m)
u	4.9 - 22.7 (m)
l'	1 - ∞ (m)
S	0 - 2.9
r	3.4 - ∞ (m)
θ	0 – 77 (degrees)
D	13.5 - 71.6 (m)
w	7.0 – 26.0 (m)
L	2.0 – 86.0 (m)

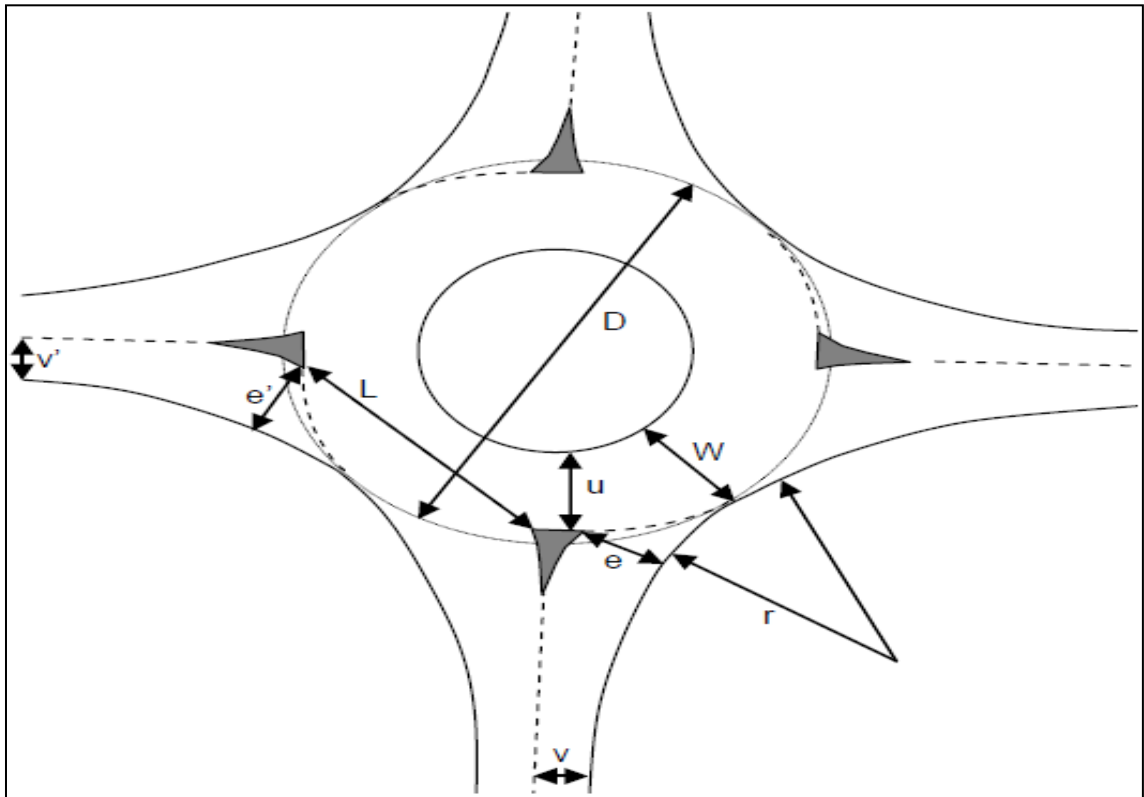


Figure 11: Kimber method geometric parameters (Kimber, 1980)

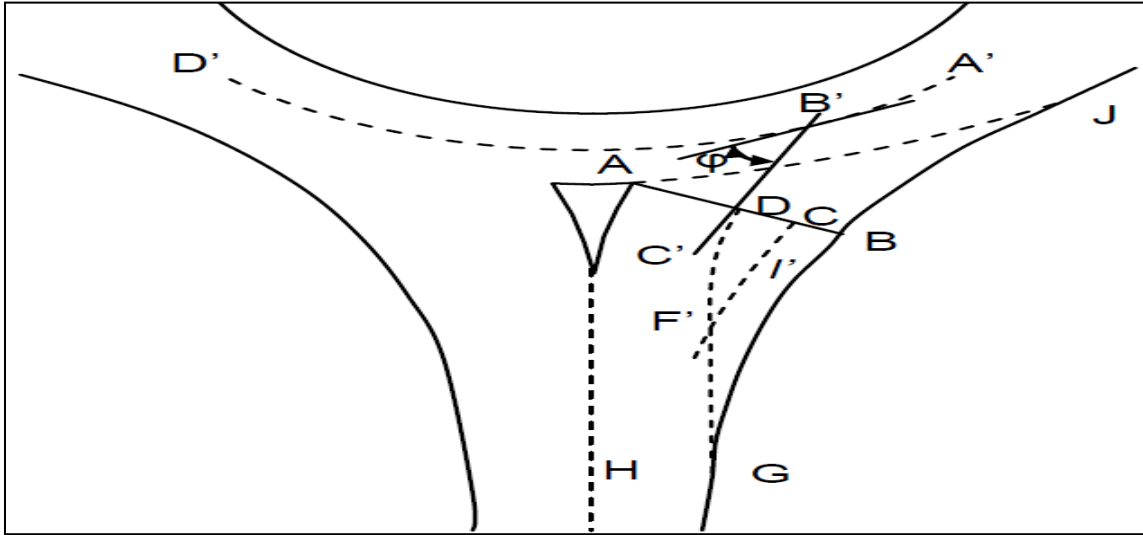


Figure 12: Kimber method geometric parameters (Kimber, 1980)

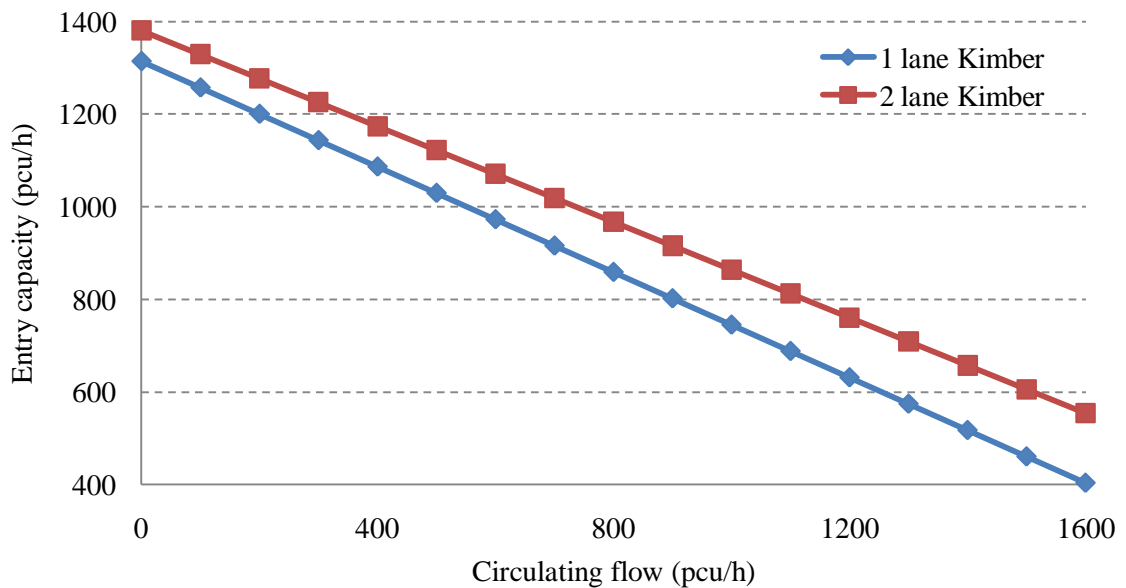


Figure 13: Entry capacity calculated values using Kimber model (Equation 15)

Notes:

- 1- The geometric parameter values for a single lane roundabout using the Kimber method is as follows: $D = 34$ m; $W = 7$ m; $e = 4$ m; $v = 3$ m; $l' = 7.5$ m; $\theta = 35^\circ$; $r = 20.8$ m (Mauro, 2010).
- 2- The geometric parameter values for a two lane roundabout using the Kimber method is as follows: $D = 56$ m; $W = 8$ m; $e = 8$ m; $v = 6.5$ m; $l' = 15.1$ m; $\theta = 35^\circ$; $r = 32.7$ m (Mauro, 2010).

2.3.2 German model (Brilon, Wu and Bondzio)

This model estimates the vehicle entry capacity at a roundabout as a function of roundabout geometry (basically the number of entry and circulating lanes) and the conflicting volume. The first version of this model was established using exponential regression with the parameters shown in Table 7 (Brilon et al., 1997; Brilon, 1991).

$$Q_e = A \exp(-B Q_c / 1000) \quad \text{Equation (22)}$$

Q_e = Entry capacity (veh/h)

Q_c = Circulating flow (veh/h)

A, B = Defined parameters

Table 7: Parameter values for Equation 22 (Brilon and Stuwe, 1990)

Number of Lanes		A	B
Entry	Circulating Roadway		
1	1	1089	7.42
2-3	1	1200	7.30
2	2	1553	6.69
3	2	2018	6.68

However, subsequent work showed that linear relation is better than the exponential relation, shown above, in terms of data variance (Brilon et al., 1997). Current version of the German model has a linear form (Equation 23) similar to the Kimber model but calibrated to field data from Germany. Parameters are provided in Table 8. The resulting relationship is illustrated in Figure 14 for a one lane and two-lane roundabout.

$$Q_e = C + DQ_c \quad \text{Equation (23)}$$

Q_e = Entry capacity (veh/h)

Q_c = Circulating flow (veh/h)

C, D = Defined parameters

Table 8: Parameters for Equation 23 (Brilon et al., 1997)

No. of Lanes Entry/Circle	C	D	N (Sample Size)*
1/1	1218	-0.74	1504
1/2 or 1/3	1250	-0.53	879
2/2	1380	-0.50	4574
2/3	1409	-0.42	295

*no. of observed 1- minute intervals

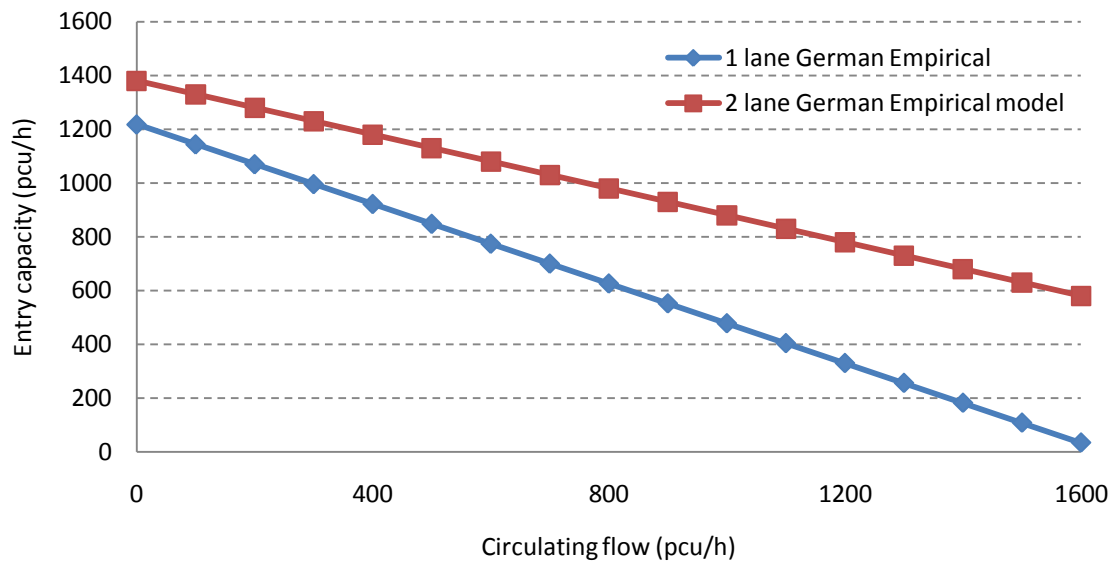


Figure 14: Entry capacity using German empirical model (Equation 23)

Note:

No. of Lanes Entry/Circle is 1/1 for one lane roundabout and 2/2 for two lane roundabout (Table 8)

2.3.3 FHWA (Robinson et al., 2000)

The FHWA method is based on the Kimber method (assuming specific values for various geometric parameters) for double and single lane roundabouts, and the German model established by Brilon, Wu, and Bondzio for urban compact roundabouts (Figure 15 and Table 9) and consequently, the FHWA method is not based on gap acceptance theory. The entry capacity and the conflicting volume have a linear relationship with an increase in the conflicting volume leading to a reduction in the entry capacity.

The two-lane roundabout entry capacity at zero circulating flow is approximately double the entry capacity of a single lane roundabout at zero conflicting flow.

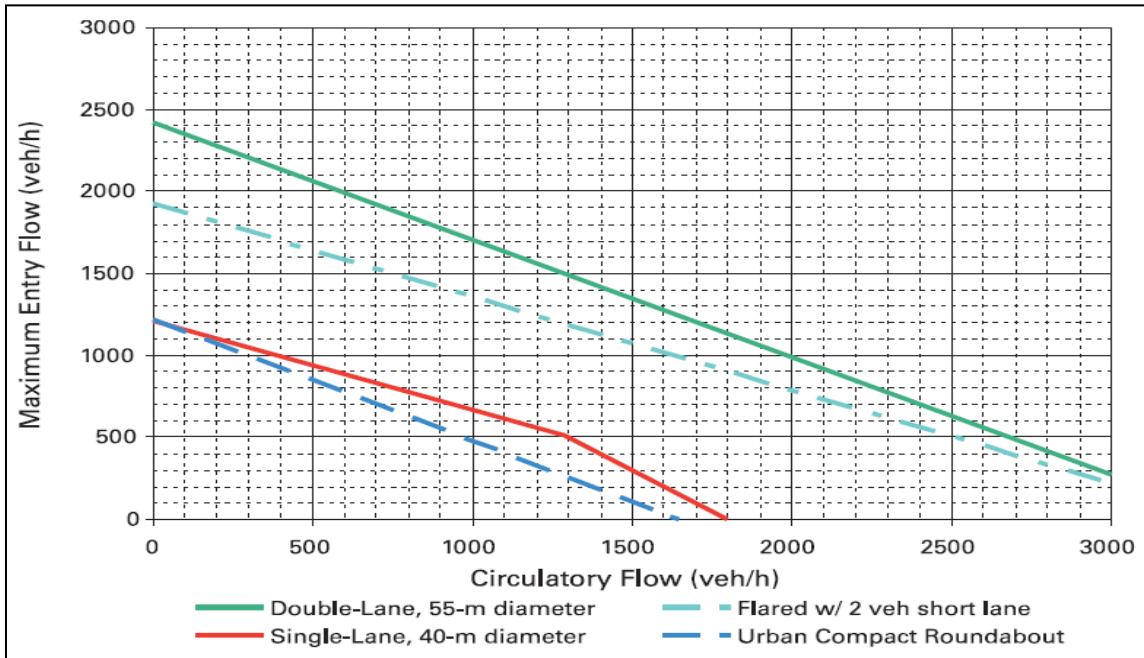


Figure 15: The entry capacity using FHWA model (Robinson et al., 2000)

Table 9: The geometric parameters used to establish the FHWA model based on the Kimber method and the German formula (Robinson et al., 2000)

Geometric Parameters	One-lane Roundabout	Two-lane Roundabout	Urban Compact Roundabout
D	40 m	55 m	It is based on the German Formula (Brilon et al., 1997) for a single lane roundabout (Equation 23)
r_e	20 m	20 m	
θ	30°	30°	
v	4 m	8 m	
e	4 m	8 m	
I'	40 m	40 m	
Q_e	$1212 - 0.5447 Q_c^*$	$2424 - 0.71 Q_c$	$1218 - 0.74 Q_c$

Q_e = Entry capacity (pcu/h)

Q_c = Circulating flow (pcu/h)

* a

2.3.4 Swiss model

According to Bovy et al., (1991) the Swiss model (Equation 24 and Figure 16) uses roundabout geometry (mainly the number of lanes and the length “ ℓ ” in the circulating lane between the exit and the entrance of an approach) and the exit and conflicting flow to estimate the entry capacity of the roundabout. The model is a linear relation between the entry capacity and vehicle distribution Q_d .

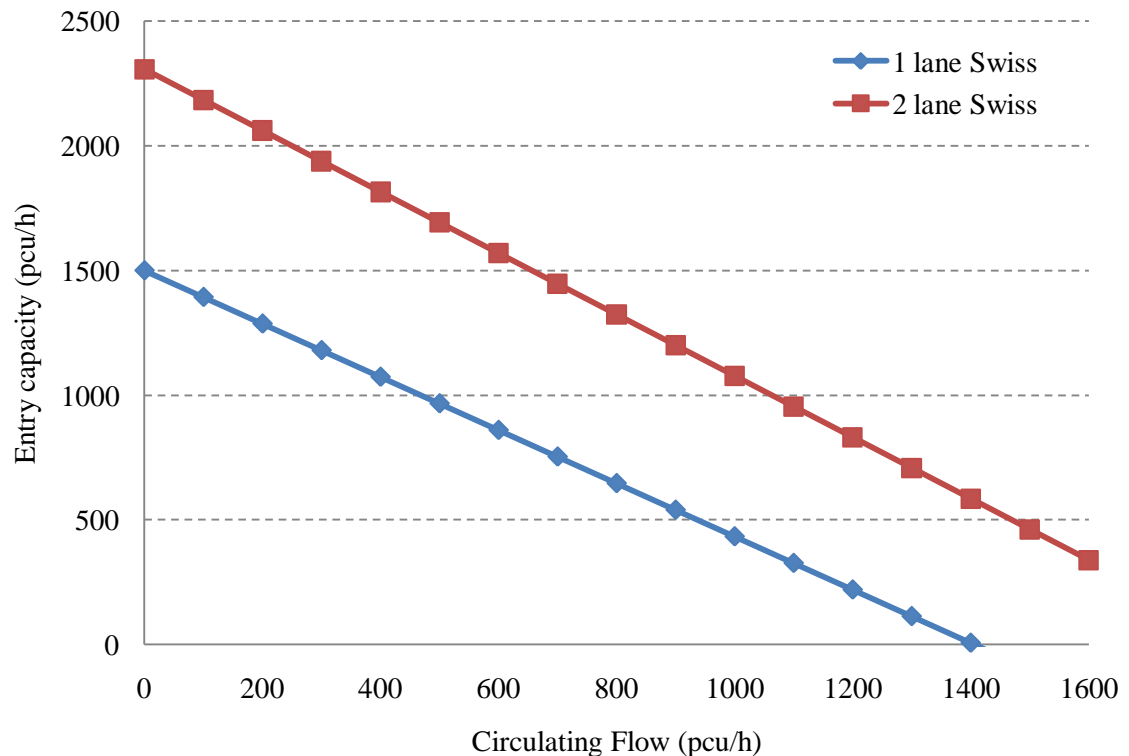


Figure 16: Entry capacity using Swiss model (Equation 24).

Note:

- 1- $\gamma = 1$ for one lane roundabout and 0.65 for two lane roundabout.
- 2- $\beta = 1$ for one lane roundabout and 0.7 for two lane roundabout.
- 3- The exiting volume and the conflicting volume are assumed to be equal in one and two lane roundabout.
- 4- ℓ is the length between point A and B (**Error! Reference source not found.**) assumed to be 22m in one and two lane roundabout.
- 5- Entry volume from each approach assumed to distribute equally to the other three legs.

This model is applicable to urban and suburban areas with a maximum island diameter range of 18 – 20 m, inscribed circle diameter range of 24 – 34 m, and flared entries (Brilon, 1991). α and β are coefficients related to the roundabout geometry. Basically, α is a parameter related to ℓ (the length between the exit and the entrance [the conflict points] in the circulating lane; see Figure 17). When ℓ increases α decreases until ℓ equals to 21 m. The α value remains constant until ℓ is equal to 27 m. After that, α drops to zero when ℓ becomes equal to 28 m. Lines b and c are the upper and lower limit of line a. a, b, c are speed lines. Line a is chosen when the circulating speed is from 20 to 25 km/hr. Line b is chosen when the circulating speed is larger than line a's speed and line c is chosen when the circulating speed is lower than line a (Figure 18). As ℓ increases, the entry capacity increases. The coefficient β is related to the number of circulating lanes. As the number of the circulating lanes decreases, the entry capacity decreases. γ is the entry lanes parameter.

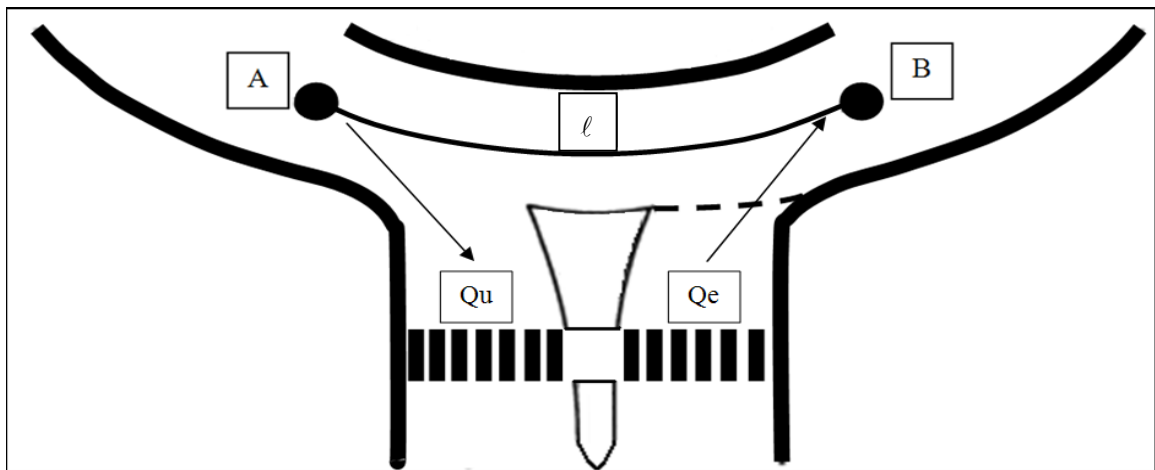


Figure 17: Vehicle volumes and the length ℓ

$$C = \frac{1}{\gamma} \left(1500 - \frac{8}{9} Q_d \right) \quad \text{Equation (24)}$$

$$\gamma = \begin{cases} 1 & \text{for one lane} \\ 0.6 \leq \gamma \leq 0.7 & \text{for two lanes} \\ 0.5 & \text{for three lanes} \end{cases}$$

$$\beta = \begin{cases} 0.9 - 1.0 & \text{for one lane} \\ 0.6 - 0.8 & \text{for two lanes} \\ 0.5 - 0.6 & \text{for three lanes} \end{cases}$$

$$Q_d = \alpha Q_u + \beta Q_c \quad \text{Equation (25)}$$

- C = Entry capacity (pcu/h)
- Q_d = Volume distribution (pcu/h)
- Q_u = Exiting volume (pcu/h)
- Q_c = Circulating conflicting volume (pcu/h)
- γ = Entry lane parameter based on the number of entry lanes
- β = Circulating lane parameter based on the number of circulating lanes

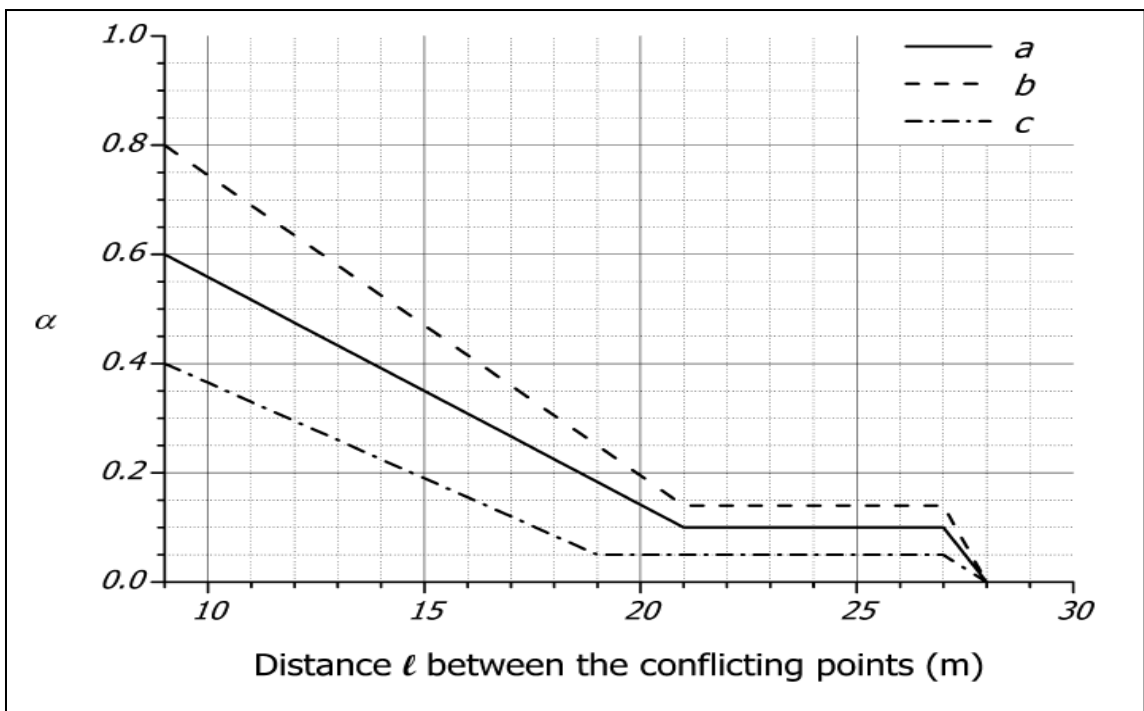


Figure 18: The relation between distance ℓ and parameter α (Mauro, 2010)

2.3.5 French model

Based on Mauro (2010), GIRABASE the French software is developed by CETE de l'Ouest of Nantes. It uses some of the geometric parameters of the roundabout (width of an entry, central island radius, circulating lane width, splitter island width at the leg) along with driver behavior (follow-up time), circulating volume, and exiting volume to estimate the capacity of a roundabout entry.

The capacity equation was developed based on an exponential regression of 63,000 vehicles in 5-10 minutes in 45 different sites (Guichet, 1997). The model (Equation 26) is general as it is applicable for all roundabout types, urban and rural, for three to eight entry legs, and for one to three circulating lanes (Guichet, 2005). The geometric parameters are indicated Figure 19. The model can be used to estimate roundabout entry capacity with geometric element ranges in Table10. The capacity estimates from the model are illustrated for a one-lane and a two-lane roundabout in Figure 20.

$$C = A e^{-Q_d C_B} \quad \text{Equation (26)}$$

$$A = \frac{3600}{T_f \left(\frac{L_e}{3.5}\right)^{0.8}} \quad \text{Equation (27)}$$

T_f = Follow-up time = 2.05 (s)

L_e = Entry width (m)

C_B = Coefficient equal to 3.525 for urban areas and 3.625 for rural areas

$$Q_d = Q_u K_a \left(1 - \frac{Q_u}{Q_c + Q_u}\right) + Q_{ci} K_{ti} + Q_{ce} K_{te} \quad \text{Equation (28)}$$

Q_d = Distributing flow at the entry (pcu/h)

Q_u = Exiting flow (pcu/h)

$$Q_c = Q_{ci} + Q_{ce} = \text{circulating flow in front of the entry (pcu/h)} \quad \text{Equation (29)}$$

Q_{ci} = Traffic volume in the inner circulating lane (close to the central island) (pcu/h)

Q_{ce} = Traffic volume on the outer circle lane (close to the entry and exit lanes) (pcu/h)

$$K_a = \begin{cases} \frac{R_i}{R_i + LA} - \frac{L_i}{L_{imax}} & \text{per } L_i < L_{imax} \\ 0 & \text{in the other Cases} \end{cases} \quad \text{Equation (30)}$$

R_i = Central island radius (m)

LA = Circle width (m)

L_i = Splitter island width (m)

$$L_{\text{imax}} = 4.55 \sqrt{R_i + LA/2} \quad \text{Equation (31)}$$

$$K_{\text{ti}} = \min \left\{ \frac{160}{LA(R_i + LA)}, 1 \right\} \quad \text{Equation (32)}$$

$$K_{\text{te}} = \min \left\{ \frac{(R_i / (R_i + LA))^2 (1 - \frac{LA-8}{LA})}{1}, 1 \right\} \quad \text{Equation (33)}$$

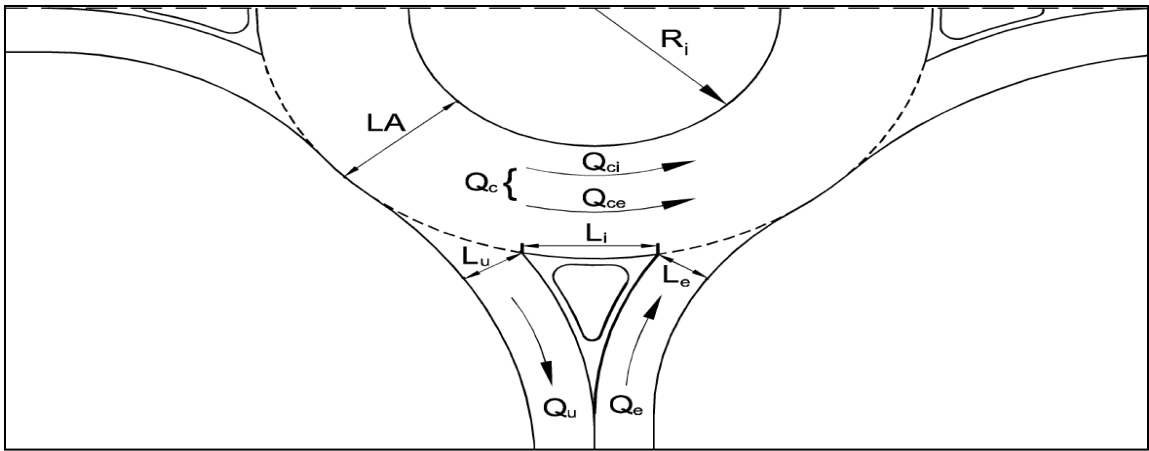


Figure 19: French model traffic volume and geometric parameters (Mauro, 2010)

Table 10: Geometric element range for French model (Mauro 2010)

Parameter	Description	Range Values
L_e	Entry lane width	3-11 m
L_i	Splitter island width	0-70 m
L_u	Exit lane width	3.5-10.5 m
LA	Circle lane width	4.5-17.5 m
R_i	Central island radius	3.5-87.5 m

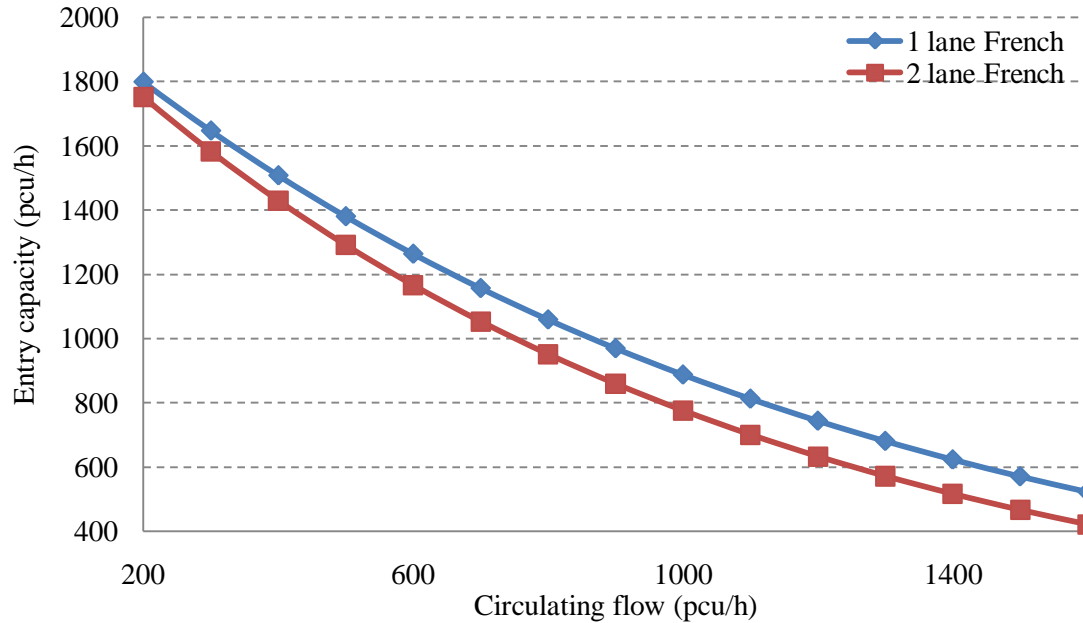


Figure 20: Entry capacity using French model (Equation 26)

Note:

- 1- In one lane roundabout the geometric parameters are:
 $L_e = 4.5\text{m}$, $L_i = 3\text{ m}$, $L_u = 4.5\text{m}$, $LA = 7\text{m}$, $R_i = 10\text{m}$.
- 2- In two lane roundabout the geometric parameters are:
 $L_e = 8\text{m}$, $L_i = 7\text{ m}$, $L_u = 8\text{m}$, $LA = 8\text{m}$, $R_i = 20\text{m}$.
- 3- The approaching vehicles from each leg assumed to distribute equally to the other three legs.

2.4 Comparison of theoretical (gap acceptance) and empirical models

All of the international models described in the previous sections have been calibrated to U.S. entry capacity data collected from the NCHRP Report 572 (Rodegerdts et al., 2007) and compared on the basis of the RMSE (Root Mean Squared Error) value. The findings from this analysis concluded (Rodegerdts et al., 2007), that model which most accurately estimates entry leg capacity for one-lane and two-lane roundabouts in the U.S. is the HCM 2000 model (Equations 3 and 4).

2.5 International pedestrian reduction factor models

The effect of pedestrians on traffic flow always appears in urban areas where pedestrians have the right-of-way over entering vehicles to cross over zebra lines (Robinson et al., 2000).

Based on Mauro (2010) there are three methods to estimate capacity reduction factors caused by pedestrians. These methods are the English method (Marlow and Maycock, 1982), the French method (Loua, 1992), and the German method (Brilon et al., 1993). Both the English and the French methods are based on queuing theory. The German method is based on data collected from roundabouts. Each method employs its entry capacity formula developed in their respective country. For all the methods, an increase in pedestrian volume and conflicting volume lead to an increase in the capacity reduction factor. For all three methods the resultant entry capacity, including the impact of pedestrians, is equal to the product of the entry capacity when there is no pedestrian volume (only conflicting circulating vehicles) multiplied by the pedestrian capacity reduction factor as shown in equation (34).

$$C_{ped} = R * C \quad \text{Equation (34)}$$

C_{ped} = Vehicle entry capacity considering impact of pedestrians (pcu/h)

R = Pedestrian capacity reduction factor

C = Vehicle entry capacity (no pedestrians crossing only vehicles) (pcu/h)

2.5.1 English method (Marlow and Maycock, 1982)

The English method is based on queuing theory, and its pedestrian reduction factor M is based on the entry capacity with vehicles only, the entry capacity with pedestrians (when there are no conflicting vehicles), and the number of vehicles between the yield line and the pedestrian cross walk.

The entry capacity of a roundabout based on pedestrian volume only (where there is no conflicting volume) is as follows:

$$Cap = \frac{Q_{ped}}{Q_{ped} \beta + (e^{Q_{ped} \alpha} - 1) (1 - e^{-Q_{ped} \beta})} 3600 \quad \text{Equation (35)}$$

Cap = Roundabout entry capacity with pedestrian volume only (no vehicles) (veh/h)

Q_{ped} = Pedestrians flow (ped/s)

$$\beta = 1/C0 (s) \quad \text{Equation (36)}$$

$C0$ = Entry capacity when there is no pedestrians nor conflicting volume based on Equation 13, and 15 (veh/s)

- α = B/v_{ped} : Pedestrian crossing time (s)
 B = The crosswalk width (m)
 v_{ped} = The pedestrian speed (m/s)
 R = The ratio of entry capacity with pedestrians only (no conflicting volume) over the entry capacity without pedestrians (with conflicting volume only)

$$M = \frac{R^{n+2} - R}{R^{n+2} - 1} \quad \text{Equation (37)}$$

$$R = \frac{Cap}{C} \quad \text{Equation (38)}$$

- n = The number of vehicles from the yield line to the pedestrian zebra crosswalk

Assuming the pedestrian cross walk width is 3.5 m for a single lane roundabout, and 7.5 m for a double lane roundabout, then M can be estimated from Equation 37. Figure 21 shows the pedestrian capacity reduction factor M (using Equation 37) as a function of the circulating traffic volume and the pedestrian volume. These results suggest that when circulating volume is low (and therefore capacity of the entry leg when no pedestrian flow exists is high) the influence of pedestrians, in terms of reducing capacity is most significant. When circulating volume increases, pedestrian flows have an increasingly smaller impact in terms of the reduction in capacity.

The computation of M is impacted by both the capacity estimated when only the pedestrian stream is considered (i.e. Equation 35) and the capacity when pedestrians are ignored. This is illustrated in Figure 22 which shows the value of M for two different cases: (1) using the English model to estimate the entry leg capacity when ignoring pedestrians (i.e. Equation 15); and (2) using the German model to estimate the entry leg capacity ignoring pedestrians (i.e. Equation 13).

The capacity reduction factor with different pedestrian volumes for one and two lane roundabouts is shown in Appendix B.

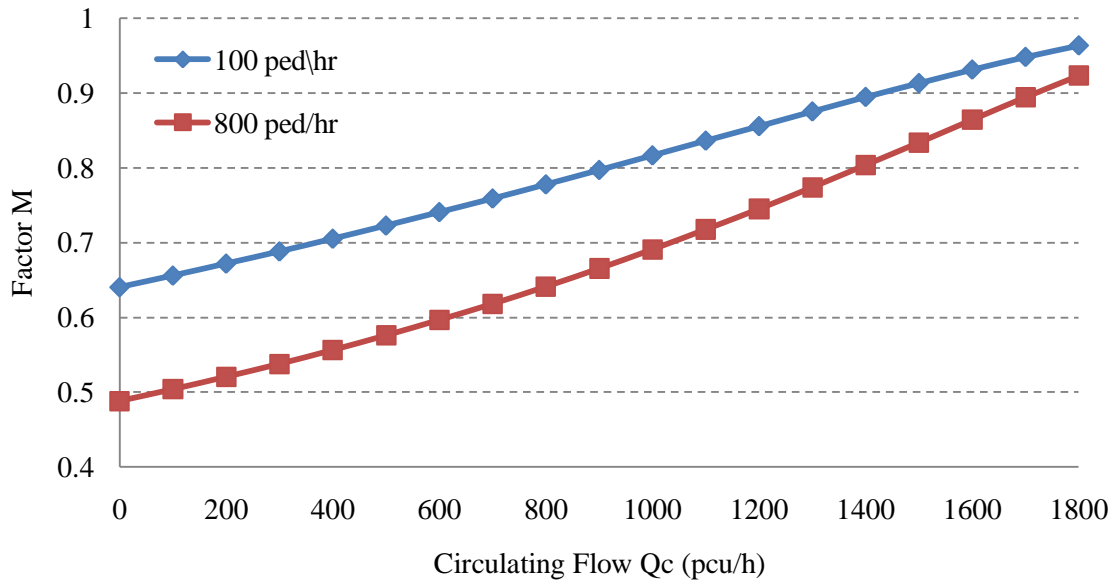


Figure 21: The impact of pedestrians on entry capacity for different pedestrian volume

Notes:

1. Entry capacity calculated using the Kimber model (Equation 15). The geometric parameter values for a single lane roundabout using the Kimber method are as follows:
 $D = 34 \text{ m}$; $u = 7 \text{ m}$; $e = 4 \text{ m}$; $v = 3 \text{ m}$; $l' = 7.5 \text{ m}$; $\theta = 35^\circ$; $r = 20.8 \text{ m}$ (Mauro, 2010)
2. The English capacity reduction factor model is used (Equation 37).

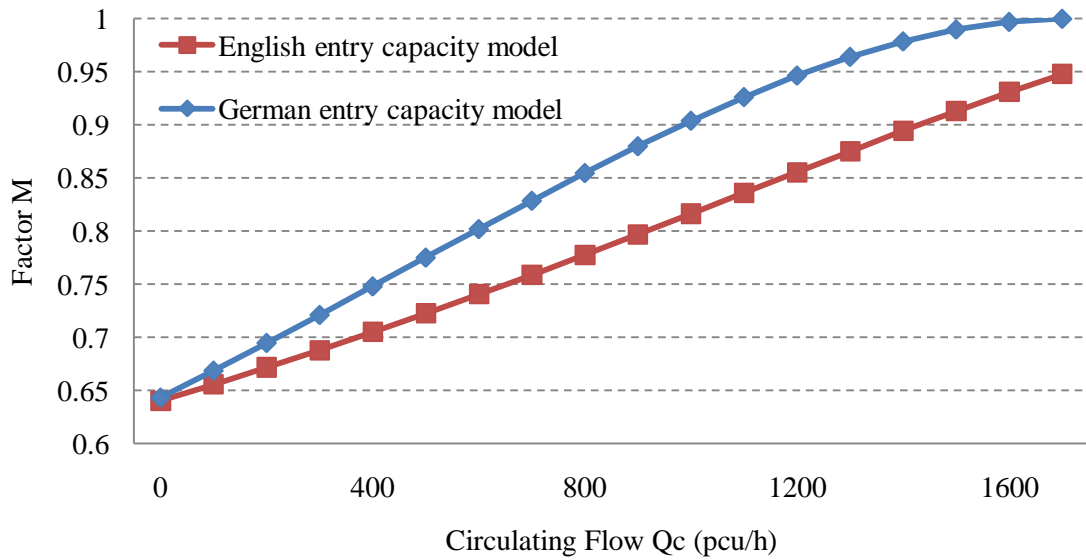


Figure 22: The impact of pedestrians on entry capacity for different entry capacity models

Note:

- 1- Pedestrian volume used 100 (ped/h) only.
- 2- Entry capacity calculated using the Kimber model (Equation 15). The geometric parameter values for a single lane roundabout using the Kimber method are as follows: $D = 34$ m; $u = 7$ m; $e = 4$ m; $v = 3$ m; $l' = 7.5$ m; $\theta = 35^\circ$; $r = 20.8$ m (Mauro, 2010).
- 3- Entry capacity calculated using German model (Equation 13). The parameter values for a single lane roundabout using the German model are as follows:
 $T = 4.1$ s, $T_0 = 2.9$ s, and $\Delta = 2.1$ s (Mauro, 2010).
- 4- The English capacity reduction factor model is used (Equation 37).

2.5.2 French method (Loua, 1992)

Similar to the English method the French method provides a roundabout entry capacity without pedestrians (Equation 26) and the reduction factor F to estimate the capacity of an entry based on pedestrian volume. The F factor is used in the same way (Equation 34) as the M factor from the English model. However, the equation used to compute the F factor (Equation 39) differs from the equation (Equation 37) used to compute the M factor.

$$F = 1 - [e^{(-k Q_d \beta)}] [1 - e^{(-Q_{ped} T)}] \quad \text{Equation (39)}$$

Q_d = Distributing flow at the entry (pcu/s) (Equation 28)

Q_{ped} = Pedestrian flow (ped/s);

$$\beta = \frac{1}{c_0} \text{ (s)} \quad \text{Equation (40)}$$

c_0 = Entry capacity when there is no pedestrians nor conflicting volume (pcu/s)

k = The number of vehicles that can be simultaneously located between the crosswalk and the yielding line

T = Analysis time period (s)

2.5.3 German method (Brilon et al., 1993)

According to Mauro (2010) the German method is based on empirical data but it has a simpler structure than both English and French models as it is based solely on pedestrian volume and conflicting volume. For both single and double lane roundabouts, M decreases with increases in the conflicting volume and/or in the pedestrian volume. This method is recommended by the FHWA for use in the U.S.

For single lane entry the reduction factor M is:

$$M = \frac{1119.5 - 0.715 Q_c - 0.644 Q_{ped} + 0.00073 Q_c Q_{ped}}{1069 - 0.65 Q_c} \quad \text{Equation (41)}$$

For double lane entry the reduction factor M is:

$$M = \frac{1260.6 - 0.381 Q_{ped} - 0.329 Q_c}{1380 - 0.50 Q_c} \quad \text{Equation (42)}$$

Q_c = Conflicting flow (pcu/h)

Q_{ped} = Pedestrian flow (ped/h)

Figure 23 illustrates the pedestrian reduction factor estimates from the English, French, and German models as a function of the circulating traffic flow.

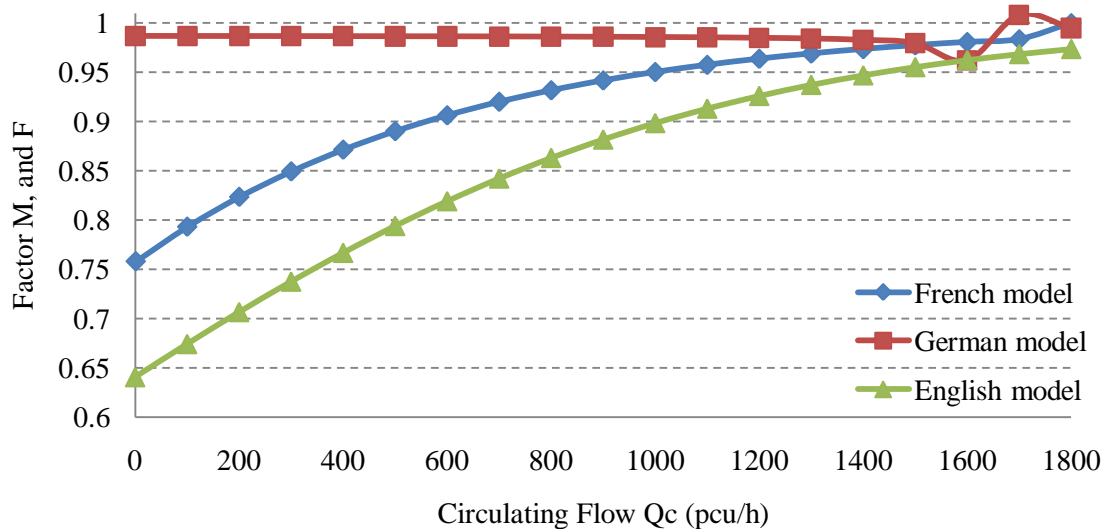


Figure 23: Comparing the capacity reduction factor for different methods

Notes:

- 1- Pedestrian volume is 100 (ped/h) only.
- 2- The entry capacity model used is Kimber method for one lane entry roundabout with the following geometry. $D = 34$ m; $u = 7$ m; $e = 4$ m; $v = 3$ m; $l' = 7.5$ m; $\theta = 35^\circ$; $r = 20.8$ m (Mauro, 2010).
- 3- German method does not use any entry capacity method in estimating the capacity reduction factor. It is based only on the conflicting volume and pedestrian volume.
- 4- The approach volume from each approach assumed to distribute equally to the other three legs in the French method. The parameters values used in the French model are as follows: $T=10$ s, $k=2$, $L_i = 7$ m, $LA= 7$ m, $L_e=4$ m, $T_f =2.05$ s, $CB= 3.525$ (Mauro, 2010).

The following observations can be made on the basis of the models reviewed in this section:

- 1- Each one of the three models for estimating the impact of pedestrians on entry leg capacity has been calibrated using data from the country in which the model was developed.
- 2- The French and English models require the use of other models to estimate the capacity of the entry leg in the absence of pedestrians.
- 3- The models provide very different estimates of the impact of pedestrians (Figure 23).
- 4- There is no a specific model to estimates of the impact of pedestrians for Canada and the U.S. which has been calibrated using Canadian and/or American data. However, the German model has been recommended for use in the U.S. (Rodegerdts, 2004).
- 5- A previous study (Rodegerdts et al., 2007) calibrated different analytical roundabout capacity estimation models to field data collected from roundabouts in the U.S. and then compared the model prediction accuracy on the basis of the RMSE. The study recommended that the HCM 2000 model be used for estimating entry leg capacity for one and two lane roundabouts in the U.S.

2.6 Simulation models

Micro- and macro-simulation software programs use different models to simulate traffic conditions in the real world. The micro-simulation packages simulate each vehicle separately. On the other hand, macro-simulation software simulates a group of vehicles together. VISSIM, PARAMICS, and AIMSUN are examples of micro-simulation software. SIDRA, RODEL, and ARCADY are examples of macro-simulation software (Nikolic and Pringle, 2010).

SIDRA is macroscopic analytical software that depends on the gap acceptance theory (Bared and Edara, 2005). RODEL and ARCADY are macroscopic empirical software programs that depend on the geometry of the roundabout and which were developed in the United Kingdom (Weber, 2010). VISSIM, PARAMICS, AIMSUN are theoretical models (microscopic simulation models) (Weber, 2010).

Recently, the Ontario Ministry of Transportation made a study to find the best model that can estimate average vehicle delay in roundabouts based on Canadian and U.S. data (Nikolic and Pringle, 2010). The presentation of the study did not include full details regarding the research, such as, the coding parameters or the Origin Destination vehicles' trips (OD pairs). However, the results concluded that all micro-simulation models performed better than the other methods. Furthermore, VISSIM and AIMSUN which provides approximately the same accuracy, performed better than PARAMICS (Figure 24). On this basis, VISSIM is selected as the micro simulation tool for modeling roundabouts within this research described in this thesis.

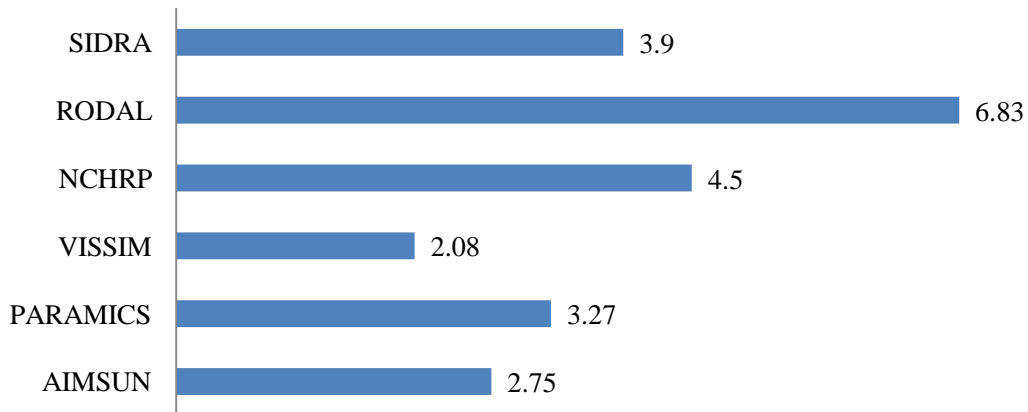


Figure 24: The RMSE values for different models based on observed and estimated entry leg delay based on the data collected by Nikolic and Pringle (2010)

Based on Trueblood and Dale, (2003), and VISSIM 5.2 User Manual (2009) VISSIM is a micro-simulation software program produced by PTV America, Inc. that is used to simulate and analyze traffic systems. Most importantly for this research is that VISSIM can model and simulate both vehicles and pedestrians within a roundabout. Unlike many other simulation models, VISSIM uses links and connectors instead of links and nodes. These links and connectors can be defined with deflection points so that the links and connectors can be curved (Figure 25).

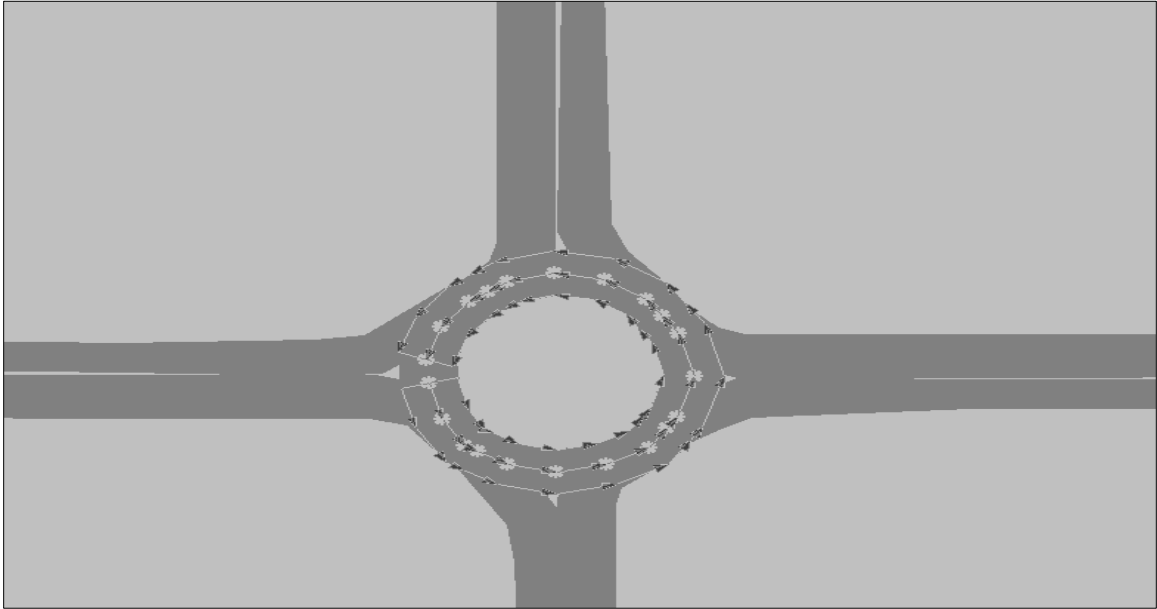


Figure 25: Deflection point in the circulatory road way as shown in VISSIM micro-simulation

VISSIM has many other features that make it one of the best models used to model the behavior of vehicles and pedestrians at roundabouts. In particular, VISSIM models the interaction between vehicles in both lateral and longitudinal positions. In addition, it uses “conflict areas” to represent gap seeking behavior in which one traffic (or pedestrian) stream must yield priority and seek gaps in one or more other traffic and/or pedestrian streams. Moreover, vehicle/driver attributes (such as vehicle dimensions, maximum acceleration/deceleration, maximum desired speed, etc.) are assigned from user-specified distributions.

2.7 Other relevant research

There are three studies reported in the literature that have some similarities to the work carried out in this thesis. These studies are:

1. Analytical Analysis of Pedestrian Effects on Roundabout Exit Capacity.
2. Effects of pedestrian crossing on roundabout capacity.
3. Simulation of Pedestrians Crossing a Street.

Each of these studies is described in more detail in the following sections.

2.7.1 Analytical Analysis of Pedestrian Effects on Roundabout Exit Capacity (Rodegerdts and Blackwelder, 2005)

The motivation for this study was the operational performance of a particular roundabout in Poway, CA. The two-lane roundabout was expected to operate near capacity and to have unusual pedestrian flows (equestrians instead of pedestrians) crossing a leg which was also expected to experience large exit volumes. A concern was raised regarding the likelihood of queues forming on the outbound leg of the roundabout as a result of vehicles having to wait for pedestrians (equestrians) crossing at the zebra line.

The study considered two boundary conditions: (1) pedestrians yield to the vehicle stream and therefore have no impact on the roundabout operations; and (2) vehicles yield to the pedestrian stream.

Given that the roundabout was located in a rural area, the study authors assumed that the true operations of the roundabout would lie somewhere between these two boundaries, even though by law vehicles are required to yield to the pedestrians.

The study estimated the fraction of pedestrians who would chose to yield to vehicles as a function of the number of suitable time headways in the conflicting traffic stream. The portion of the pedestrian flow that yielded to vehicles had no impact on vehicle operations and therefore could be ignored.

For the portion of the pedestrian flow that did not yield to pedestrians, a method was developed to estimate the impact on vehicle operations. The method assumed that whenever pedestrians were in the crosswalk, vehicles were required to stop and a queue would form. If the queue spilled back into the circulating roadway, then the queue is assumed to block all entries to the circulating roadway at all entry legs.

The methods proposed in this study have several limitations:

1. The method does not consider the length of the queue in the circulating roadway. Rather the method makes the assumption that all entry leg capacities become zero as soon as a queue spills back into the circulating roadway. This assumption is overly restrictive.

2. The consequence of the assumption identified in the previous point is that the capacity of an entry leg becomes zero even when all vehicles entering at that entry leg exit the roundabout before encountering the tail of the queue in the circulating roadway. This result is clearly not valid.
3. The study examined conditions in a rural area in which a relatively high proportion of pedestrians may be expected to yield to vehicles. However, in many urban areas, with higher pedestrian flows and lower vehicle speeds, it may be expected that a low proportion of pedestrians will yield to vehicles. Furthermore, in many jurisdictions (including the Region of Waterloo), road designers are encouraging pedestrians to assume the right of way and are educating drivers to yield right of way. Consequently, roundabouts should be designed and evaluated under the expectation that (over time) the proportion of pedestrians yielding to vehicles will be very small.

2.7.2 Simulation of Pedestrians Crossing a Street (Boenisch and Kretz, 2010)

This study examined ways of modeling pedestrian and vehicle interactions within the VISSIM simulation model. In particular, they examined the use of “conflict areas” within the VISSIM model. They simulated a two-way street with pedestrians crossing (no zebra line) the street mid-block. Vehicles are assumed to have right of way over the pedestrians. The authors used the “conflict area” feature in VISSIM with the default values, to model this interaction and specified that vehicles had the right of way. However, the study concluded that even when pedestrians must yield right of way to vehicles, and therefore it can be expected that pedestrians have no impact on vehicle delays, the model results indicated that vehicles did experience delays caused by pedestrians. The study observed that sometimes pedestrians accept time headways that are insufficiently long to enable them to cross the street without causing arriving vehicles to slow down and sometimes even stop. The study also observed that there appears to be insufficient pedestrians’ data for calibrating pedestrian behavior at uncontrolled crossings.

The lack of data on which to calibrate pedestrian behaviour (particularly with respect to whether or not they chose to yield to vehicles) is not an issue because in this thesis the assumption is made that pedestrians have right of way and cross at a zebra crossing. Consequently, for these conditions, we expect vehicles to yield to pedestrians.

2.7.3 Effects of pedestrian crossing on roundabout capacity (Duran, 2010)

This study used the micro simulation model VISSIM to study the impact of pedestrian volume and the cross walk location (i.e. distance from the circulating roadway) on the roundabout entry capacity (i.e. pedestrian capacity reduction factor). The VISSIM model was calibrated to travel time data from NCHRP project 3-65 for a two lane roundabout. Four different pedestrian volumes and cross walk locations were examined. The traffic volume and distribution is used from the NCHRP project 3-65 DVD video data during the morning and the afternoon peak hours. The research did not consider the warm-up period in the simulation runs but the simulation was run for 3600 seconds with 10 different random seeds. The roundabout geometry in VISSIM was coded using Google Earth pictures. The conflict area feature from VISSIM was used in the merge area of the two traffic streams. The conflict feature requires the specification of three parameters, namely Front Gap, Rear Gap, and Safety Distance Factor. The authors calibrated these parameters using the field data from the NCHRP project and found the best values to be: Front Gap = 1.5 s; Rear Gap = 0.6 s; and Safety Distance Factor = 0.9.

The results of the study showed that the entry capacity estimated from the HCM 2010 model closely matched those estimated by the VISSIM model. These findings confirmed the validity of using VISSIM to model roundabout operations. However, the study did not develop an analytical model for estimating the delays to vehicles traversing the roundabout as a function of pedestrians' flows.

Chapter 3 Methodology

3.1 Introduction

This chapter aims to (1) highlight the limitations of the analytical models described in the previous chapter with respect to estimating vehicle delay based on pedestrians volume; and (2) propose an analytical model that takes into consideration these shortcomings.

As mentioned earlier, modern roundabouts are unsignalized intersections that give right-of-way to pedestrians over vehicles. Therefore vehicles entering or exiting the roundabout are required to look for suitable gaps between the crossings pedestrians. Consequently, it is possible to identify four sources of delay that vehicles may experience as a result of pedestrians crossing the approach leg. The analytical models that estimate vehicle entry capacity considering pedestrian flows (i.e. Equation 37, 39, 41, and 42) consider only one of these sources. This chapter aims to develop a model that estimates all delay sources.

The four delay sources caused by pedestrians are (Figure 26):

Source 1: Entering vehicles yield to pedestrians and vehicles in the entry leg.

Source 2: Exiting vehicles yield to pedestrians in the exit lane.

Source 3: The queue in the exit lane spills back into the circulating roadway causing delays to vehicles in the circulating roadway.

Source 4: The queue in the circulating roadway spills back to upstream entry legs and blocks vehicles on the entry legs from entering the circulating roadway.

Based on the literature review there is a lack of field data that covers a sufficiently large range of vehicle and pedestrian volumes and that captures all vehicle delays (not only those experienced on the entry leg). Consequently, it is not possible to establish an empirical model. In Chapter 2 it was shown that the VISSIM simulation model has been demonstrated to generate a realistic estimate of vehicle delay and considered one of the best models for simulating roundabouts. As a result, within this research, roundabout performance data (including vehicle delays) are generated using the VISSIM micro-simulation software.

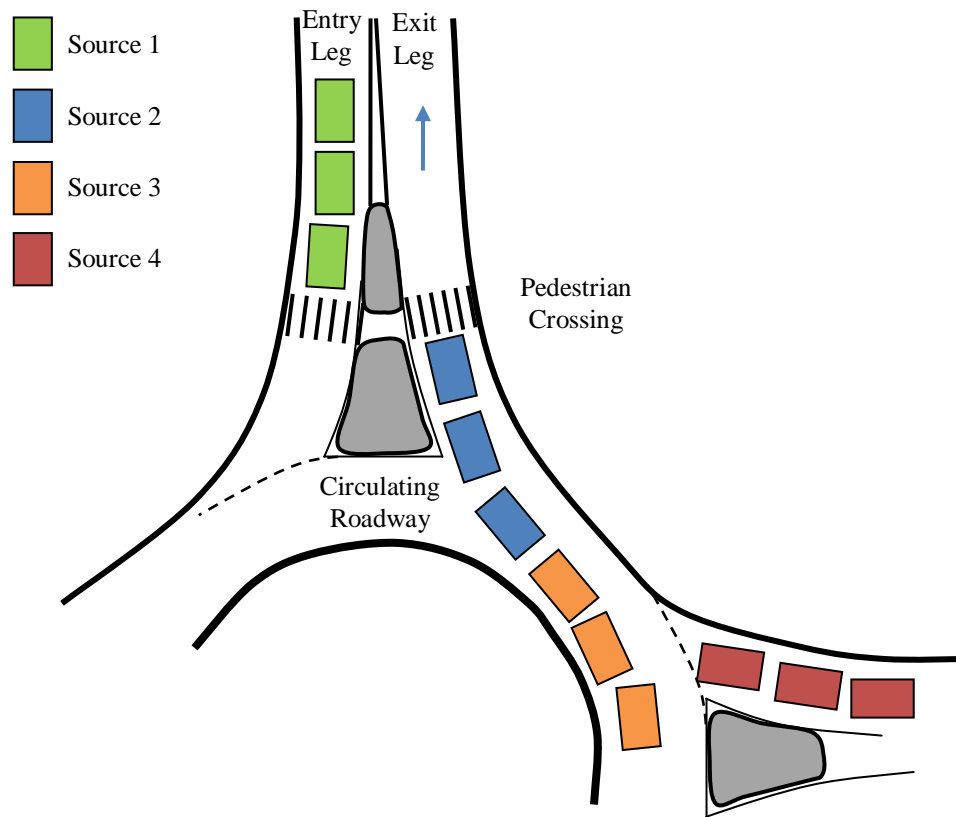


Figure 26: Sources of delay caused by conflicts with pedestrian streams

3.2 Coding VISSIM

One advantage to using a simulation model instead of collecting field data is the ease with which measures of performance can be extracted from the model. In the context of this research, it is necessary to obtain delays for each vehicle as it traverses the roundabout. A single lane roundabout was simulated for a range of vehicle and pedestrians volumes. Average vehicle delay for each O-D pair was captured on the basis of simulation results from each simulation run. Three two-lane roundabouts are coded in VISSIM that have the same geometries as three different sites in the Region of Waterloo. These field sites are used for validating the model results.

This section describes the roundabout scenarios simulated; the values selected for key VISSIM parameters; and the results of several validation case studies. The results obtained from simulating the roundabout and the analysis of their results are provided in Chapter 4.

3.3 Definition of roundabout geometry

Within the context of this study, roundabouts are assumed to have 4 approach legs. Single lane roundabouts are assumed to have a single entry lane and a single exit lane on each approach leg and a single lane on the circulating roadway. Two-lane roundabouts are assumed to have two entry lanes and two exit lanes on each approach leg and two lanes on the circulating roadway. The geometric parameters associated with one lane and two lane roundabouts are provided in Table 11. These values fall within Canadian design recommendation and the as built conditions of the three field sites discussed within this thesis.

Roundabout having the geometric characteristics defined in Table 11 were coded in VISSIM. The one-lane roundabout was used to calibrate and validate the proposed analytical model described later in this chapter. The two-lane roundabout was used to compare the VISSIM results with field data.

Table 11: The geometry of one-lane and two-lane roundabout

The inscribed diameter case	One lane	Two lane
Inscribed diameter (m)	34	55
Entry radius (m)	20	23
Exit radius (m)	20	23
Entry width per lane (m)	4.5	3.5
Approach width per lane (m)	4	3.5
Departure width per lane (m)	4	3.5
Exit width per lane (m)	4.5	3.5
Circulatory road width per lane (m)	6	3.5

Note:

Figure 3 shows the roundabout characteristics identified in the table above.

3.4 VISSIM modelling coding and assumptions

A detailed description of the coding of the VISSIM model is presented in Appendix C. The significant coding assumptions are described here.

3.4.1 Model inputs

Each approach leg to the roundabout was assumed to be 2500 m long so that any excessive queuing could be observed. All vehicle flows on the entry legs were distributed equally to the other three exits. Pedestrian flow was assumed to cross only a single entry/exit leg. This assumption was made to isolate the impact of pedestrian flows on delays to vehicles entering the roundabout and delays to vehicles exiting the roundabout. Pedestrians were assumed to have right of way and vehicles on the entry and exit leg were required to yield right of way. Vehicles yield to pedestrians only when the pedestrian was occupying the pedestrian crossing on the vehicle leg. For example, a vehicle using the entry leg will yield to pedestrians on the entry leg pedestrian crossing but will not yield to the pedestrians in the exit leg crossing, regardless of which direction the pedestrian is walking. Pedestrian walking speed is stochastic with a mean of 5km/h; a minimum of 4 km/h; and a maximum of 6 km/h.

The right-of-way is for vehicles circulating in the roundabout. The approach vehicle yields to the circulating vehicles.

1. In a two-lane roundabout, the approach vehicle in the left hand lane must yield to vehicles in both lanes in the circulating roadway.
2. In a two-lane roundabout, the approach vehicle in the right hand lane yields only to the vehicles in the outer lane of the circulating roadway.
3. In a one-lane roundabout, entering vehicles must yield to all conflicting vehicles.

The conflict area feature in VISSIM is used to simulate the right-of-way. It affects vehicle behavior by way of three parameters (i.e. front gap, rear gap, and safety distance). Front gap is the time that the yielding vehicle requires to enter the roundabout. The time starts when the yielding vehicle begins to enter the roundabout and after the circulating vehicle passes the entry approach and ends after the yielding vehicle enters the roundabout.

Rear gap is the time in seconds from the time when the vehicle on the yielding approach passes the conflict area to the time when the vehicle on the circulating roadway has just entered the conflict area on the circulating roadway. Safety distance is a factor used for the merging approaches like the entrance to the roundabout and the circulating road. It is a factor multiplied by the safety distance of the vehicle on the circulating roadway to estimate the minimum headway required by the yielding vehicle to enter the major road. The roundabout entry capacity decreases when the three parameters (front gap, rear gap, and safety distance) increase.

For cars and heavy good vehicles (HGVs), the desired speed is 50 km/h; minimum entrance speed is 48 km/h; maximum entrance speed is 58 km/h. The speed limit of vehicles on the circulating roadway is 35 km/h. Vehicles are assumed to begin decelerating as they approach roundabout a minimum of 30 m from the yield line.

3.4.2 Model output is recorded

Delay is measured for each vehicle within the simulation. The time is recorded when a vehicle passes the upstream data collection point. The time is also recorded when the vehicle passes the downstream recording point. The difference between the recorded times is the vehicle travel time. Delay is calculated as the travel time minus the time to travel at free speed.

The upstream data collection point was located 1500 m upstream of the yield line on each approach leg. The downstream data collection point was located at the downstream end of the zebra crossing of each exit lane. Delay was compiled for all O-D pairs separately for one lane roundabouts and averaged for all O-D pairs for each approach for two lane roundabouts. This is done to serve the calibration and validation proposes of the analytical model for one lane roundabouts, and to serve the validation propose with field data for two lane roundabouts.

Volume entering the circulating roadway was measured for all entry legs by placing a vehicle counter at the yield line on each entry lane on each leg. The traffic stream was assumed to consist of 2% heavy vehicles and 98% cars. In all simulation runs, output was selected for analysis after a suitable warm-up period had elapsed. This warm-up period is necessary because when the simulation begins, the network is empty of vehicles and performance measures extracted during this time are not indicative of the loaded network.

For all simulation runs, a warm-up period of 1800 seconds was used. The simulation was run for 5400 seconds so data were obtained over a 1 hour period.

3.5 Experimental Design

The goal of the research is to estimate the average vehicle delay on the basis of each O-D pair as a function of approach vehicle volume and pedestrian volume.

For one lane roundabout a full factorial experimental design was constructed with these factors. The full factorial design implies $8 \times 4 = 32$ scenarios. For two lanes roundabout 3 scenarios of experimental design were constructed. Each scenario was replicated 10 times, each time with a different random number seed. Outputs (i.e. Average vehicle delay) were averaged over the 10 replications and stored in a data base.

The one lane roundabout factors are as follows:

- 1- Roundabout geometry (n=1).
- 2- Entry volume from all approaches (n=4; 100, 200, 300, 400 veh/h).
- 3- Pedestrian volume (n=8; 1, 200, 300, 400, 500, 600, 700, 800 ped/h in total in both directions).

The two lane roundabout vehicle composition and geometry are taken from three sites in the Region of Waterloo (See Appendix D for more details).

3.6 Proposed model:

The proposed method is based on gap acceptance and queuing models for estimating vehicle delay for each source in one lane modern roundabout and is calibrated based on VISSIM results.

The model is constructed to be applicable to each leg of a single lane roundabout. In the context of the model development, it is assumed for simplicity that pedestrians cross at only one leg of the roundabout although the model can be applied when pedestrians cross any number of the approaches.

The approach legs are numbered as follows. Leg 1 is the leg at which pedestrians cross and remaining legs are numbered clockwise around the roundabout (Figure 27).

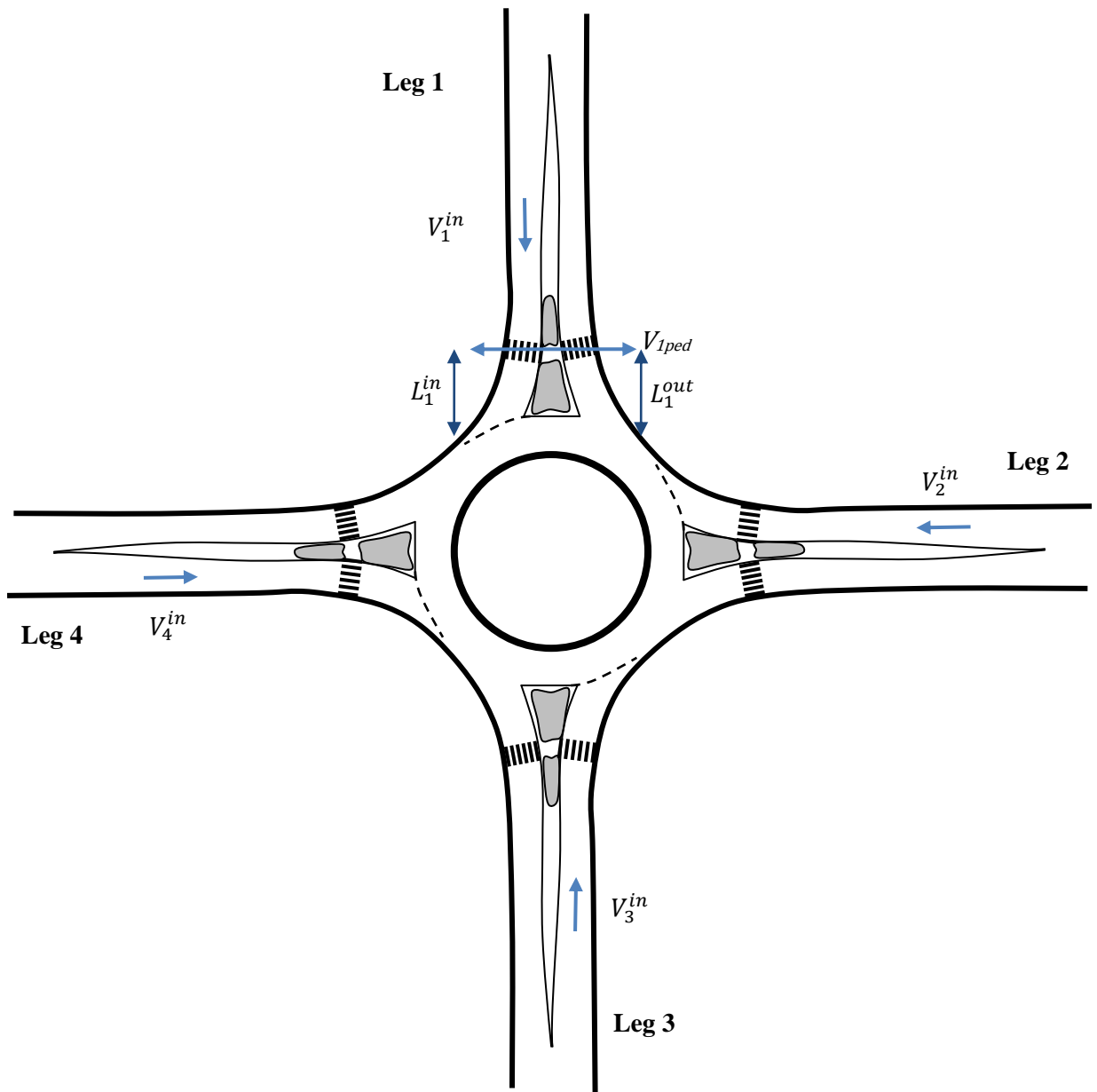


Figure 27: Roundabout configuration used for model

Variables are defined with respect to Figure 28.

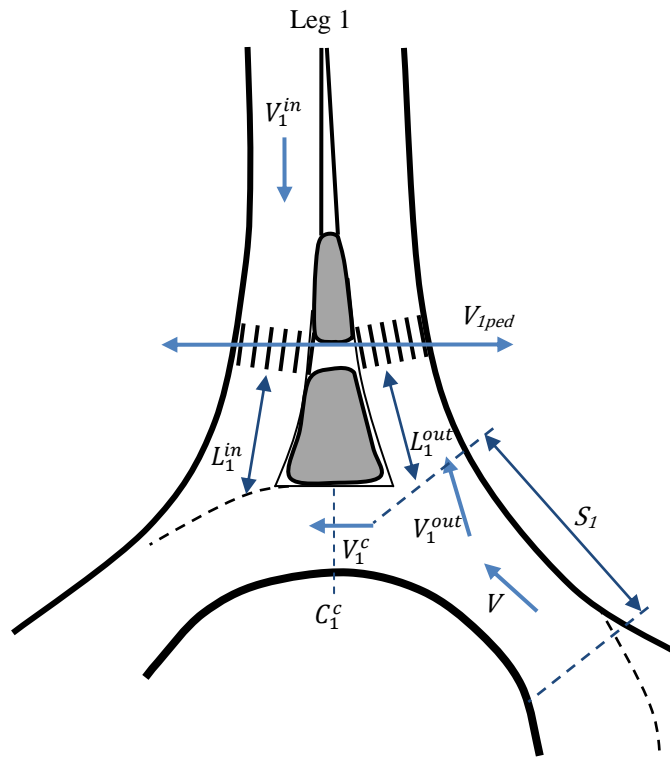


Figure 28: Definition of parameters used in proposed model

- C_2^{base} = Capacity of the entry lane at Leg 2 when no queue exists on the circulating roadway (veh/h)
- C_1^c = Capacity of the circulating roadway between the exit and entry lanes of Leg 1 (veh/h)
- C_2^{in} = Capacity of the entry lane of Leg 2 (veh/h)
- C_2^{in-min} = Capacity of entry lane of Leg 2 when a queue is present within the circulating roadway (veh/h)
- L_1^{in} = Length of the storage area between the pedestrian crossing and the merge (m) on the entry lane.
- L_1^{out} = Length of the storage area between the circulating roadway and the pedestrian crossing (m).
- S_1 = Maximum queue storage between the exit lane at leg 1 and the entry lane at leg 2 (# vehicles)

- t_c = Minimum time headway within the circulating roadway traffic stream required for a vehicle on the entry lane to enter the circulating roadway (s)
- t_f = Minimum time required for the non-first vehicle on the entry lane to make use of a time headway in the circulating roadway traffic stream to enter the roundabout (s)
- t_{cped}^{in} = Minimum time headway within the pedestrian stream required for a vehicle on the entry lane to pass the pedestrian crossing (s)
- t_{cped}^{out} = Minimum time headway within the pedestrian stream required for a vehicle on the exit lane to pass the pedestrian crossing (s)
- t_{fped}^{in} = Minimum time required for the non-first vehicle on the entry lane to make use of time headway in the pedestrian stream to pass the pedestrian crossing (s)
- t_{fped}^{out} = Minimum time required for the non-first vehicle on the exit lane to make use of time headway in the pedestrian stream to pass the pedestrian crossing (s)
- T = Analysis time period (h)
- V_1^c = Demand on circulating roadway between the exit and entry lanes of Leg 1 (veh/h)
- V_1^{out} = Demand on exit lane of Leg 1 (veh/h)
- V_1^{in} = Demand on entry lane of Leg 1 (veh/h)
- V_{1ped} = Pedestrian demand crossing Leg 1 in both directions combined (ped/h)
- V = Demand upstream of exit lane of Leg 1 (veh/h)

3.6.1 Source 1: Delay at entry leg

The method assumes that the pedestrian cross walk is very close to the circulating road ($L_1^{in} = 0$). Consequently, vehicles entering Leg 1 should seek a gap between both vehicle and pedestrians volume at the same time. Based on this assumption the entry capacity formula from the HCM (Equation 2) is modified in three ways:

1. The conflicting volume is composed of both pedestrians crossing the cross walk and vehicles within the circulating roadway;

2. The critical time (t_c) in the numerator in Equation 2 is expanded to two critical gaps values, one related to the time required to enter the circulating roadway (the same as in Equation 2) and the other the critical time require to pass the crosswalk (t_{cped}^{in});
3. In a similar way, the follow up time in the denominator in Equation 2 is expanded to two terms.

The result of these modifications is Equation 43.

$$C_{Source1} = \frac{(V_c^1 + V_{ped1})e^{-(V_c^1 t_c + V_{ped1} t_{cped}^{in})/3600}}{1 - e^{-(V_c^1 t_f + V_{ped1} t_{fped}^{in})/3600}} \quad \text{Equation (43)}$$

The entry vehicle average delay at Leg 1 is estimated using the HCM delay equation (Equation 44) taking into account the entry capacity from Equation 43 and entry volume at Leg 1

$$d_{Source1} = \frac{3600}{C_{Source1}} + 900T \left[\left(\frac{V_1^{in}}{C_{Source1}} - 1 \right) + \sqrt{\left(\frac{V_1^{in}}{C_{Source1}} - 1 \right)^2 + \frac{\left(\frac{3600}{C_{Source1}} \right) \left(\frac{V_1^{in}}{C_{Source1}} \right)}{450T}} \right] \quad \text{Equation (44)}$$

3.6.2 Source 2: Delay at exit lane

Delay at the exit lane is estimated using the HCM entry capacity model (Equation 2) but in this case the conflicting volume is the pedestrian volume only,

$$C_{Source2} = \frac{V_{1ped} e^{(-V_{ped1} t_{cped}^{out})/3600}}{1 - e^{(-V_{ped1} t_{fped}^{out})/3600}} \quad \text{Equation (45)}$$

$$d_{Source2} = \frac{3600}{C_{Source2}} + 900T \left[\left(\frac{V_1^{out}}{C_{Source2}} - 1 \right) + \sqrt{\left(\frac{V_1^{out}}{C_{Source2}} - 1 \right)^2 + \frac{\left(\frac{3600}{C_{Source2}} \right) \left(\frac{V_1^{out}}{C_{Source2}} \right)}{450T}} \right] \quad \text{Equation (46)}$$

3.6.3 Source 3: Delay within circulating roadway due to queue spillback

In order to capture this delay source the vehicle storage area L_1^{out} is assumed to be close to zero. Therefore, the queue starts to form as soon as the exiting vehicle stops to find a gap between the pedestrian volumes in the exit lane (similar to source 2) and the exit capacity is calculated using Equation 45. When the queue spills back into the circulating roadway, the capacity of the circulating roadway is a function of the capacity of the circulating roadway downstream of the queue, the capacity of the exit lane, and the proportions of the flow in the circulating roadway that exit at Leg 1 and that continue past the exit at leg 1 (Figure 29). Thus, we can view the capacity of this section of the circulating roadway as a shared lane. The capacity of the circulating roadway downstream of the diverge at exit 1 is assumed to be a constant (C_1^c). The shared capacity is estimated using Equation 47 (HCM, 2000) and the delay using the shared capacity, and circulating vehicle volume is estimated using Equation 48.

$$C_{shared} = \left[\frac{v_1^{out}/V}{C_1^{out}} + \frac{v_1^c/V}{C_1^c} \right]^{-1} \quad \text{Equation (47)}$$

Delay is estimated using the HCM equation as

$$d_{source3} = \frac{3600}{C_{shared}} + 900T \left[\left(\frac{V}{C_{shared}} - 1 \right) + \sqrt{\left(\frac{V}{C_{shared}} - 1 \right)^2 + \frac{\left(\frac{3600}{C_{shared}} \right) \left(\frac{V}{C_{shared}} \right)}{450T}} \right] \quad \text{Equation (48)}$$

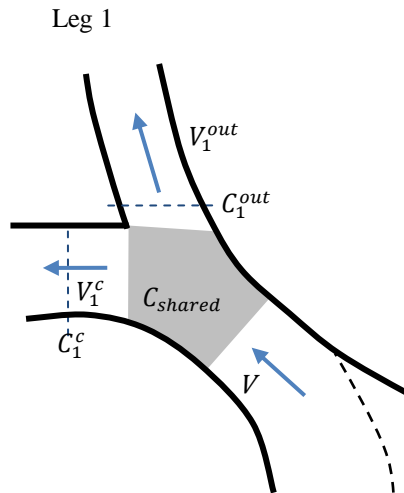


Figure 29: Treating the circulating roadway as a shared lane

3.6.4 Source 4: Delay due to queue spill back into circulating roadway

The last source of delay occurs when queue forms within the circulating roadway and spills back upstream to block the upstream (i.e. Leg 2) entry.

When this occurs, the capacity of the entry leg is expected to decrease to some minimal value.

When the queue does not block the entry leg, then entry capacity of this approach can be estimated using Equation 43 which is re-written below to clarify the appropriate leg indices.

$$C_2^{base} = \frac{(V_c^2 + V_{ped2}) e^{-(V_c^2 t_c + V_{ped2} t_{cped}^{in})/3600}}{1 - e^{-(V_c^2 t_f + V_{ped2} t_{fped}^{in})/3600}} \quad \text{Equation (49)}$$

However, when the entry from Leg 2 is blocked by a queue spilling back from the exit lane at Leg 1, then this source of delay (source 4) is formed. Under these conditions, capacity is estimated using another model (Figure 30).

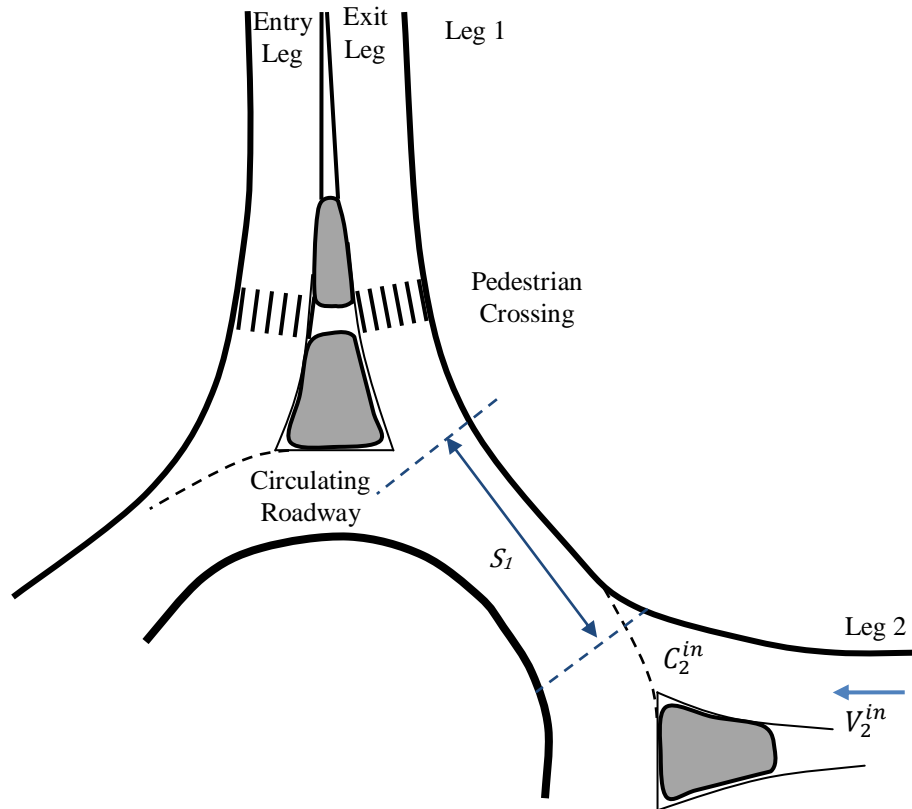


Figure 30: Queue spill back impacting entry capacity of next upstream leg

Assuming an M/M/1 queuing system (i.e. Poisson arrivals, exponential service times, and a single server) the probability that the number of vehicles in the queue exceeds the number of vehicles that can be stored in S_l , can be computed. The estimated probability required two additional assumptions, namely (1) that the queuing system has reached steady state; and (2) that the system is under-saturation (i.e. $V < C_{shared}$). Assuming these two conditions are met, then the probability that more than N vehicles exist in the queue (Mannering, 2008) is calculated using Equation 50.

$$P(n > N) = \left(\frac{V}{C_{shared}} \right)^{N+1} \quad \text{Equation (50)}$$

The entry capacity of Leg 2 is equal to minimal constant value (C_2^{in-min}) if the number of vehicles in the queue (n) in the circulating lane exceeds the number that can be stored S_l . This minimal capacity (which is greater than zero) is used to reflect the behaviour of vehicles on the Leg 2 approach “forcing” their way into the circulating flow. Therefore, the entry capacity for Leg 2 is computed using Equation 51.

$$C_2^{in} = \max \left((1 - P(n > N)) C_{base}^2, C_2^{in-min} \right) \quad \text{Equation (51)}$$

Delay is estimated using the HCM equation

$$d_{Source4} = \frac{3600}{C_2^{in}} + 900T \left[\left(\frac{V_2^{in}}{C_2^{in}} - 1 \right) + \sqrt{\left(\frac{V_2^{in}}{C_2^{in}} - 1 \right)^2 + \frac{\left(\frac{3600}{C_2^{in}} \right) \left(\frac{V_2^{in}}{C_2^{in}} \right)}{450T}} \right] \quad \text{Equation (52)}$$

3.6.5 Proposed Analytical experimental design

Figure 27 illustrates the layout of a single lane roundabout and Table 12 provides the geometric parameters used to simulate a roundabout in VISSIM. The coding method has been discussed in the previous section. The detailed code and specification used in the simulation is provided in Appendix C.

Each OD pair movement has its source of delay as shown in Table 13. Therefore, the delay for each OD pair is the sum of the delay sources experience during the vehicle OD movement (Table 13).

Unlike the analytical model VISSIM delay results are on the basis of OD movements. The way VISSIM was coded means it is not possible to observe delays directly by the individual source. However, the following equations (Equation 53, 54, 55, and 56) can be used to convert delay extracted from VISSIM from the OD delay form to source delay form.

Table 12: Characteristics of single lane roundabout use for case study

Roundabout Characteristic	Value
Inscribed diameter	34m
Entry radius	20m
Exit radius	20m
Entry lane width	4.5 m
Exit lane width	4.5 m
Cross walk width on entry lane	6 m
Cross walk width on exit lane	5.2 m
L_1^{in}	7 m
L_1^{out}	7 m
Circulatory road width	6 m

$$\hat{d}_{Source1} = \frac{1}{3}(\hat{d}_{1-2} + \hat{d}_{1-3} + \hat{d}_{1-4}) \quad \text{Equation (53)}$$

$$\hat{d}_{Source2} = \hat{d}_{3-1} - \hat{d}_{3-4} \quad \text{Equation (54)}$$

$$\hat{d}_{Source3} = \hat{d}_{4-1} - \hat{d}_{Source2} \quad \text{Equation (55)}$$

$$\hat{d}_{Source4} = \max\{0, \hat{d}_{2-1} - \hat{d}_{Source2} - (\hat{d}_{3-4} - \hat{d}_{3-2})\} \quad \text{Equation (56)}$$

Table 13: Sources of delays associated with each O-D pair

O-D Pair	Source
1-2	1
1-3	1
1-4	1
2-1	4+3+2
2-3	4+3
2-4	4+3
3-1	3+2
3-2	---
3-4	3
4-1	3+2
4-2	---
4-3	---

Chapter 4: Results and Data Analysis

This chapter describes the process used to (1) validate VISSIM entry capacity results with field data; (2) validate average vehicle delay from VISSIM with field data; and (3) Calibrate and validate the proposed analytical model.

The Canada and the United States current recommended (Rodegerdts et al., 2007) practice to estimate roundabout entry capacity in the absence of pedestrians is the HCM 2000 roundabout entry capacity model. If pedestrian volume exists, then the FHWA recommends the use of the German pedestrian capacity reduction factor (Equations 41 and 42). Average vehicle delay is estimated using the HCM 2000 delay equation (Equation 5). This research estimates the average vehicle delay for a one-lane roundabout based on the pedestrian and conflicting volumes using the micro-simulation software VISSIM 5.2, HCM 2000 and the proposed model. A comparison is done between these three models.

Prior to using VISSIM to examine the impacts of pedestrians validation was conducted to ensure the model was producing reliable results. This was done by validating the roundabout entry capacity and average vehicle delay from VISSIM to field data results. This is followed by comparison between the pedestrian capacity reduction factor between VISSIM and the international methods. This validation effect is described in the next section.

A presentation of the calibration and validation of the new proposed model is in the next section. The meaning of the results and comparison between VISSIM, proposed models, and existed analytical models are presented and discussed.

4.1 VISSIM validation

The literature review in Chapter 2 indicates that VISSIM has already been compared to other models and field data and found to perform well. Consequently, the validations carried out in this study are limited to:

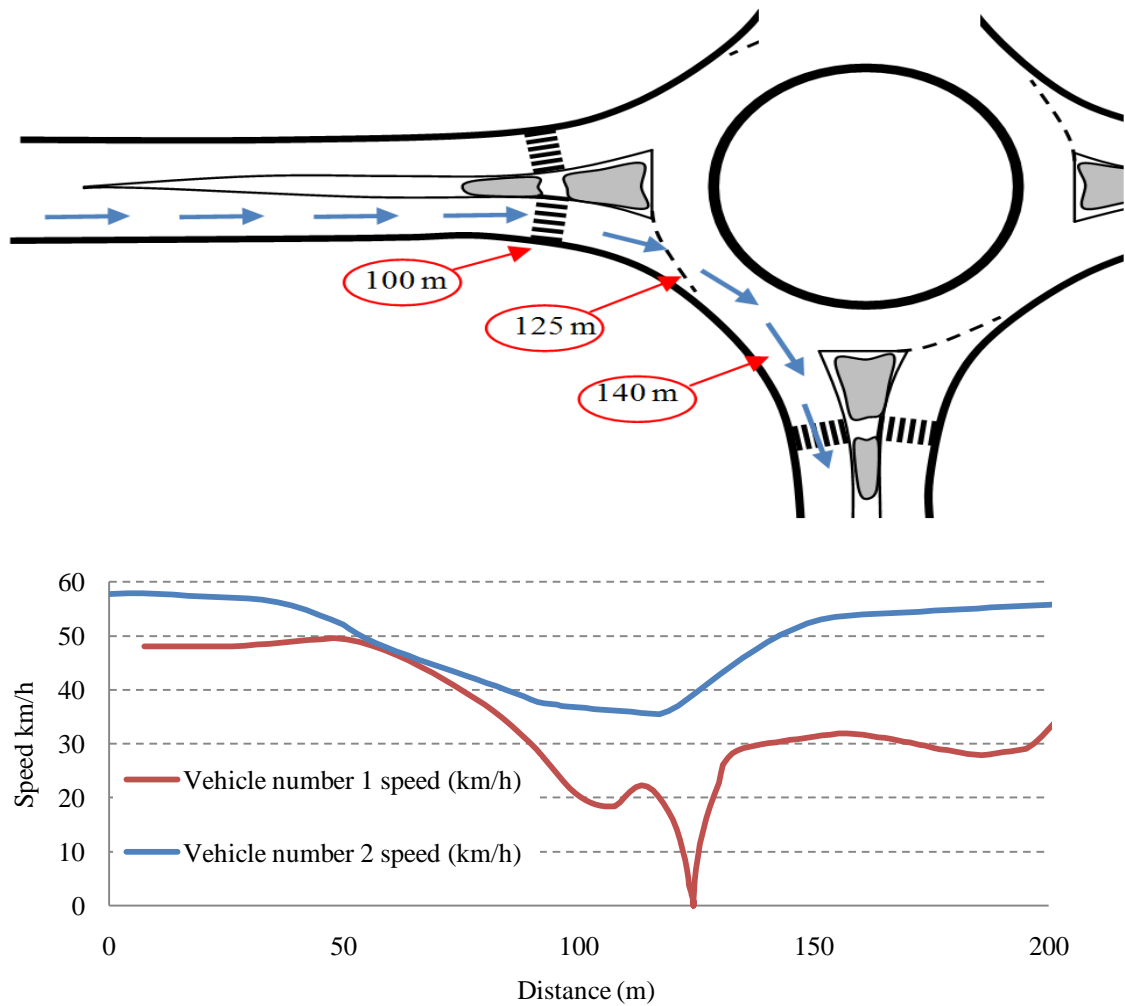
- 1- Examining the credibility of vehicle speed behavior.
- 2- Comparing the average vehicle delay from VISSIM with field data and HCM 2000 model.

3- Comparing entry capacity from VISSIM with field data and HCM 2000 model.

The literature review in Chapter 2 also indicates that there is insufficient field data for pedestrian crossings the roundabout legs to permit the development of empirical models. Furthermore, field data collection efforts in Waterloo Region at three sites failed to provide data with a sufficient number of pedestrian crossings.

4.1.1 Vehicle trajectory in VISSIM

As part of the validation of the VISSIM model, trajectories of individual vehicles were extracted from the simulation. Figure 31 includes the results of one such run.



Distance in (m)	Position of the vehicle description	Feature existed in the code
0	approaching the roundabout	Vehicle drive based on its free speed (50km/h)
80	the speed mark or posted speed	(30km/h)
100	pedestrians crossing	Conflicting area with pedestrians
125	the roundabout entry	Reduction speed in the circulating roadway (30 km/h)
140	the exit of the roundabout	No features available
150	pedestrians crossing line in the exit	No features available
200	the departure lane	No features available

Figure 31: Vehicle trajectory for left movement

The trajectory in Figure 31 shows the vehicle number 1 traveling along the approach at the speed limit of 50 km/h and then reduces speed when approaching the zebra crossing to yield to pedestrians and then coming to a stop to yield to circulating vehicles. Vehicle number 2 travels along the approach at slightly above the speed limit of 50 km/h and then reduces speed to enter and traverse the roundabout. This trajectory was obtained from a vehicle making a right turn movement in a single lane roundabout.

These trajectories show the expected behaviour of the vehicle changing speeds in response to geometric constraints (i.e. reducing speed to enter the circulating roadway due to the roadway curvature) and in response to seeking gaps in pedestrian and vehicle streams.

4.1.2 Vehicle delay from field data, VISSIM and HCM

As part of the validation of the VISSIM model, average vehicle delay were extracted from the simulation and compared to field data collected from three roundabouts in the Region of Waterloo. These roundabouts are: (1) University Ave W at Ira Needles; (2) Erb St. W at Ira Needles; and (3) Sawmill Rd. at Arthur St. S (HW 85).

The data were collected when a queue existed on the selected roundabout approach leg. Data were collected over a period of 120 minutes at University Ave W/ Ira Needles; 60 minutes at Erb St. W/ Ira Needles; and 60 minutes at Sawmill Rd. / Arthur St. S (HW 85). For all three roundabouts, the average vehicle delay was collected for the critical lane as follows:

Data were collected using a video recorder. From the video recording, the vehicle type and time at which the vehicle passed a predetermined location upstream of the queue was recorded. Then the vehicle type and time at which the vehicle entered the roundabout was recorded. The theoretical travel time from the approach location until the vehicle passed the yield line at the roundabout entry when there were no conflicting vehicles and no leading vehicles is the free flow travel time. The free flow travel time is assumed to be the minimum observed travel time when there were no conflicting vehicles and no leading vehicles. The vehicle delay is the difference between the travel time, when the roundabout had vehicles or the entry approach was queued, and the free flow travel time. The average delay for all vehicles is the average vehicle delay. The summary of the collected data is as follows:

Table 14: Data collected from the three roundabouts in the region of Waterloo

Roundabout location	Description of queue length as noticed	Recording period	Number of lanes	Road Condition
University Ave W/ Ira Needles	Low	2 hours (3:00 – 5 PM)	One-lane and flared	Excellent (sunny day and dry road)
Erb St. W/ Ira Needles	Medium	1 hour (2:30 – 3:30 PM)	One-lane and flared	Excellent (cloudy day and a very light snow)
Sawmill Rd. / Arthur St. S (HW 85)	High	1 hour (4:14 – 5:14 PM)	One-lane and flared	Ok (cloudy day and a moderate snow)

Note:

The detailed VISSIM code for this part is available in Appendix C and D.

The Average vehicle delay, maximum queue length and the ratio of average vehicle delay over the maximum queue length is calculated, measured, and generated from the three methods HCM 2000, field data, VISSIM respectively as shown in the following tables.

Table 15: Summary of the average vehicle delay and maximum queue length observed from different sites

Field Site	University	Erb	HWY 85
Average vehicle delay (s/veh)	5.60	10.23	8.45
Maximum queue length (m)	40.37	90.00	154.00
Average vehicle delay (s/veh)/Maximum queue length (m)	0.14	0.11	0.05

Table 16: Summary of the average vehicle delay and maximum queue length from different sites using HCM 2000 model

Site name	University	Erb	HW 85
Average vehicle delay (s/veh)	15.5	9.8	15.7
Maximum queue length (m)	59	23.4	57
Average vehicle delay (s/veh)/Maximum queue length (m)	0.26	0.42	0.27

Table 17: Average vehicle delay and maximum queue length generated from VISSIM code for University Avenue with Ira Needles site

Statistical measures	One flared lane (VISSM)		
	Mean	95% upper limit of the mean	95% lower limit of the mean
Average vehicle delay (s/veh)	5.38	5.75	5.01
Maximum queue length (m)	89.00	89.00	89.00
Average vehicle delay (s/veh)/Maximum queue length (m)	0.06	0.06	0.06

Table 18: Average vehicle delay and maximum queue length generated from VISSIM for Erb Street with Ira Needles site

Statistical measures	One flared lane (VISSM)		
	Mean	95% upper limit of the mean	95% lower limit of the mean
Average vehicle delay (s/veh)	7.88	8.30	7.46
Maximum queue length (m)	59.00	59.00	59.00
Average vehicle delay (s/veh)/Maximum queue length (m)	0.13	0.14	0.13

Table 19: Average vehicle delay and maximum queue length generated from VISSIM for Arthur Street and Sawmill Road site (HWY 85)

Statistical measures	One flared lane (VISSM)		
	Mean	95% upper limit of the mean	95% lower limit of the mean
Average vehicle delay (s/veh)	12.30	12.67	11.93
Maximum queue length (m)	65.00	65.00	65.00
Average vehicle delay (s/veh)/Maximum queue length (m)	0.19	0.19	0.18

Based on the comparison between average vehicle delays (field data collected from the three sites in Waterloo rejoin) with VISSIM and HCM 2000 delay model, VISSIM provides better estimate of vehicle delay than the HCM. VISSIM RMSE compared to field data is 2.6; HCM2000 RMSE value compared to field data is 7.1.

However, it needs to be noted that average vehicle delays from field data are relatively low as the roundabouts are operating between LOS A and B (Figure 32).

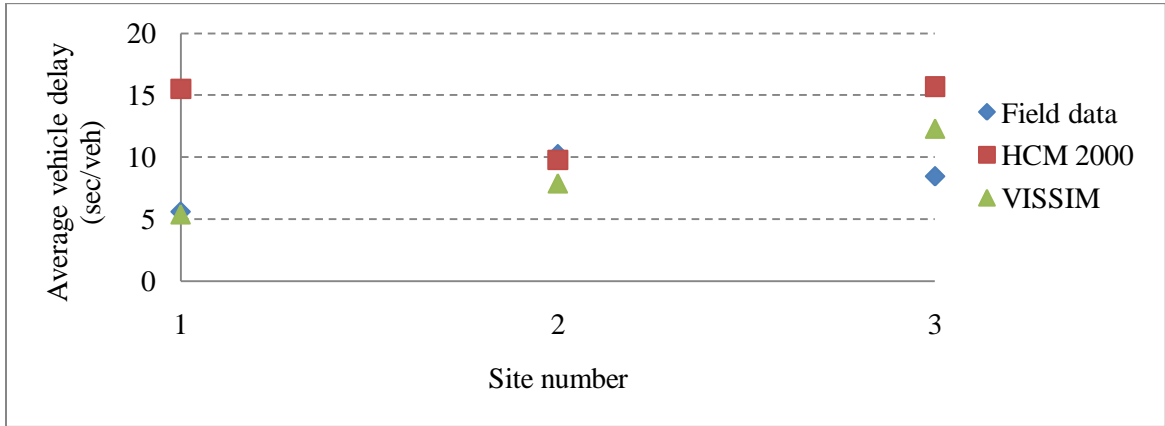


Figure 32: Average vehicle delay from different sites

VISSIM provides better estimates in terms of delay divided by the maximum queue length than does the HCM 2000 model when compared with the field data. VISSIM RMSE compared to field data is 0.09, HCM2000 RMSE value compared to field data is 0.2 (Figure 33).

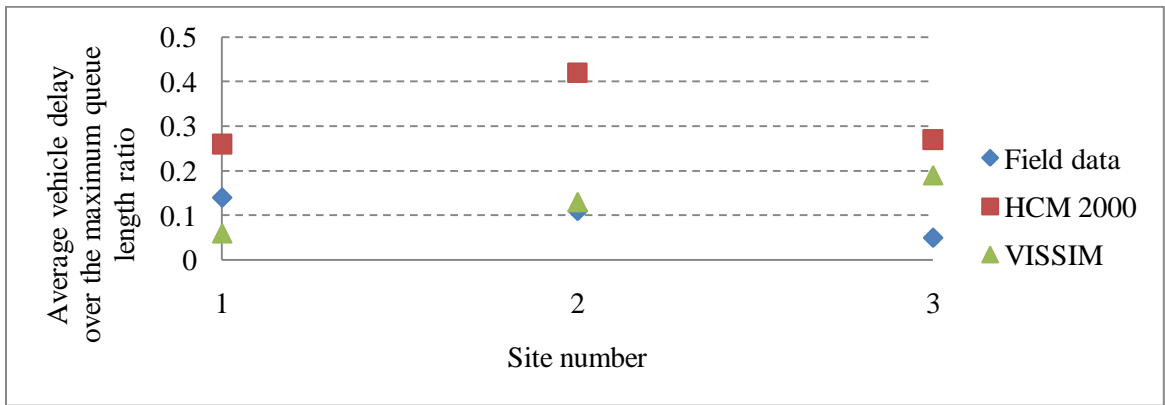


Figure 33: Average vehicle delay over the maximum queue length ratio

The detailed coding for the three sites is in Appendix D.

4.1.3 Entry capacity from VISSIM, Field data and HCM 2000 model

It was not possible to collect the entry capacity data from roundabouts located within Waterloo Region because these roundabouts currently operate with relatively low traffic volumes and very low pedestrian volumes and therefore are highly under-saturated.

Consequently observing and recording entry volumes measures demand not capacity. However, the research (Simulated capacity of roundabouts and impact of roundabout within a progressed signalized road) by Bared and Edara (2005) collected entry capacity data for one- and two-lane roundabouts from several sites in the USA. Data were collected from fifteen single lane roundabouts and from seven two-lane roundabouts.

VISSIM was validated on the basis of entry capacity field data for one and two lane roundabout from the Bared and Edara (2005) research. The roundabout geometry and the roundabout entry capacity from the field data used in Bared and Edara (2005) research are shown in Table 20 and Table 21.

Table 20: The roundabout geometry for one- and two-lane roundabouts found from research and coded in VISSIM (Bared and Edara, 2005)

Roundabout type	Single Lane	Dual Lane
Inscribed circle diameter	35m	55m
Entry radius	20m	40m
Exit radius	20m	40m
Entry width	4.5m	8.5m
Approach width	4.0m	7.3m
Departure width	4.0m	7.3m
Exit width	4.5m	8.5m
Circulatory road width	6.0m	9.5m

1- Validating one-lane roundabout from VISSIM to field data

The features used in coding the roundabout in VISSIM are described in Chapter 3. Figure 34 provides the resulting entry lane capacities. When compared with the HCM 2000 and field data, the roundabout entry capacity results from VISSIM appear to be too high at low conflicting volumes (less than about 300 veh/h). At high conflicting volume (more than 800 veh/h) VISSIM over estimates capacity compared to the field data but match the HCM estimates more closely.

The RMSE and the average percentage error based on roundabout entry capacity between VISSIM code and field data is 187.9 and 24.1 consecutively. The RMSE and the average percentage error based on roundabout entry capacity between HCM code and field data is 68.6 and 12.0 respectively.

Table 21: The entry capacity for one and two-lane roundabout based on the geometry in Table 20 (Bared and Edara, 2005)

Observation No.	Conflicting Flow (veh/h)	Maximum Entry Flow based on Field Data (veh/h)	
		one-lane roundabout	two-lane roundabout
1	120	1020	-
2	300	852	1620
3	480	690	-
4	600	588	1290
5	720	480	-
6	900	312	990
7	1200	-	750
8	1500	-	552
9	1800	-	372

2- Validating the two-lane roundabout from VISSIM to field data

The features used in coding the roundabout in VISSIM are described in Chapter 3. Figure 35 shows the estimation of the entry capacity of both lanes in two lane roundabout using VISSIM code (two lane roundabout without flare [See Appendix C for more details]) and field data. From Figure 35 it can be observed that VISSIM over estimates entry capacity at very low and very high conflicting volume but provides results that are very similar to the field observations for conflicting volumes around 900 vehicles per hour. The RMSE value and average percentage error value between the estimated roundabout entry capacities from VISSIM compared to field data is 374.4, and 43.9 respectively.

Figure 36 shows the estimation of the entry capacity of the critical lane in two lane roundabout using VISSIM and HCM data. The roundabout entry capacity results from VISSIM code (two lane roundabout without flare [See Appendix C for more details]) matches with the HCM 2000 model. The roundabout entry capacity results from VISSIM tend to be nearly constant under high conflicting volumes. This could be explained by the driver behavior used in VISSIM, the minimum headway time, and the origin and destination (OD) demand. The RMSE value and average percentage error value between the estimated roundabout entry capacities from VISSIM compared to HCM 2000 is 118.98 and 18.15 respectively. Based on the validation above VISSIM provides different trend in estimating roundabout entry capacity for one and two lane roundabout compared to field data and HCM 2000 entry capacity model results. Despite these differences VISSIM is used because it captures all sources of vehicle delay.

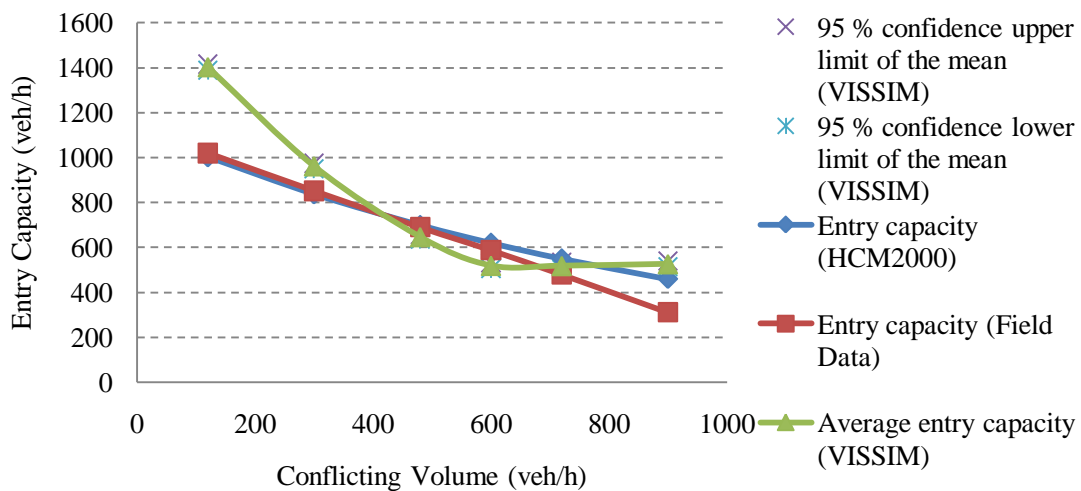


Figure 34: VISSIM, field data, and HCM 2000 entry capacity results for one-lane roundabouts

Based on the validation results it appears that, for the conditions observed (which were at a high level of service), VISSIM provides better estimates of average vehicle delay than the HCM 2000. In addition, the trajectories extracted from VISSIM appear to be realistic, although no quantitative evaluation was conducted. Based on these calibration and validation results, it is concluded that the VISSIM model is able to provide credible estimates of vehicle delays at roundabouts.

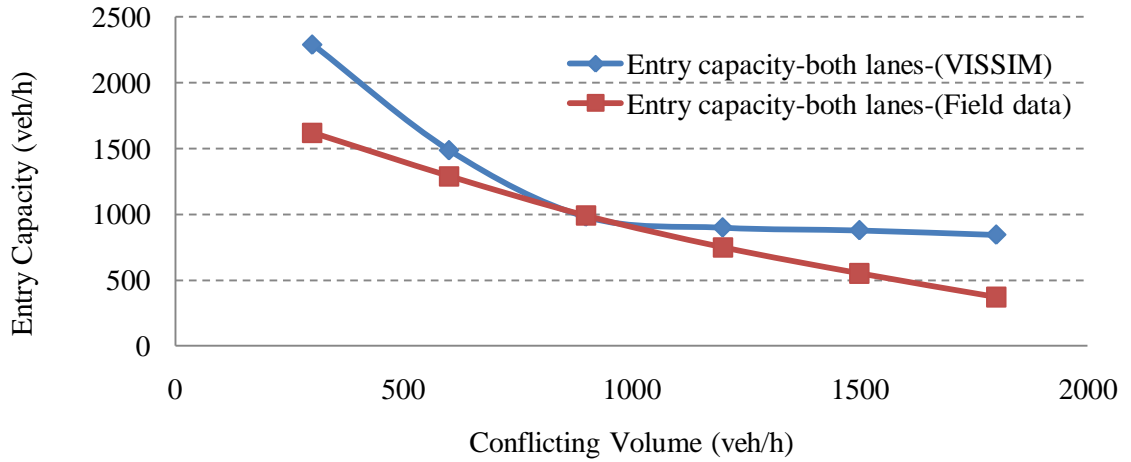


Figure 35: Examining the entry capacity of both lanes in VISSIM and field data for two-lane roundabouts

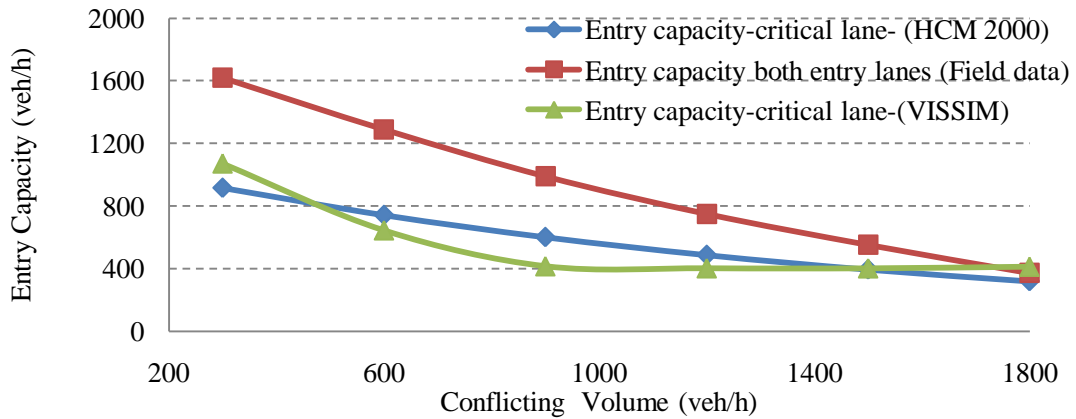


Figure 36: Examining the entry capacity of critical lane in VISSIM, and HCM 2000 for two lane roundabout

4.2 Calibration of the proposed analytical model

The proposed model is calibrated based on minimizing the root mean squared error (RMSE) between the O-D delay estimated from the proposed model and those obtained from VISSIM (Equation 57). Because the aim of the proposed model is to estimate accurately vehicle delay under an acceptable Level of Service F ($d > 50$ s/veh) or better, the maximum vehicle delay (d_{max}) was set to be 60 seconds/vehicle. The other parameters were constrained by maximum, minimum values as shown in Table 22.

The entry volume used is 400 (veh/h) from all entries and the pedestrians volume ranged from 1 to 800 (ped/h) as shown in the experimental design sections. Using the target equation (Equation 57) and the constraints specified in Table 22 the optimal set of parameter values was obtained as provided in Table 22.

$$RMSE = \sqrt{\frac{1}{n} \sum_{i=1}^I \sum_{j=1, j \neq i}^J E_{i-j}} \quad \text{Equation (56)}$$

$$E_{i-j} = \begin{cases} (\hat{d}_{i-j} - d_{i-j})^2 & \hat{d}_{i-j} \leq d_{max} \\ (d_{max} - \min(d_{max}, d_{i-j}))^2 & \text{otherwise} \end{cases} \quad \text{Equation (57)}$$

Table 22: Parameters in Proposed Model

Model Parameter	Minimum Value	Maximum Value	Optimal Value	Units
C_1^c	1000	1300	1162	veh/h
C_2^{in-min}	25	150	55	veh/h
S_l	4	8	4	veh/h
t_c	4.1	6	4.5	s
t_f	3.1	4	3.1	s
t_{cped}^{in}	2.25	6	6.0	s
t_{cped}^{out}	2.25	6	5.0	s
t_{fped}^{in}	2.25	4	4.0	s
t_{fped}^{out}	2.25	4	2.3	s

4.3 Validation of proposed analytical model

The proposed model was evaluated by comparing the delay estimates provided by the model to estimates obtained from other sources, including VISSIM, and existing analytical models. These comparisons are carried out to evaluate the accuracy of the proposed model and the existing models and have been divided into parts as follows:

Part A: Comparison of vehicle delay source 1 from VISSIM with existing analytical models.

Based on VISSIM validation in the previous section, VISSIM proved that it has a realistic estimation of vehicle delay compared to field data. All the existing analytical models failed to capture source 3 to 4 of delay. Consequently the comparison is based on delay from source 1 only to find the best model to represent the field data. There are different entry capacities and capacity reduction factor models as discussed in Chapter 2. These models are coded in excel sheet and their calculated capacity results compared to results from their references (see Appendix B) to make sure that the incorporation of the analytical methods within the spreadsheets was done correctly. The HCM delay model is used for each combination of entry capacity and capacity reduction factor to estimate the delay from each model. The delay extracted from these combinations and VISSIM results are calculated and generated based on the experimental design shown in Chapter 3 and then compared. The delay from VISSIM is based on OD pairs and the delay for all OD pair in source 1 are averaged. The comparison is based on the RMSE value. This comparison is to show which model provides estimates of delay that are most similar to the VISSIM results.

Based on the results in Table 23 the combination of models that best represent the VISSIM results in terms of replicating Source 1 delays is the Australian entry capacity model combined with the French capacity reduction factor model. Note that for all model combinations, delay is estimated using the HCM 2000 delay model.

The average vehicle delay based on the HCM 2000 entry capacity model (i.e. the first row in Table 23) combined with the three capacity reduction factor (German, English, and French) models for different pedestrian volume and 400 (veh/h) entry volume are shown in Figure 37.

As can be observed, the German and English pedestrian capacity reduction models lead to significant under-estimation of Source 1 delay when pedestrians' volumes exceed approximately 200 ped/h. Furthermore, it is observed that the German and English models have the same trend with respect to the estimated delay.

Table 23: RMSE values for different entry capacity and capacity reduction factor models based on VISSIM delay results

Capacity Model	Pedestrian Reduction Model		
	German (Equation 41)	English (Equation 37)	French (Equation 39)
HCM2000 (Equation 3)	40.4	38.0	27.7
Australian (Equation 8)	39.9	39.0	25.7
German (Gap Acceptance) (Equation 13)	42.8	41.4	38.1
Kimber (Equation 15)	44.2	43.3	42.5
German (Empirical) (Equation 23)	40.4	38.0	26.4
FHWA (Table 9 a)	43.6	42.3	41.0
Swiss (Equation 24)	44.3	43.7	42.6
French (Equation 26)	45.7	45.5	45.3
RMSE of Best Model	25.7		
RMSE of Worst Model	45.7		

Figure 38 shows the regression line for each of the capacity reduction factor models used to estimate vehicle delay using the HCM entry capacity and delay model based on delay Source 1. These results confirm the observations from Figure 37 that the French pedestrian capacity reduction model combined with the HCM 2000 entry capacity models provides the best fit of the VISSIM results.

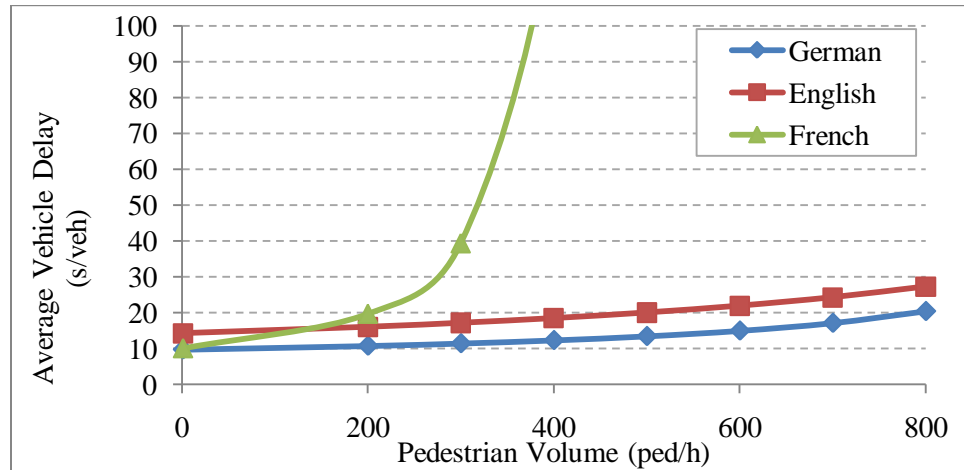


Figure 37: Vehicle delay based on different capacity reduction factor models

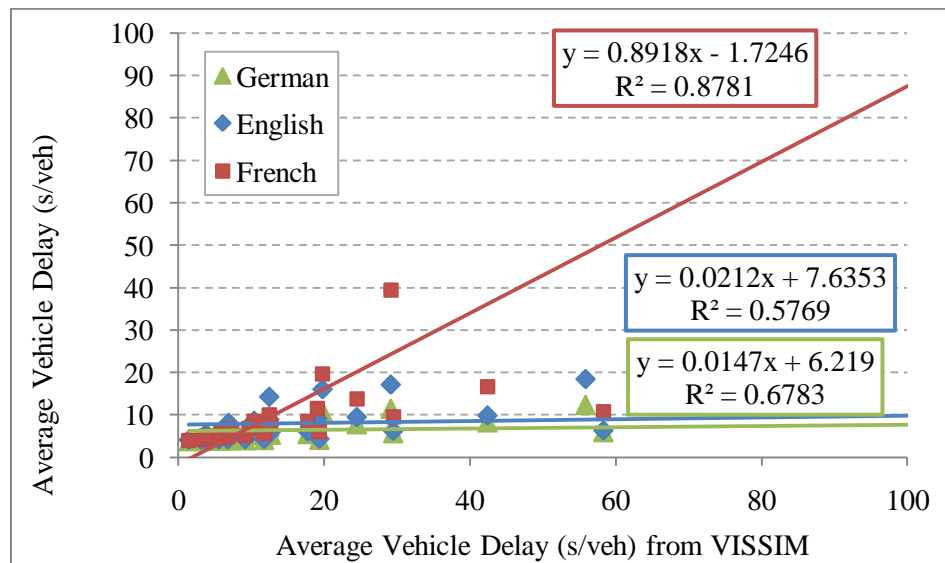


Figure 38: Regression lines for different capacity reduction factor models

Part B: Comparison of models with respect to all sources of vehicle delay

The previous section showed that the Australian entry capacity model combined with the French pedestrian capacity reduction factor is best able to replicate the VISSIM estimates of Source 1 delays.

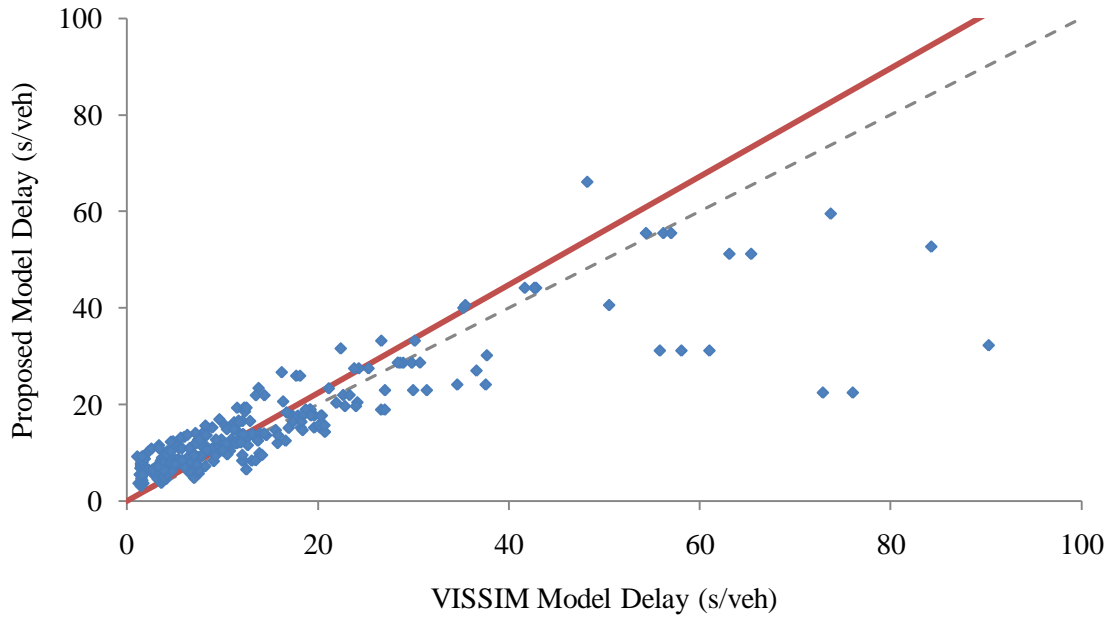
This is in contrast to the findings from an NCHRP report (Rodegerdts, 2007) and Rodegerdts (2004) which recommended the HCM 2000 entry capacity model and the German pedestrian capacity reduction factor model be used for application within the USA.

Given that the current recommended practice within Canada and the USA appears to be the use of the HCM and German models, these models are used in this section.

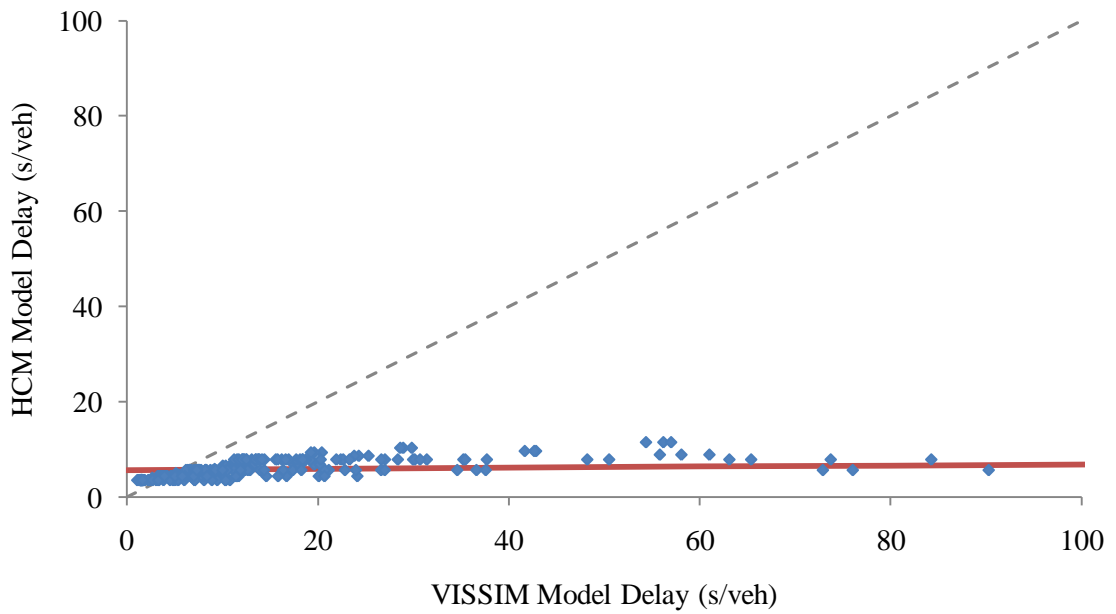
To estimate the accuracy of the proposed model and the combination of the HCM and German models in capturing all vehicle delay sources the following comparison is made. Average vehicle delays which are less than 100 seconds for each OD pairs as estimated from the proposed model, the HCM/German models, and the VISSIM model are compiled in Figure 39. A limit of 100 seconds was selected since the focus is on practical conditions (Level of Service F or better) and including estimation errors associated with highly oversaturated conditions is not valuable. The figure contains dashed lines and solid lines. The dashed line is the perfect correlation between VISSIM and the models. The solid line is the linear regression between the delays obtained from VISSIM and the delays estimated by the models. Table 24 shows the statistical results of the regressions. The R^2 value for the proposed model is higher than the HCM implying that the proposed model is much better able to explain the variation in the observed delays than is the HCM/German model.

Table 24: Regression results

		Proposed Model	HCM Model
Slope	Value	1.121	0.012
	t-statistic	39.2	16.5
Intercept	Value	0 ^a	5.63
	t-statistic	---	42.3
Adjusted R ²		0.84	0.49
Number of Obs.		288	288
^a The intercept was not significantly significant (t=-1.1) and therefore the regression was carried out again with the constant set equal to zero.			



(a) Proposed Model



(b) HCM Model

Figure 39: Comparison of estimated delays obtained from the proposed and HCM analytical models with the delays obtained from VISSIM

Part C: Compare vehicle delay from the proposed model, and HCM with VISSIM results based on leg 1, leg 2, and OD 4-1

From the previous comparison it is shown clearly that the proposed model captures all delay sources unlike the HCM. This part aims to estimate the accuracy of the proposed model and the HCM model in capturing different vehicle delay sources (from Leg 1, Leg 2, and OD 4-1).

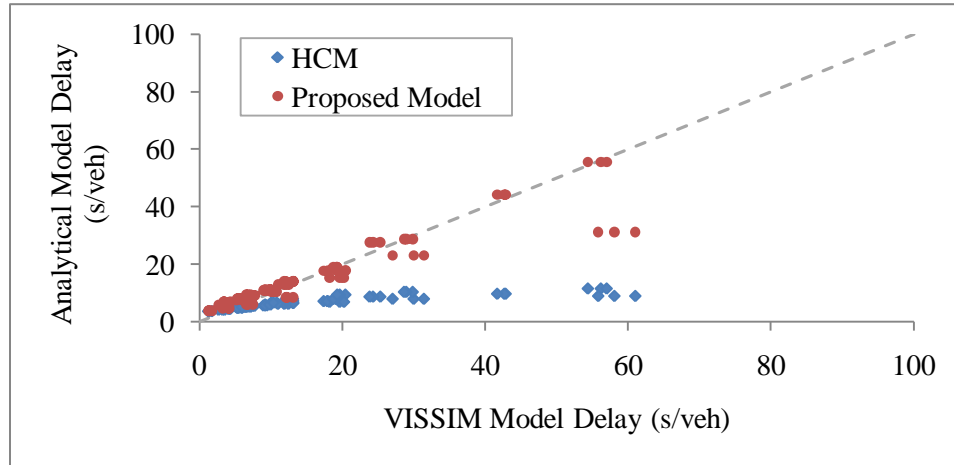
A comparison is between the proposed model and the HCM/German models for estimating Source 1 delays at Leg 1 only. Figure 40a shows the resulting comparisons.

It is expected that the HCM/German models would provide superior accuracy since they are designed specifically to address Source 1 delays. However, the results suggest that the proposed model is more accurate even for Source 1 delays. (RMSE Proposed model = 6.5 s; RMSE HCM/German model = 39.8 s).

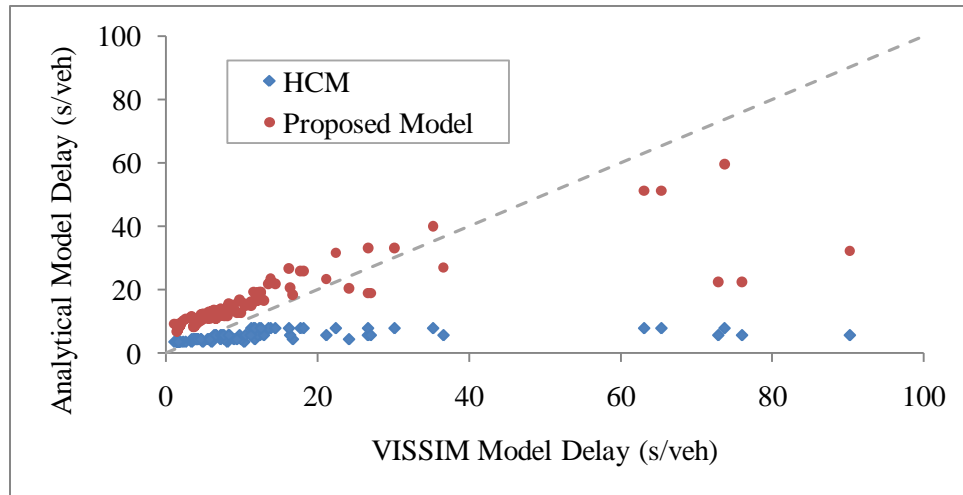
A second comparison was made with respect to the delays experienced by vehicle entering at Leg 2. Vehicles entering Leg 2 could experience Source 4 delays if the queue from the exit at Leg 1 spilled back and extended to the entrance of Leg 2. If this does not occur, then vehicles entering at Leg 2 will experience only Source 1 delays. Keep in mind the method assumed no pedestrians volume in any approach other than approach 1 (Leg 1). The impact of Source 4 delays is shown in Figure 40b. The delays estimated by the combined HCM/German model are very low and do not change very much as a function of the circulating conflicting volume. On the other hand, as shown in Figure 40b the proposed model captures the occurrences of queues spilling back from the exit to Leg 1 and leading to much higher delays at entry Leg 2. It is clear that for these cases, the proposed model is more accurate in estimating this source of delay than the HCM/German model. The RMSE of the Proposed model = 12.9 seconds and the RMSE of the HCM model = 18.5 seconds. Note, however, that despite being superior to the HCM/German model, the proposed model underestimates Source 4 delay when delay is very high.

The last comparison was conducted to examine the ability of the proposed model to estimate delays for vehicles that experience three delay sources (i.e. source 1, 2, and 3) combined. This is achieved by examining the delay experiences of vehicles traversing the roundabout from origin 4 to destination 1.

Vehicles entering Leg 4 conflict with circulating vehicles only (pedestrian volume is equal to zero) and therefore experience Source 1 delay. In the circulating roadway these vehicles experience Source 3 delays when the queue spills back from the exit lane at Leg 1 into the circulating roadway. And finally, these vehicles experience Source 2 delays when they seek a gap between pedestrians on the exit at Leg 1.



(a) Delays to vehicles entering via Leg 1



(b) Delays to vehicles entering via Leg 2

Figure 40: Comparison of estimated delays obtained from the proposed and HCM analytical models with the delays obtained from VISSIM by entry leg

Vehicle delay results from the proposed model and the HCM/German model for OD 4-1 are shown in Figure 41. The results indicate that the HCM/German model under-estimates vehicle delay (OD 4-1) compared to VISSIM results. This is expected as the HCM/German model considers only delay Source 1. Conversely, the proposed model captures all three sources of delay (source 1, 2, and 3) and therefore is much more accurate than the HCM/German model. This is confirmed by the RMSE values ((RMSE Proposed model = 4.6 s; RMSE HCM/German = 13.1 s).

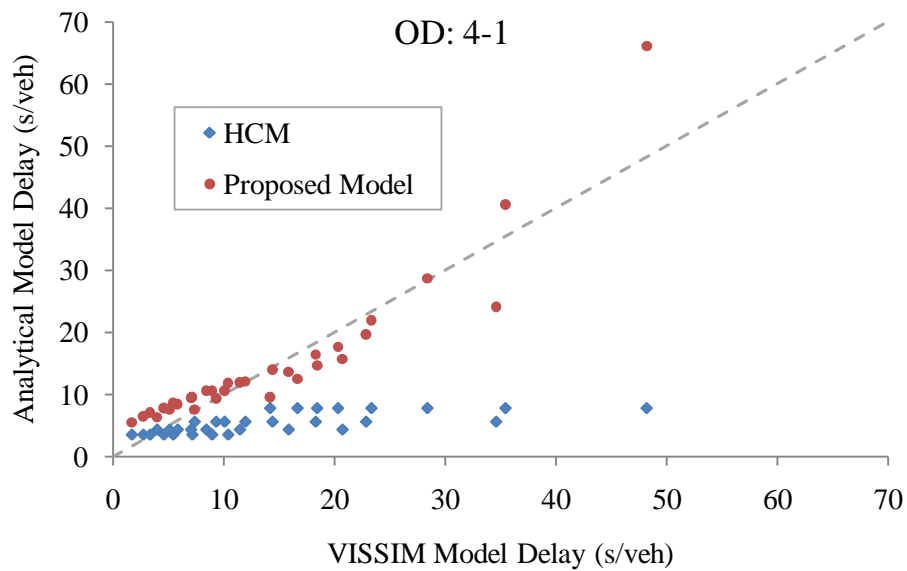


Figure 41: Comparison of estimated delays obtained from the proposed and HCM analytical models with the delays obtained from VISSIM for OD 4-1

Chapter 5: Conclusions and Recommendations

Modern roundabouts are an unsignalized intersection design that accommodates both vehicles and pedestrians. The convention within North America is that pedestrians have right-of-way over vehicles when crossing the zebra line on the approach leg. As a result, vehicle must yield right-of-way to pedestrians and may incur delays. Pedestrians crossing the approach leg of a roundabout can cause delays to vehicles traversing the roundabout in 4 ways. Some of these vehicle delay sources are not captured by the existing analytical models and consequently these models over-estimate the level of service that roundabouts are likely to provide when significant pedestrian flows are present.

The goals of this thesis were to (1) examine the magnitude of the influence that pedestrians are likely to have on roundabout operations, particularly under the assumption that vehicles must and do yield right-of-way to pedestrians in the crosswalk; and (2) develop an analytical method that could be used to estimate delays to vehicles traversing the roundabout as a function of vehicle and pedestrians flows.

The results in this thesis show that the influence of pedestrians on vehicle delays can be much larger than is captured with most existing analytical models. Ignoring these effects can lead to the design and construction of roundabouts which will have an effective service life which is much shorter than originally anticipated.

The model proposed in this thesis was calibrated and validated using data from the VISSIM model. The comparisons carried out suggest that the proposed model is much more accurate than the HCM/German models currently recommended for use in North America.

The proposed model is based on well understood traffic and queuing theories and can be applied in practice to assess single lane roundabouts.

The following recommendations are made:

1. There is evidence available in the literature (e.g. Oh and Sisiopku, 2000) that even when vehicles are required by law to yield to pedestrian flows, a relatively large portion of vehicles in the USA fail to do so.

It is anticipated that over time, as roundabouts become more common and drivers become more experienced with driving through roundabouts, that this proportion will decrease. Nevertheless, it is recommended that the proposed model be extended to consider as an input the proportion of vehicle which yield right of way to pedestrians.

2. The model be extended to be applicable to two-lane roundabouts.
3. The model be extended to explicitly consider the distance between the circulating roadway and the crosswalk rather than assuming that this distance is equal to zero.
4. The model be used to assess the service life implications for typical roundabout designs by examining the level of service of the roundabout (in terms of vehicle delays) as a function of growth in the pedestrian and vehicle flows. This should lead to design criteria related to the maximum pedestrian flows rates that can be supported by various roundabout designs at specified levels of service.
5. The proposed model should be validated using field data – but specifically for conditions in which a large proportion of drivers yield to pedestrians. Obtaining these field data will be challenging given the limited number of roundabouts which currently have moderate to high pedestrian volumes and the general lack of consensus/understanding by drivers and pedestrians about who has the right-of-way at the zebra crossings.

References

- Alisoglu, S. (2010) "Roundabouts v. Signalized intersections: A comprehensive Analysis"
Kansas Government Journal, July 2010.
- Angelastro, M. (2010) "The Influence of Driver Sight Distance on Crash Rates and Driver Speed
at Modern Roundabouts in the United States" ITE Journal, INSTITUTE OF
TRANSPORTATION ENGINEERS, July 2010.
- Bared, J. and Edara, P. (2005) "Simulated Capacity of Roundabouts and Impact of Roundabout
Within a Progressed Signalized Road" Transportation Research Circular, E-C083,
Proceedings of the National Roundabout Conference, Vail Colorado, May 22-25, 2005.
- Boenisch, C. and Kretz, T. (2010) "Simulation of Pedestrians Crossing a Street" PTV AG,
Karlsruhe, Germany, 2010.
- Bovy, H., Dietrich, K. and Harmann, A. (1991) "Guide Suisse des Giratoires" Lausanne,
Switzerland, 1991.
- Brilon, W. and Stuwe, B. (1990) "Capacity and Safety of Roundabouts in West Germany"
Proceedings 15th ARRB Conference, Vol. 15, Part 5, 1990.
- Brilon, W. (1991) "Intersections Without Traffic Signals" Springer-Verlage, Vol. II, Berlin,
1991.
- Brilon, W., Stuwe, B. and Drews, O. (1993) "Sicherheit und Leistungsfähigkeit von
Kreisverkehrsplätzen" (Safety and capacity of roundabouts) Research Report, Ruhr-
University Bochum, Bochum, Germany, 1993.
- Brilon, W., Wu, N. and Bondzio, L. (1997) "Unsignalized Intersection in Germany - A State of
the Art 1997" Proceedings of the Third International Symposium on Intersections Without
Traffic Signals, Portland, Oregon, USA, July 1997, pp. 61-70.
- Cowan, R. J. (1975) "Useful headway models" Transportation Research, Vol. 9, No 6, 1975, pp.
371-375.

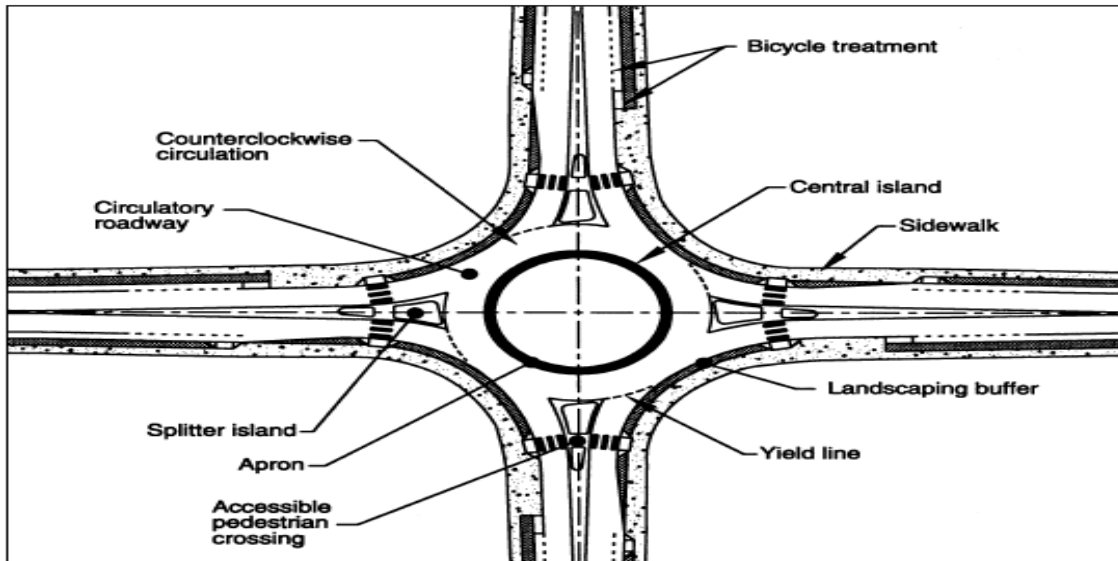
- Duran, C. (2010) “Effects of pedestrian crossing on roundabout capacity” University of Texas, El Paso, USA, 2010.
- Guichet, B. (1997) “Roundabouts in France: Development, Safety, Design and Capacity” University of Idaho, Proceedings of the Third International Symposium of Intersections Without Traffic Signals, Portland, Oregon, USA, 1997.
- Guichet, B. (2005) “Roundabouts in France and new use” TRB Transportation Research Board, Proceedings of the National Roundabout Conference, Vail, Colorado, USA, 2005.
- Hallmark, S., Fitzsimmons, E., Isebrands, H. and Giese, K. (2009) “EVALUATING THE TRAFFIC FLOW IMPACTS OF ROUNDABOUTS IN SIGNALIZED CORRIDORS” 2010 Annual Meeting of the Transportation Research Board, Paper #10-1309, 2009.
- HCM (2000), “Highway Capacity Manual – 2000” TRB Transportation Research Board, Washington, D.C., 2000.
- “How to Navigate Modern Roundabouts” (<http://www.wcroads.org/news/roundabouts/navigate.htm>), Minnesota Department of Transportation, 2011.
- Jacquemart, G. (1998) “Modern Roundabout Practice in the United States” TRB Transportation Research Board, Synthesis of Highway Practice 264, Washington, D.C., 1998.
- Kimber, R. (1980) “Traffic Capacity of Roundabouts” Transportation and Research Laboratory, Laboratory Report LR942, Crawthorne, Berkshire, U.K., 1980.
- “L'Arc De Triomphe” (<http://www.kstate.edu/roundabouts/ada/photos/larcdetriomphe.htm>), Kansas State University, 2002.
- Louah, G. (1992) “Panorama critique des modeles français de capacité des carrefours giratoires” Actes du séminaire international “Giratoires 92,” Nantes, France, 1992.
- Manning, F., Washburn, S. and Kilareski, W. (2008) “Principles of Highway Engineering and Traffic Analysis – Fourth Edition”, Wiley, 2008.
- Marlow, M. and Maycock, G. (1982) “The effect of zebra crossings on junction entry capacities”, Transport and Road Research Laboratory, SR 724 Monograph, 1982.

- Mauro, R. (2010) “Calculation of Roundabouts Capacity, Waiting Phenomena and Reliability” Springer, 2010.
- Nikolic, G. and Pringle, R. (2010) “OPERATIONAL ANALYSIS OF ROUNDABOUTS” Ontario Traffic Council and ITE, Traffic Software Packages Workshop, Richmond Hill, Toronto, Ontario, Canada, November 23, 2010.
- Oh, H. and Sisiopku, V. (2000) “Probabilistic Models for Pedestrian Capacity and Delay at Roundabouts” Transportation Research Circular, E-C018, Proceedings of the 4th International Symposium on Highway Capacity, Maui, Hawaii, USA, June 27–July 1, 2000, pp. 459-470.
- “Region of Waterloo” (<http://www.regionofwaterloo.ca/en/gettingaround/roundabouts.asp>), 2001.
- Robinson, B., Rodegerdts, W., Scrbrough, W., Kittelson, R., Troutbeck, W., Brilon, L., Bondzio, K., Courage, M., Kyte, J., Mason, A., Flannery, E., Myers, J., Bunker, J. and Jacquemart, G. (2000) “Roundabouts: An informational Guide” Federal Highway Administration – FHWA, Publication number FHWA-RD-00-067, Turner Fairbank Highway Research Center, McLean, Virginia, USA, 2000.
- Rodegerdts, L. and Blackwelder, G. (2005) “Analytical Analysis of Pedestrian Effects on Roundabout Exit Capacity” Transportation Research Circular, E-C083, Proceedings of the National Roundabout Conference, Vail, Colorado, May 22-25, 2005.
- Rodegerdts, L., Blogg, M., Wemple, E., Myers, E., Kyte, M., Dixon, M., List, G., Flannery, A., Troutbeck, R., Brilon, W., Wu, N., Persaud, B., Lyon, C., Harkey, D. and Carter, D. (2007) “Roundabouts in the United States” TRB Transportation Research Board, NCHRP Report 572, Washington, D.C, 2007.
- Tanner, J. (1962) “A theoretical analysis of delays at uncontrolled intersection” Biometrika, Vol. 49, No. 1 and 2, 1962, p. 163-170.
- “The City of Waterloo “ (<http://www.waterloo.ca/DesktopDefault.aspx?tabid=1721>), 2001.

- “Three-leg Multi-Lane Roundabout in East Lansing, Michigan”
(http://attap.umd.edu/UAID_agus.php?UAIDType=7&iFeature=3), An Applied Technology and Traffic Analysis Program, 2011.
- Troutbeck, R. (1989) “Evaluating the Performance of a Roundabout” Australian Road Research Report SR 45, 1989.
- Trueblood, M. and Dale, J. (2003) “Simulating Roundabouts With VISSIM” Institute of Transportation Engineers/Transportation Research Board, 2nd Urban Street Symposium, Anaheim, California, USA, July 28-30, 2003.
- “VISSIM 5.20 User Manual” PTV AG, Karlsruhe, Germany, 2009.
- “Waterloo Region approves two new roundabouts”
(<http://swo.ctv.ca/servlet/an/local/CTVNews/20110125/roundabouts-approved-110125?hub=SWOHome>), CTV NEWS, 2011.
- Weber, P. (2010) “Introduction to RODEL and ARCADY for Roundabouts” Ontario Traffic Council and ITE, Traffic Software Packages Workshop, Richmond Hill, Toronto, Ontario, Canada, November 23, 2010.

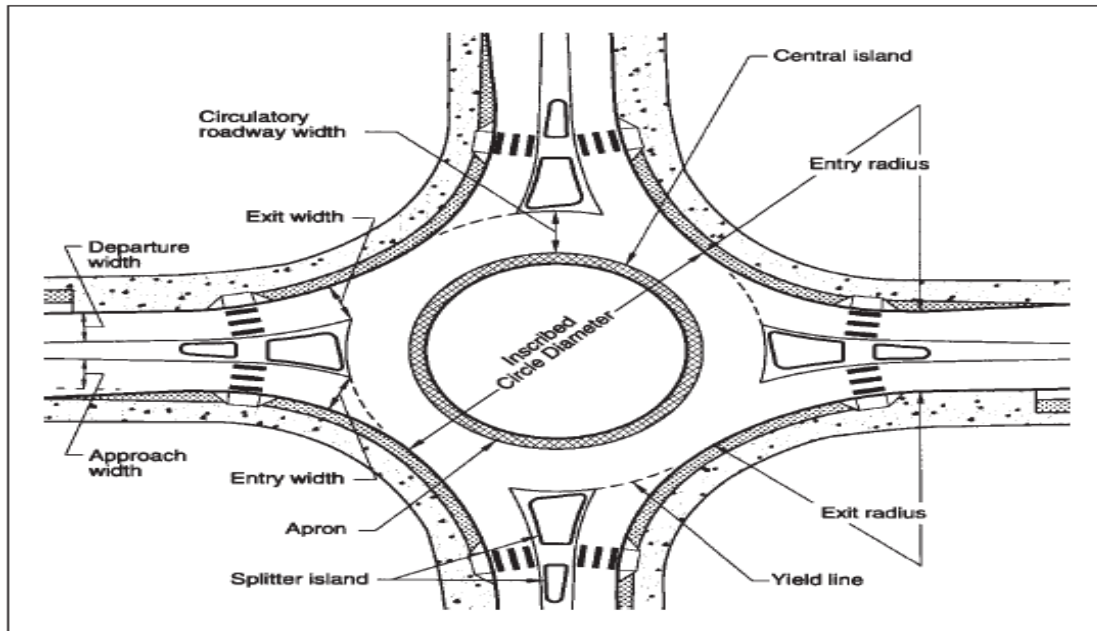
Appendix A: Roundabout features, diminutions, and key words

This appendix describes the roundabout features and diminutions that are necessary to understand the roundabout terminology. In addition, it contains the research symbols and key words that are used in the thesis. These key words will ease the understanding of the thesis content.



Feature	Description
Central island	The island in the middle of a roundabout around which vehicles circulate.
Splitter island	The island between the entrance and the exit of a roundabout lane that separates traffic and provides a safe area for pedestrians.
Circulatory roadway	The road around which vehicles circulate the central island in a counter clockwise direction (in Canada and The United States).
Apron	A low rise curb around the circulating island and joining to the circulatory road.
Yield line	A marking line that separates the circulating road from the entering road.
Accessible pedestrian crossings	The pedestrian crossing line, “the zebra line”, at roundabout entrance and exit.
Bicycle treatments	A lane that allows cyclists the choice to circulate with vehicles or with pedestrians.
Landscaping buffer	An identifier of vehicle and pedestrian paths and separates them.

Figure 42: Roundabout features (Robinson et al., 2000)



Dimension	Description
Inscribed circle diameter	The largest circulatory road diameter from the north approach entering yield line to the south approach entering yield line.
Circulatory roadway width	The width of the circulating road. It is larger than a vehicle width by a small proportion.
Approach width	The width of the roundabout upstream of the approach or after the pedestrian crossing line far from the yield line.
Departure width	The width of the roundabout downstream of the departure or after the pedestrian crossing line far from the exit line.
Entry width	The width of the road at the yield line.
Exit width	The width of the road at the exit line.
Entry radius	The radius of the entry curve from the pedestrian cross line at the entry road until the circulatory roadway.
Exit radius	The radius of the exit curve from the pedestrian cross line at the exit road until the circulatory roadway.

Figure 43: Roundabout dimensions (Robinson et al., 2000)

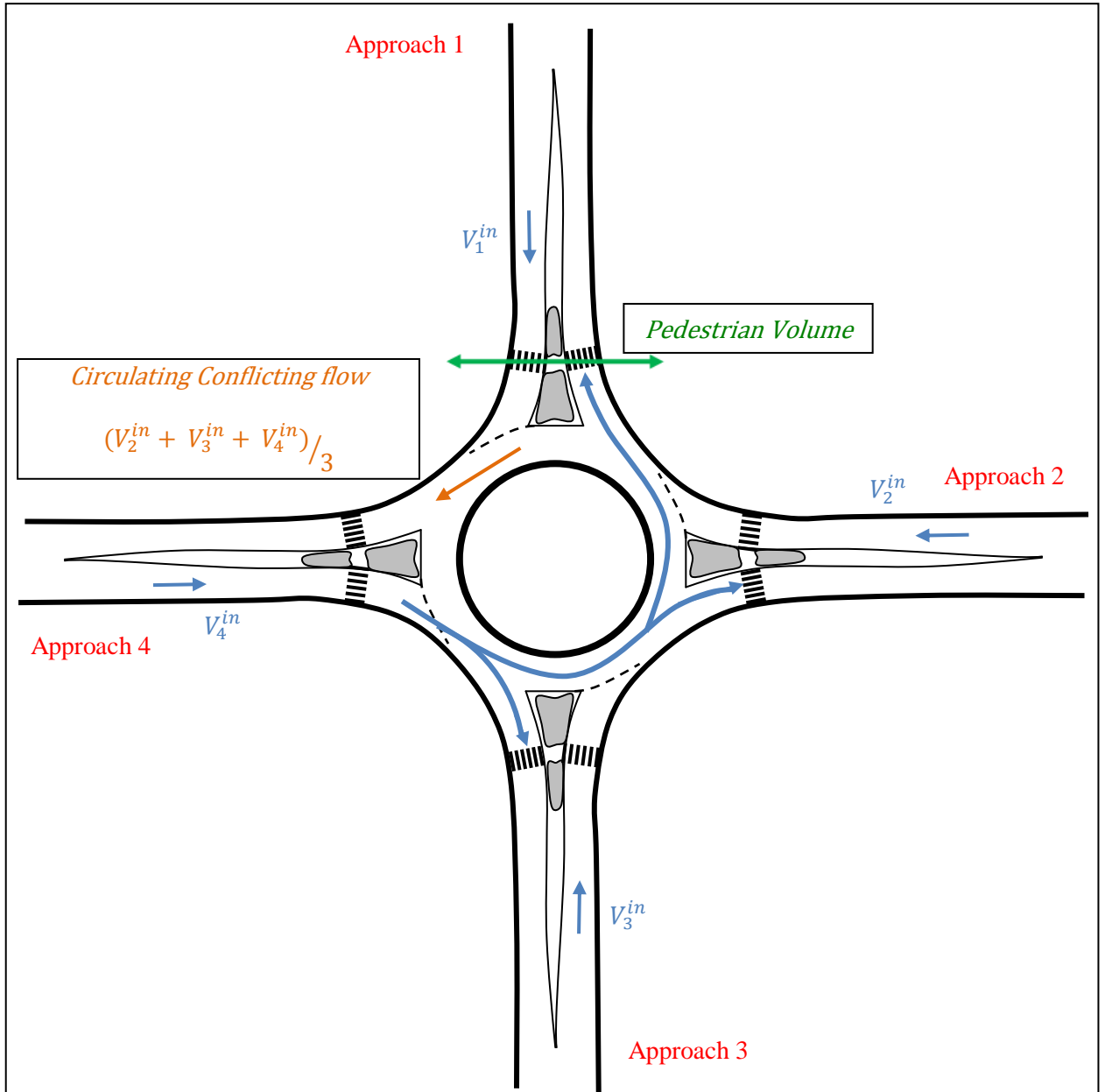


Figure 44: Approach numbering for one lane roundabout

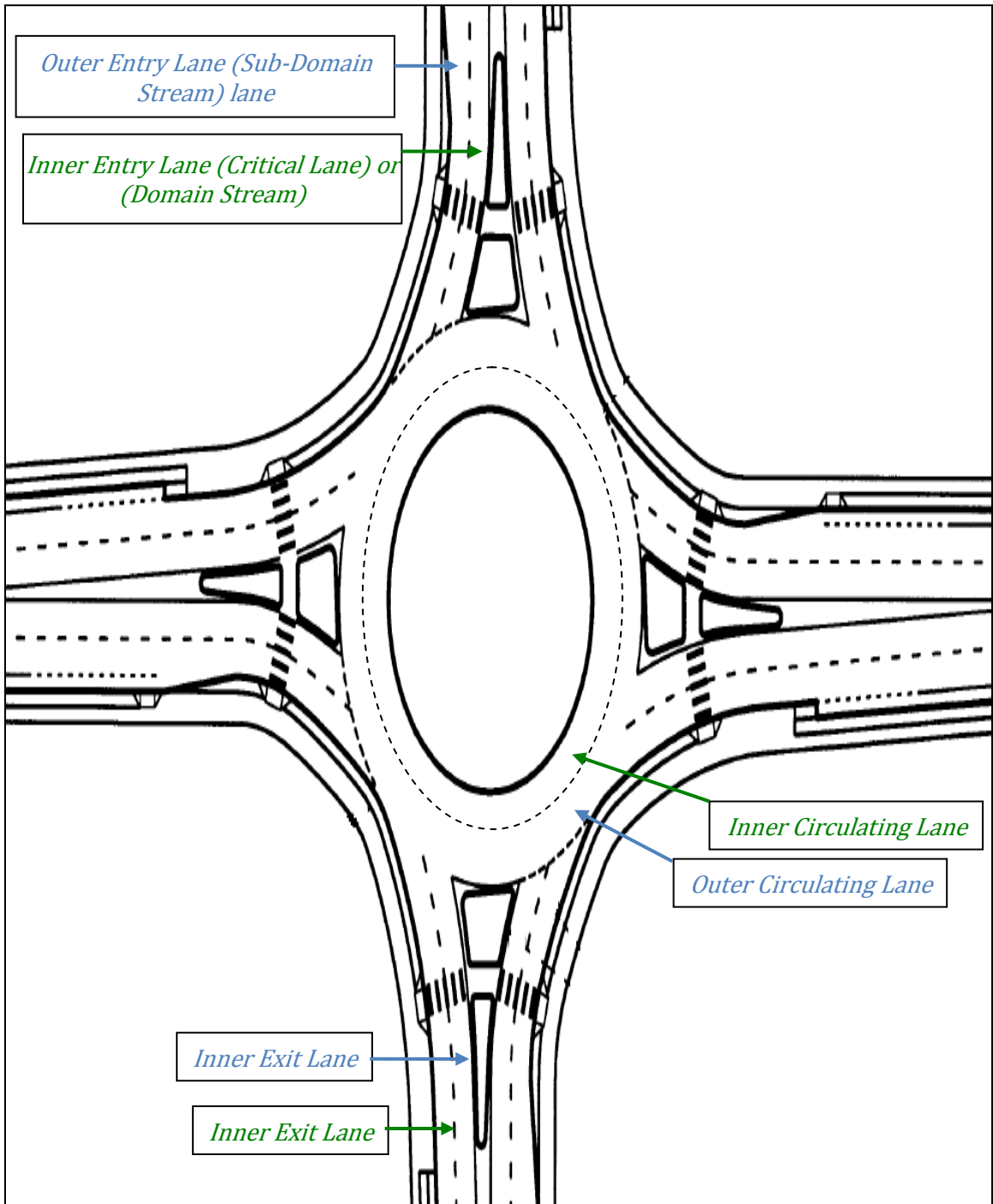


Figure 45: Inner and Outer lanes in Two-lane roundabout (Robinson et al., 2000)

Table 25: Key words used in the research and their description

key words	Description
Inner lane in the entering side	The inner lane in the entering side is the lane that is close to the pedestrians' island (Figure 45).
Outer lane in the entering side	The outer lane in the entering side is the lane that is farthest from the pedestrians' island (Figure 45).
Inner lane in the exiting side	The inner lane in the existing side is the lane that is close to the pedestrians' island (Figure 45).
Outer lane in the exiting side	The outer lane in the existing side is the lane that is farthest from the pedestrians' island (Figure 45).
Inner circulating lane	The circulating lane near the central island (Figure 45).
Outer circulating lane	The circulating lane near the entry and exit lanes (Figure 45).
Pedestrian Volume	The only approach that has pedestrian volume in this research is Approach 1 (see Figure 44).
Entry volume	The entry volume from one approach assumed to distribute equally to the other three exit legs (e.g., vehicle demand from approach 4 distribute equal magnitude of vehicle volume to the other three legs (see Figure 44)).
Conflicting or circulating volume	The vehicle volume that conflicts with the entering vehicles (e.g., entering vehicles from Approach 1 conflict with vehicles in the circulating roadway (see Figure 44). The value of the conflicting volume is the sum of V_2^{in} , V_3^{in} , V_4^{in} divided by 3.
Roundabout entry	The area where the yield line and pedestrians cross walk is.
Roundabout approach	The area upstream from the pedestrian crosswalk.
Roundabout departure	The area downstream from the pedestrian crosswalk from the exiting side.
HCM 2000	Highway Capacity Manual
FHWA	Federal Highway Administration

key words	Description
ICD	Inscribed Circle Diameter
pcph	Passenger car per hour
h	Hour
RMSE	Root Mean Square Error
MAPE	Mean Absolute Percentage Error
Seed	Is a number used in VISSIM the micro-simulation software to generate random distribution

Appendix B: Entry capacity and capacity reduction factor from existed analytical models

This appendix shows the comparison of entry capacity and capacity reduction factor between the coded models in excel with the calculated entry capacity and capacity reduction factor from their references. This comparison is made to insure that the analytical model done in the excel sheet is done correctly. The summary of the comparison is shown in the table below and the detailed resultant entry capacity and capacity reduction factor from the references and the excel sheet are shown in the figures below.

Table 26 : Comparing entry capacity and capacity reduction factor results from references to the calculated using the equations

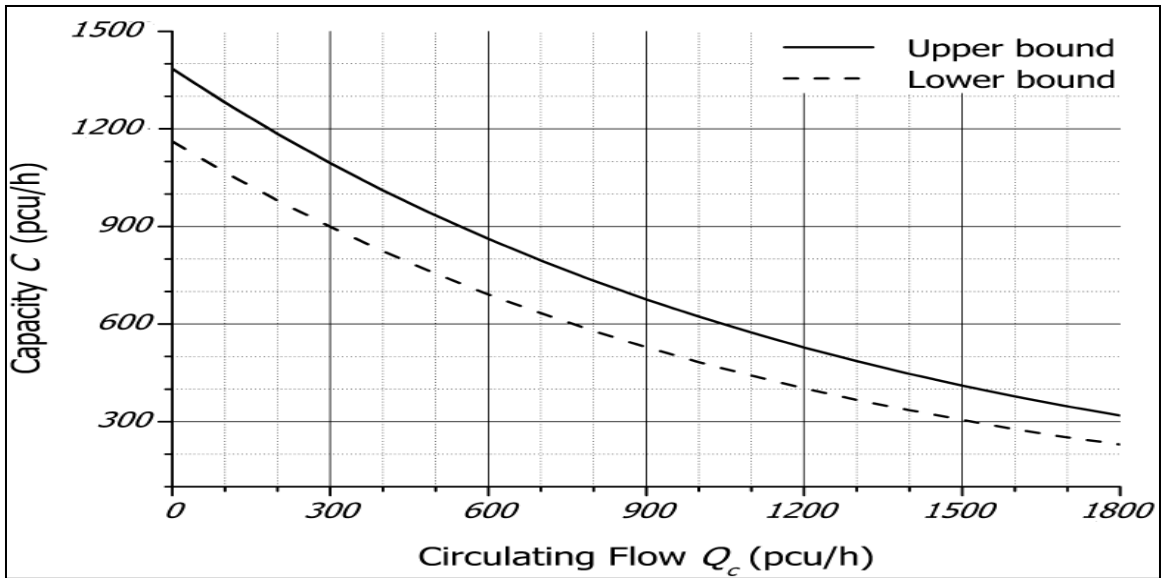
		results are from equation comparing to the reference figure		
		The same	Almost the same	Not the same
Entry Capacity	One lane roundabout			
	Model	The same	Almost the same	Not the same
	HCM 2000		√ (lower bound not single lane)	
	Australian			√ (Troutbeck compared to Tanner model)
	German (Gap Acceptance)	√		
	Kimber	No reference figure		
	German (Empirical)	√		
	FHWA	√ before deflection point (1800veh/h) circulating volume		
	Swiss	No reference figure		
French	No reference figure			
Capacity Reduction Factor	English method with English entry capacity model		√	
	English method with German entry capacity model		√	
	German	√		
	French method with French entry capacity model	√		

Note:

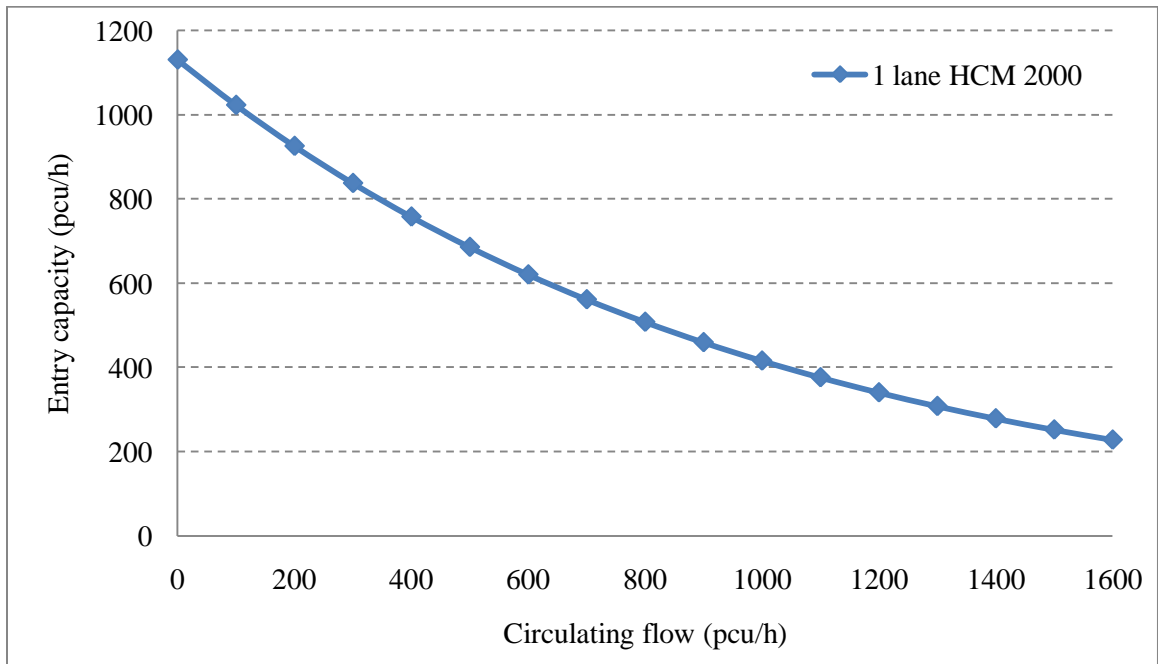
- 1- The small difference in the entry capacity values between the reference and the used model is as follows: HCM entry capacity results from the reference is for Lower bound and it is compared to the single lane roundabout entry capacity model results (Equation 3).
- 2- The Kimber model geometric parameter used is based on (Mauro, 2010).
- 3- There are no entry capacity figures from references for Swiss and French models.
- 4- The French capacity reduction factor has some assumptions. The geometry and the vehicle distribution are assumed. The vehicle distribution is 1/3 of entry vehicle exit to the other three exits.
- 5- Troutbeck equation is used to calculate the roundabout entry capacity. The reference used Tanner equation with Avent and Taylor headway values [$T= 2.5$, $T_0= 2.1$, $\Delta= 2.2$ for 1 lane roundabout) (Mauro, 2010).
- 6- The FHWA model did not include an analytical model to estimate entry capacity for conflicting volume more than 1800 veh/h.
- 7- The reason of the small difference between the estimated capacity reduction factor from the model and the reference in the English capacity reduction factor models is as follows: the pedestrians cross walk location and pedestrians walking speed are assumed as they are not specified in the reference (they make a different in estimating capacity reduction factor).
- 8- The German capacity reduction factor does not need entry capacity values.
- 9- The French capacity reduction factor model does not need value for entry capacity from the German model as value of B is chosen from the reference to be 2.57 ($B = 1/$ entry capacity at zero conflicting volume).

Entry capacity models:

HCM (HCM, 2000)



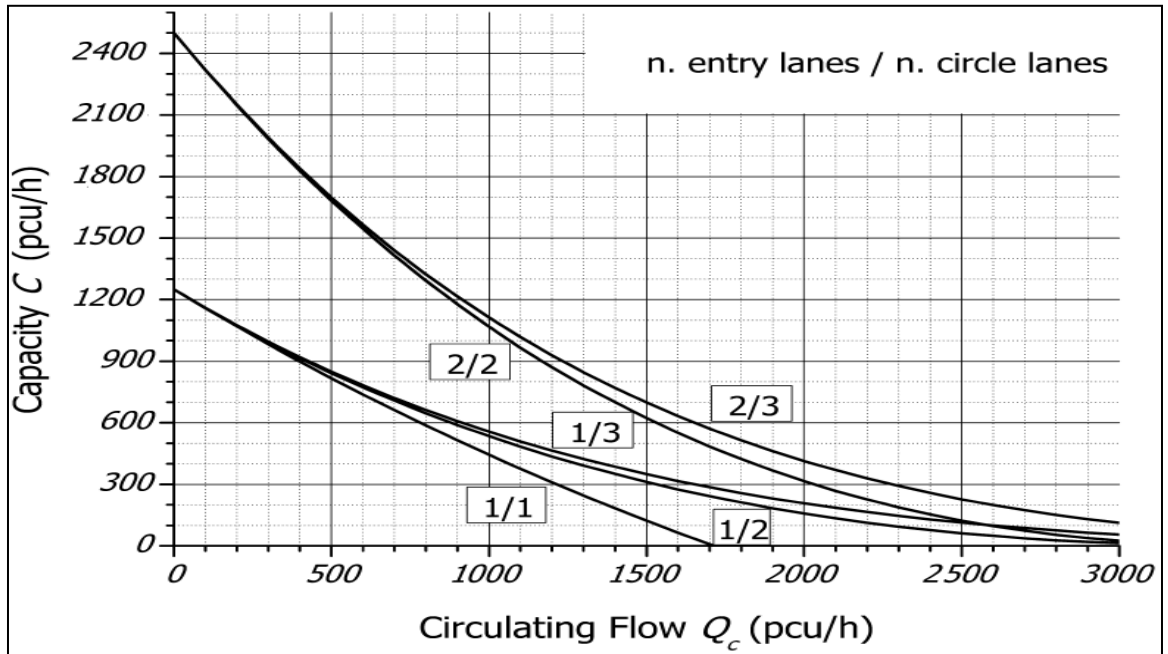
a) Reference estimates



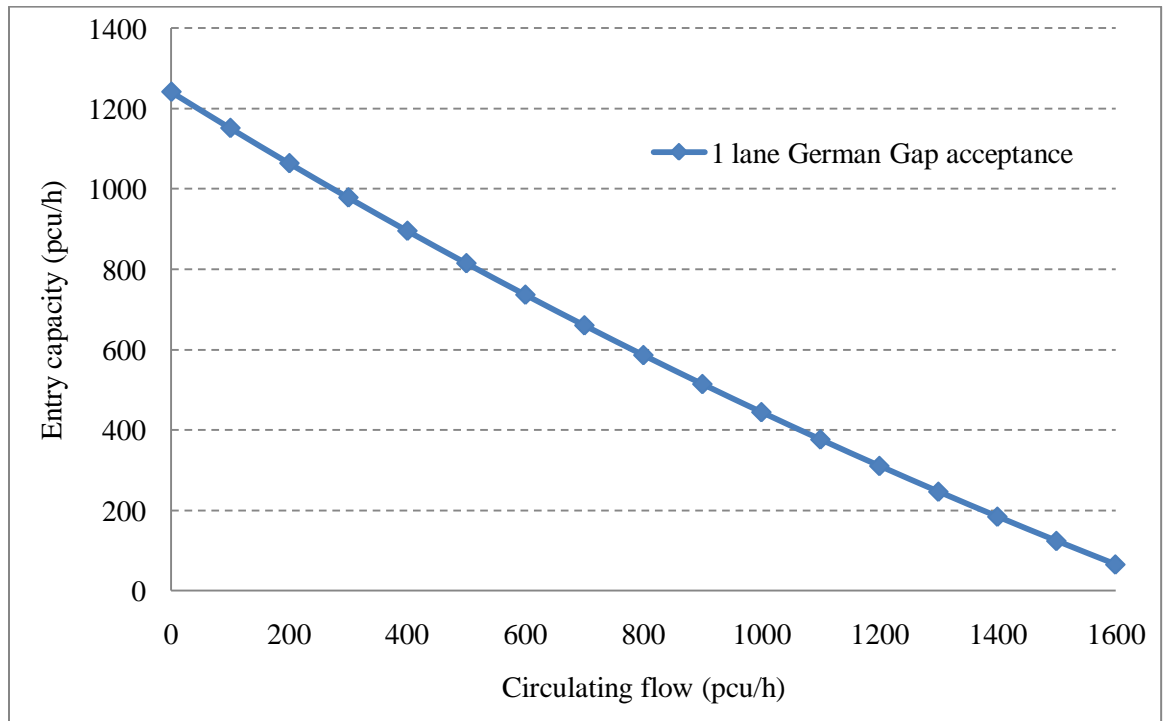
b) Model estimates

Figure 46: HCM entry capacity model

German (Gap Acceptance) (Brilon et al., 1997)



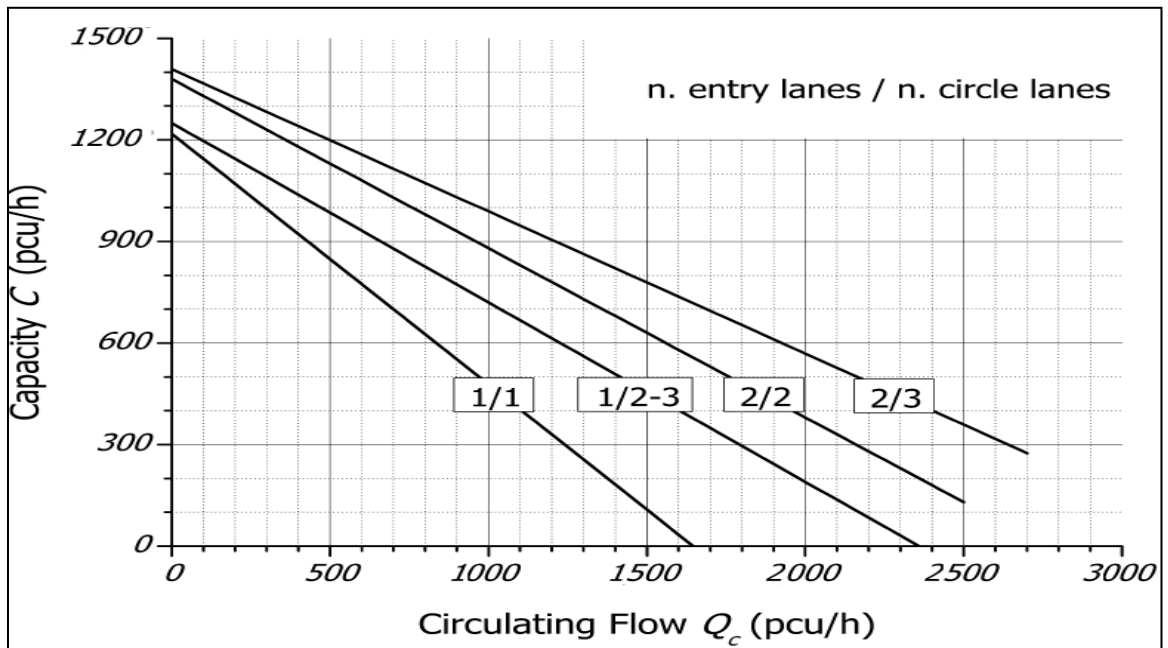
a) Reference estimates



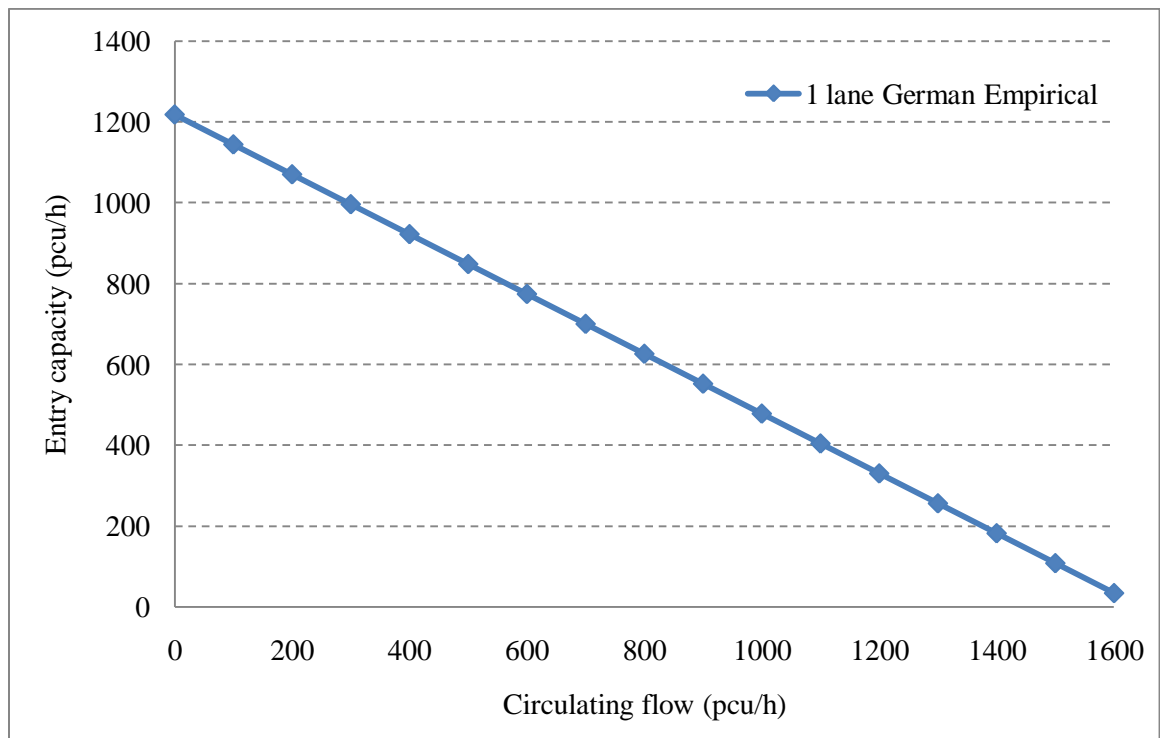
b) Model estimates

Figure 47: German (Gap Acceptance) entry capacity model

German (Empirical) (Brilon et al., 1997)



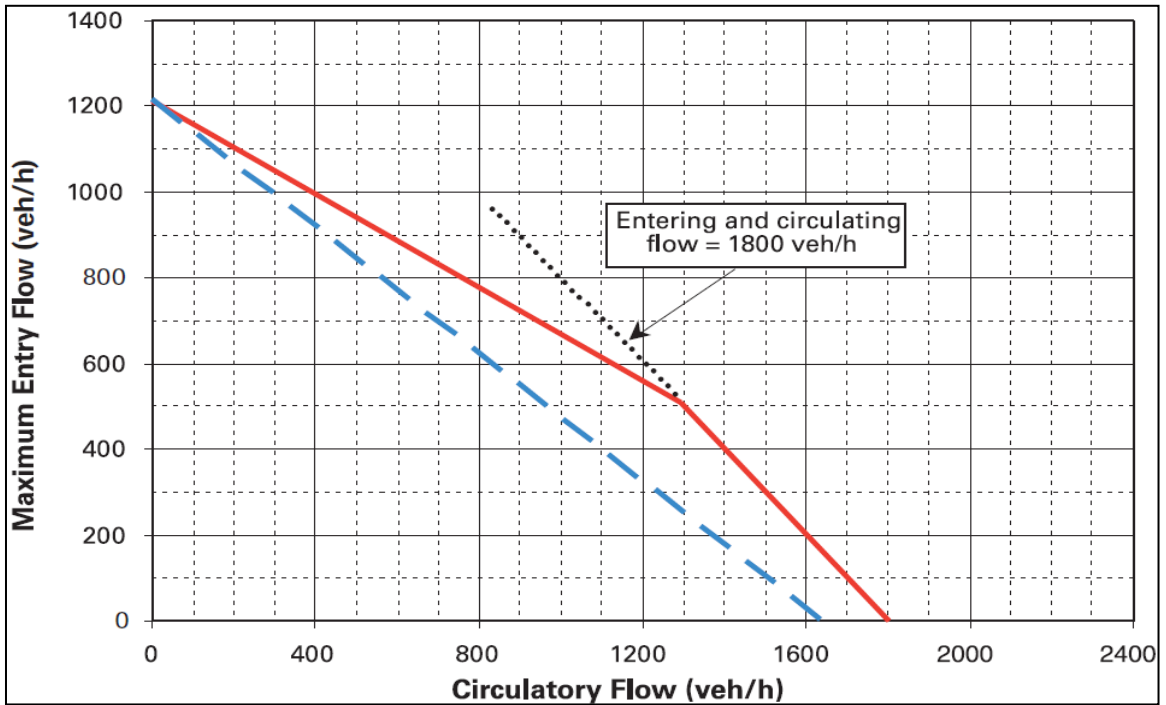
a) Reference estimates



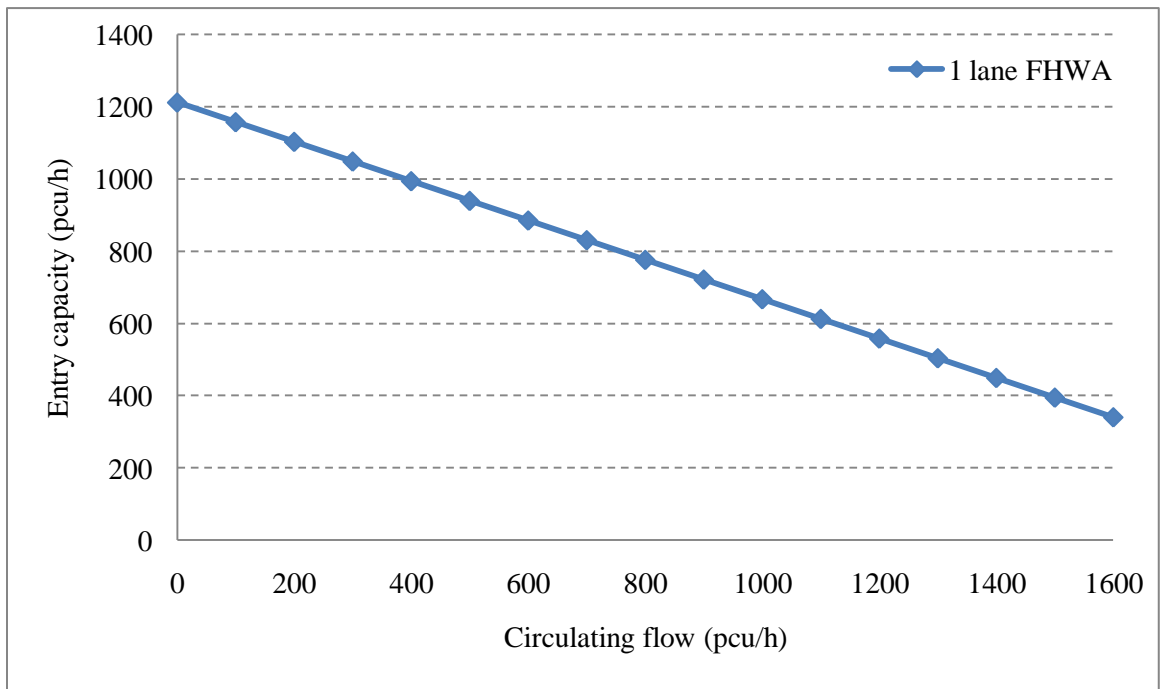
b) Model estimates

Figure 48: German (empirical) entry capacity model

FHWA 2000 (Robinson et al., 2000)



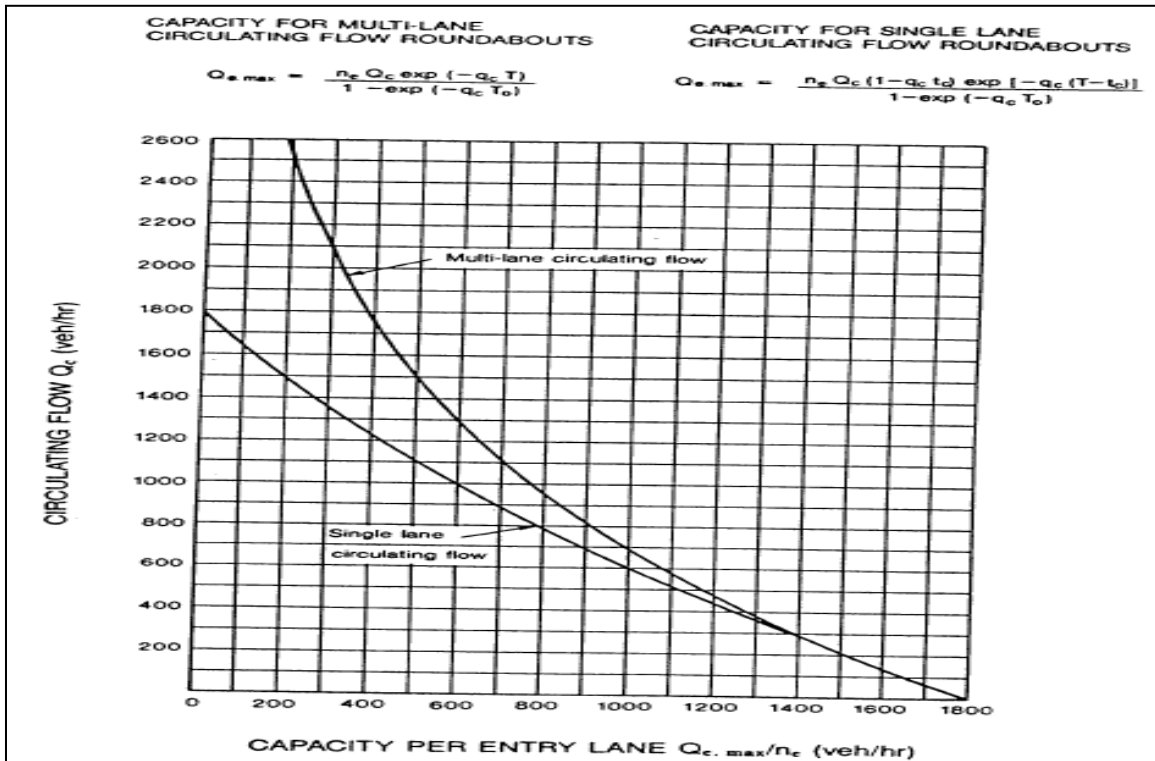
a) Reference estimates



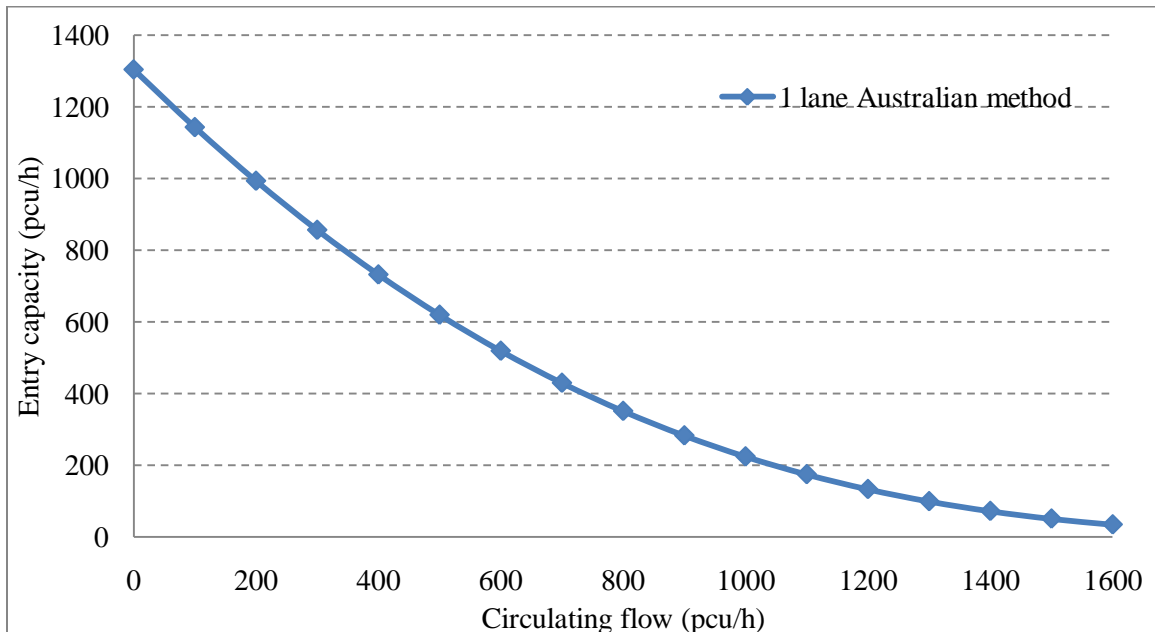
b) Model estimates

Figure 49: FHWA entry capacity model

Australian Troutbeck's model for capacity (Mauro, 2010)



a) Reference estimates



b) Model estimates

Figure 50: Australian entry capacity model

Kimber (Kimber, 1980)

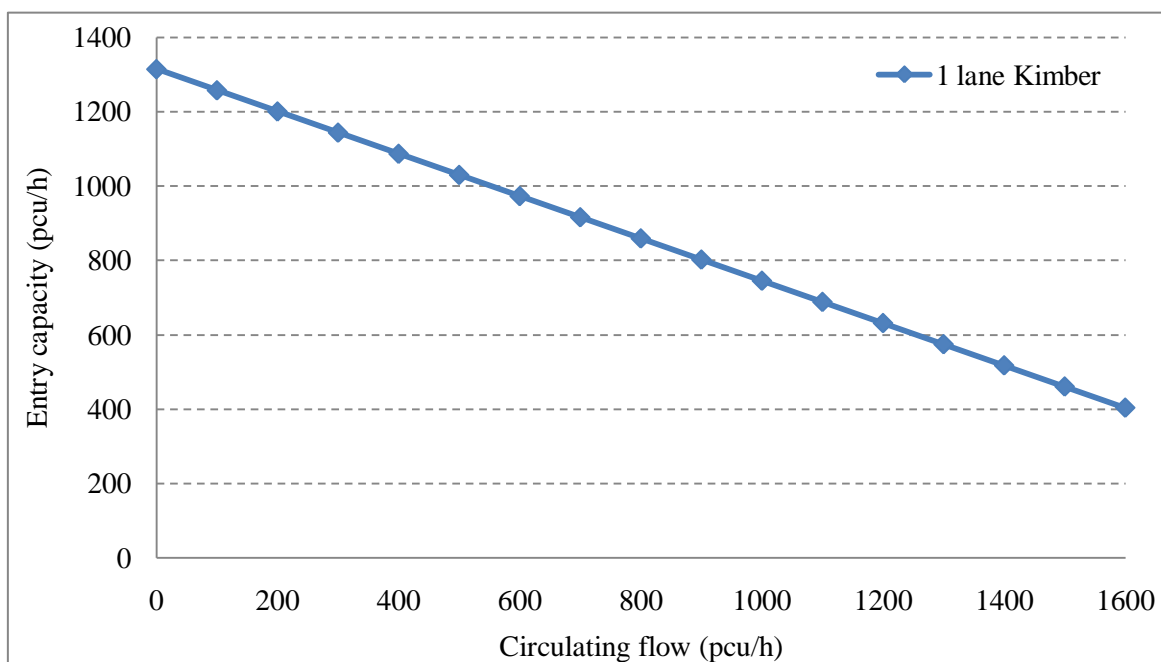


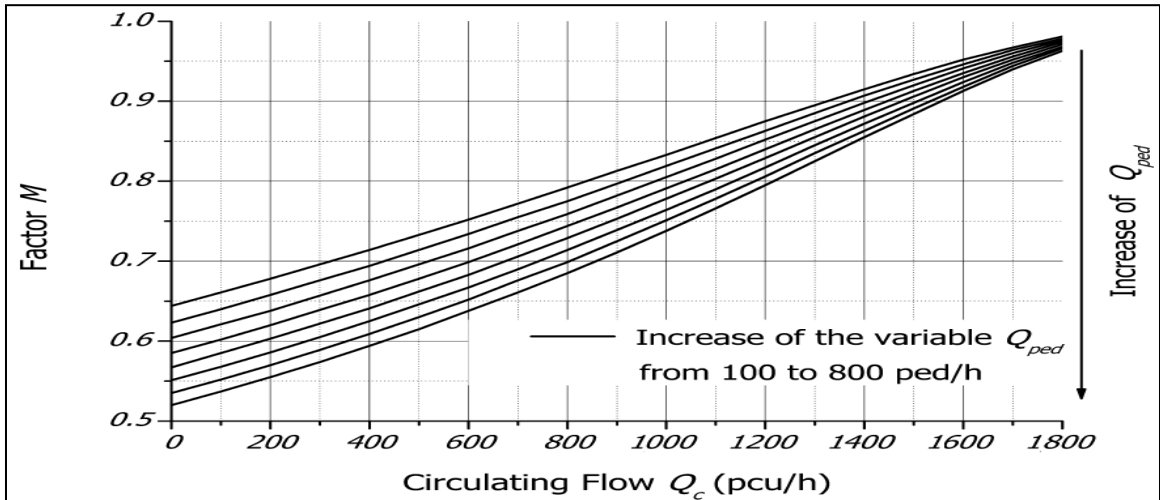
Figure 51: Kimber entry capacity model

Geometry used in Kimber Figure for one lane roundabout based on (Mauro, 2010).

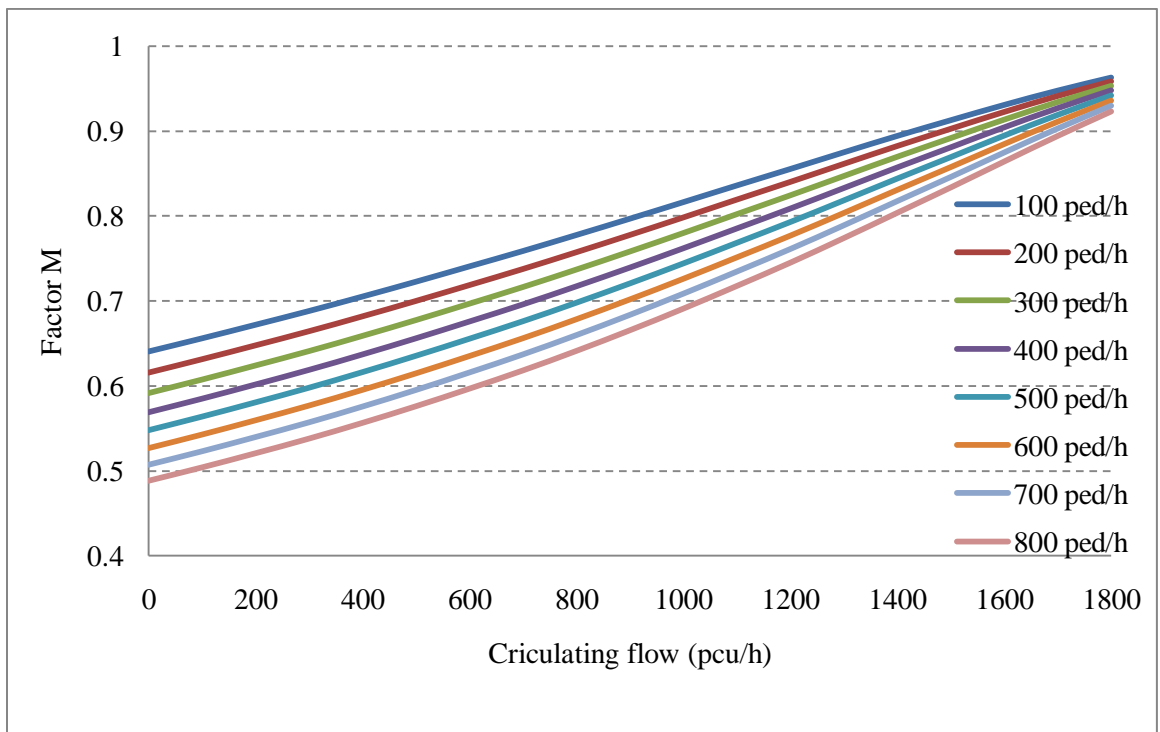
Geometry parameters	Used in the equation
e (m)	4.5
v (m)	3
l' (m)	7.5
D (m)	34
θ (°)	35
r (m)	20
F (Y-intercept)	1314

Capacity Reduction Factor:

English capacity reduction factor and English entry capacity model (Marlow and Maycock, 1982)



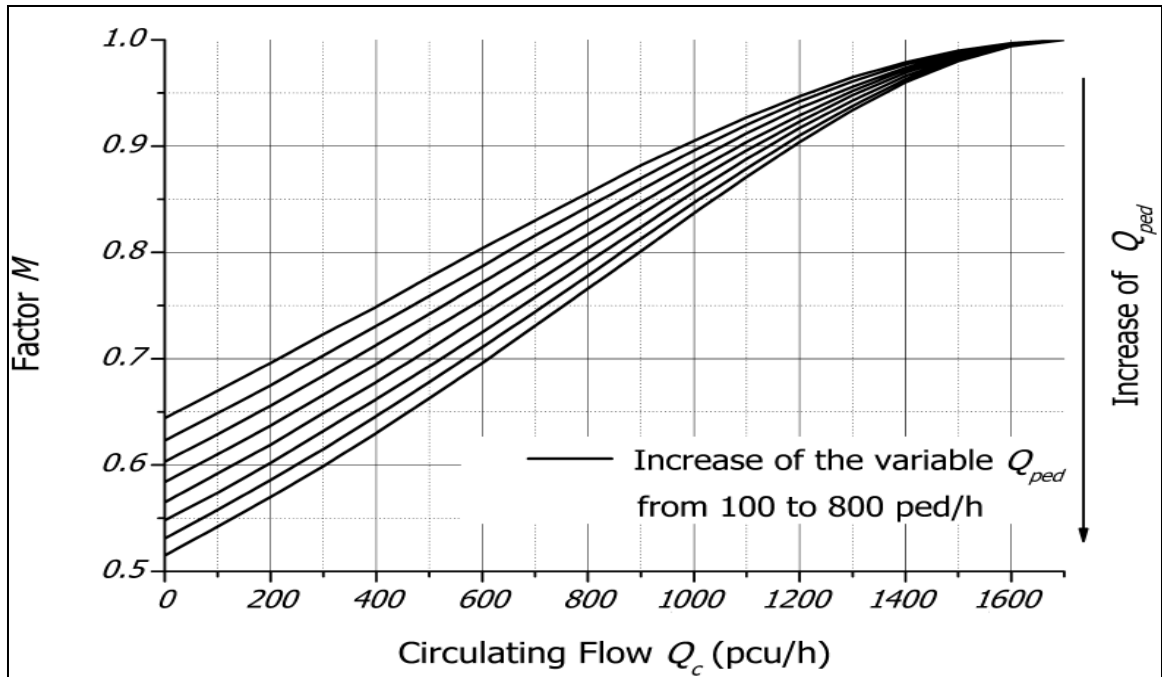
a) Reference estimates



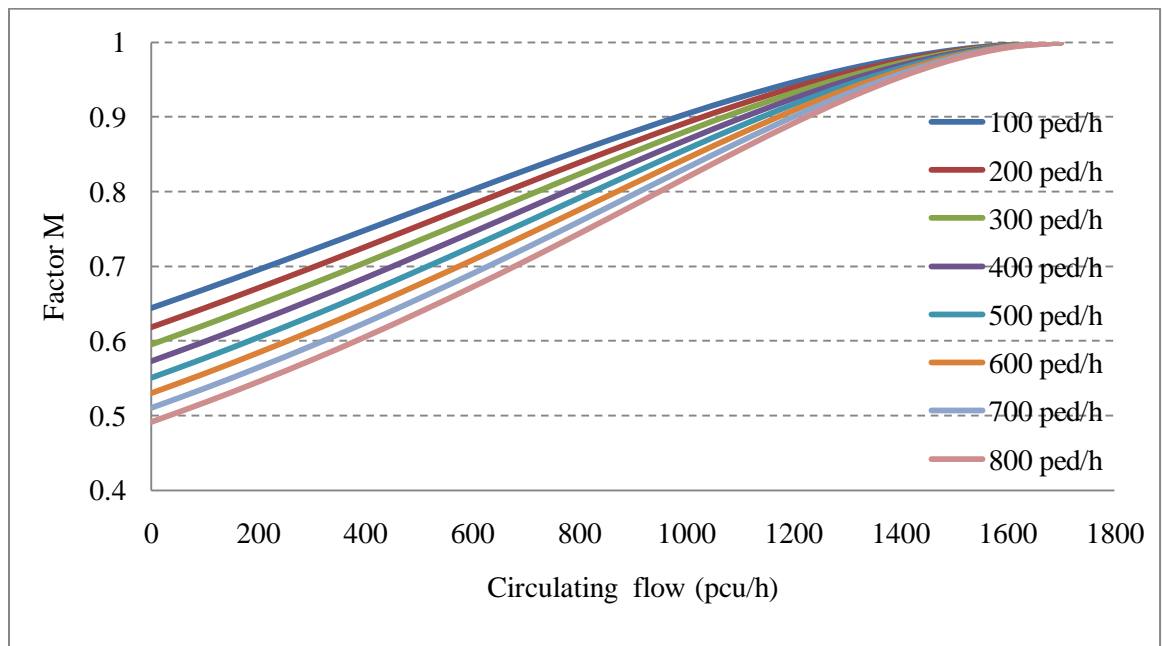
b) Model estimates

Figure 52: English entry capacity and capacity reduction factor model

English capacity reduction factor and German entry capacity model (Marlow and Maycock, 1982)



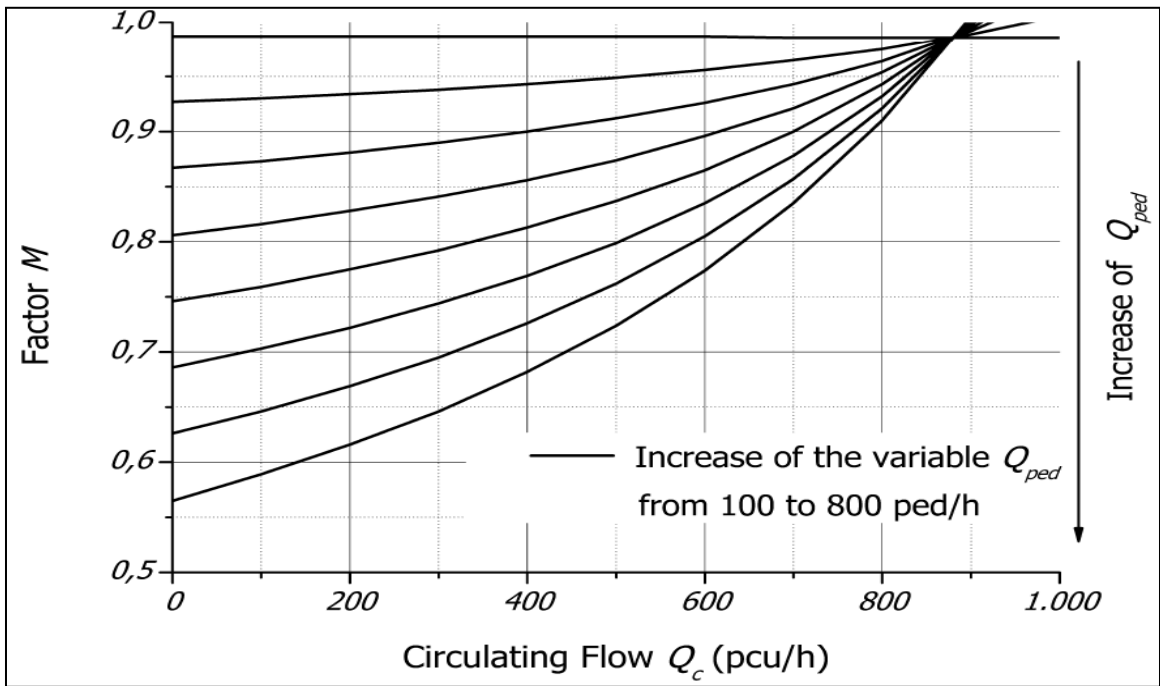
a) Reference estimates



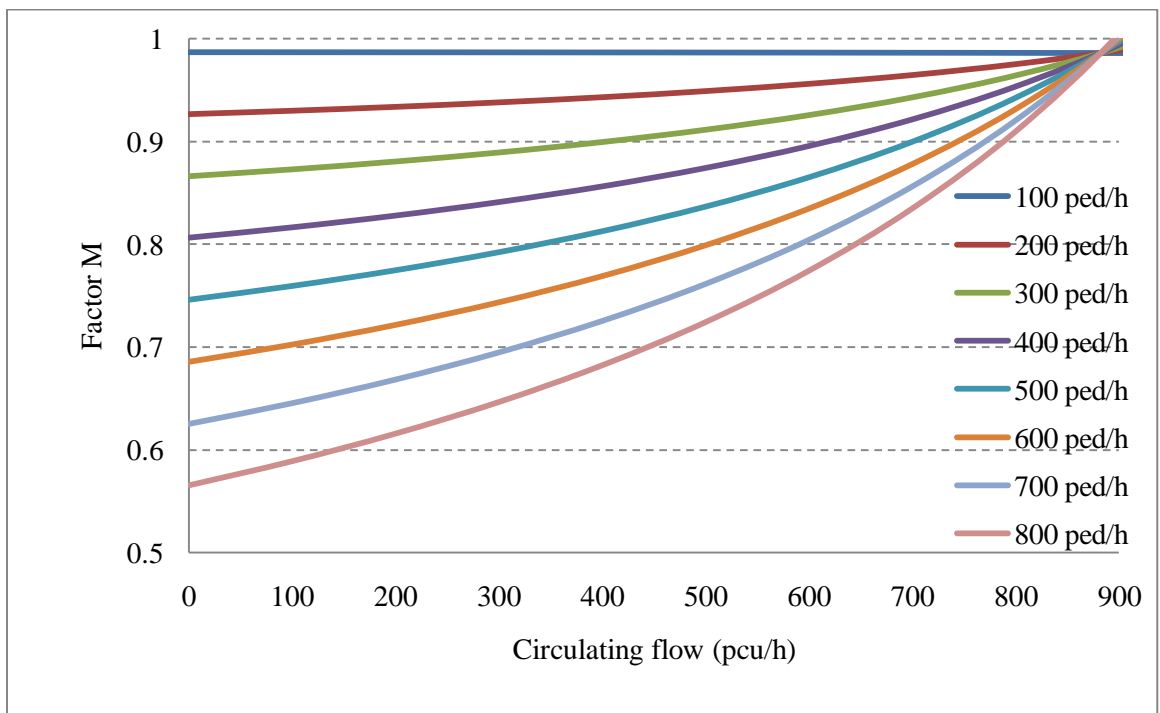
b) Model estimates

Figure 53: English capacity reduction factor and German entry capacity models

German capacity reduction factor (Brilon et al., 1993)



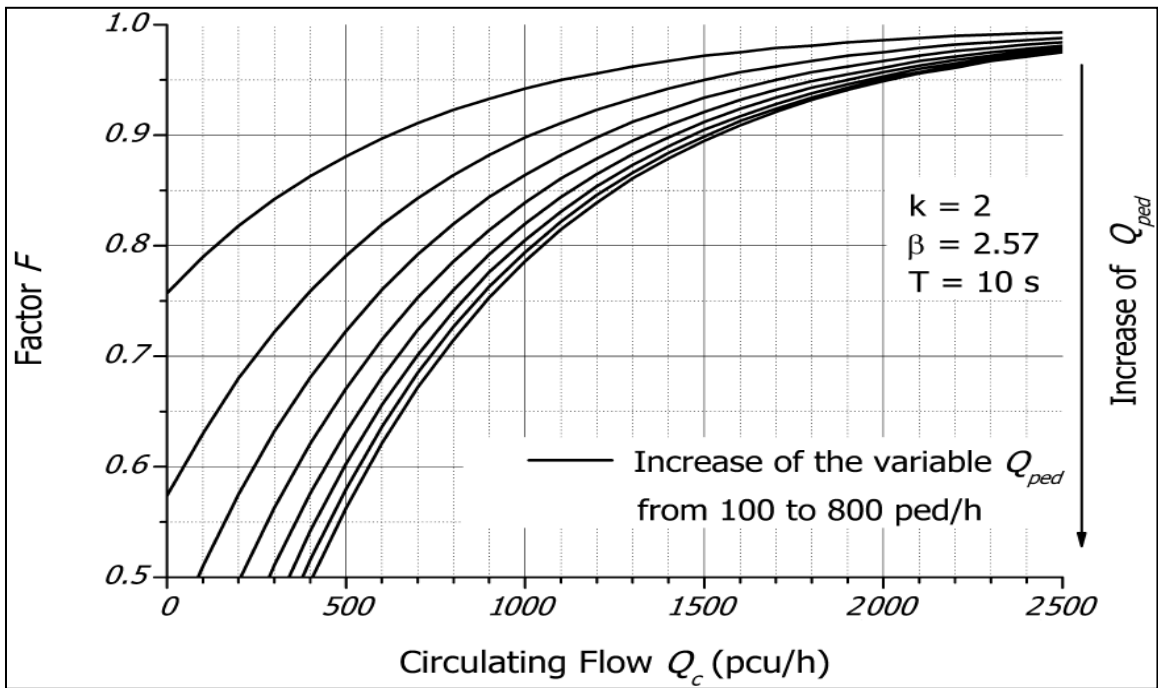
a) Reference estimates



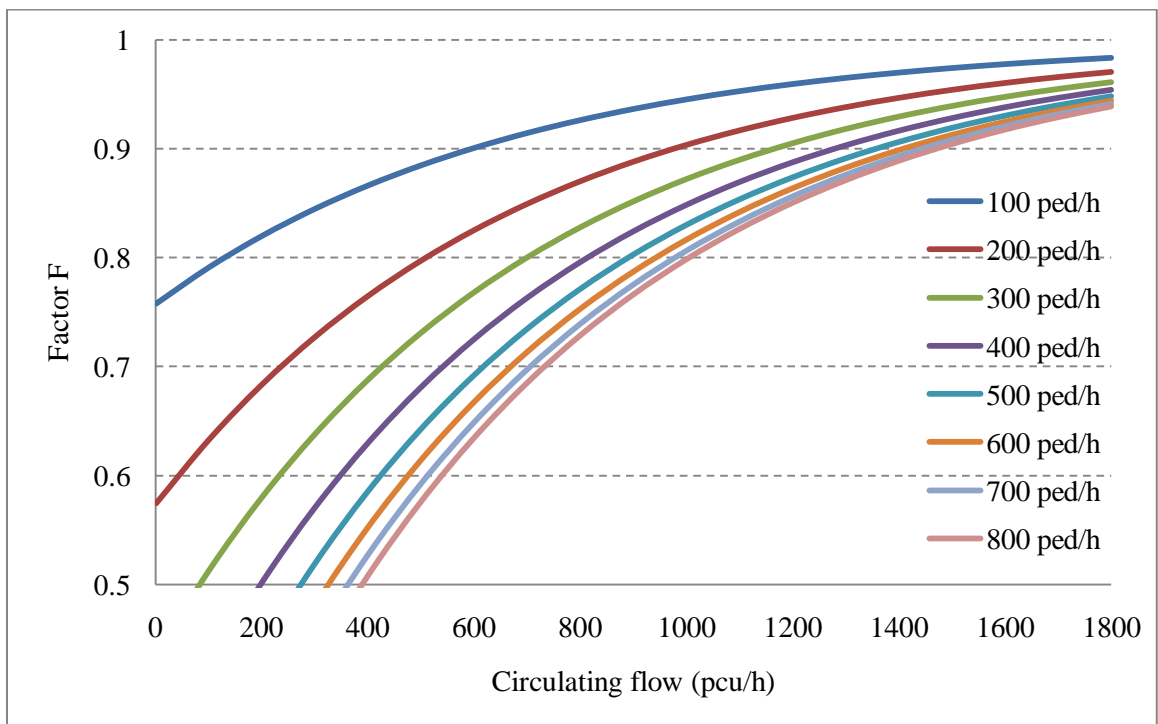
b) Model estimates

Figure 54: German capacity reduction factor model

French capacity reduction (Loua, 1992)



a) Reference estimates



b) Model estimates

Figure 55: French capacity reduction factor model

Appendix C: Coding the roundabout in VISSIM 5.2

A one- and two-lane four-leg symmetrical roundabout with different ICDs, vehicle volume, and pedestrian volume were coded using VISSIM 5.2 based on (Trueblood & Dale, 2003), and (VISSIM 5.20 User Manual, 2009). The following steps demonstrate this coding:

- 1- Set driver behavior used in VISSIM (default values) (see Figure 56 and Figure 57).

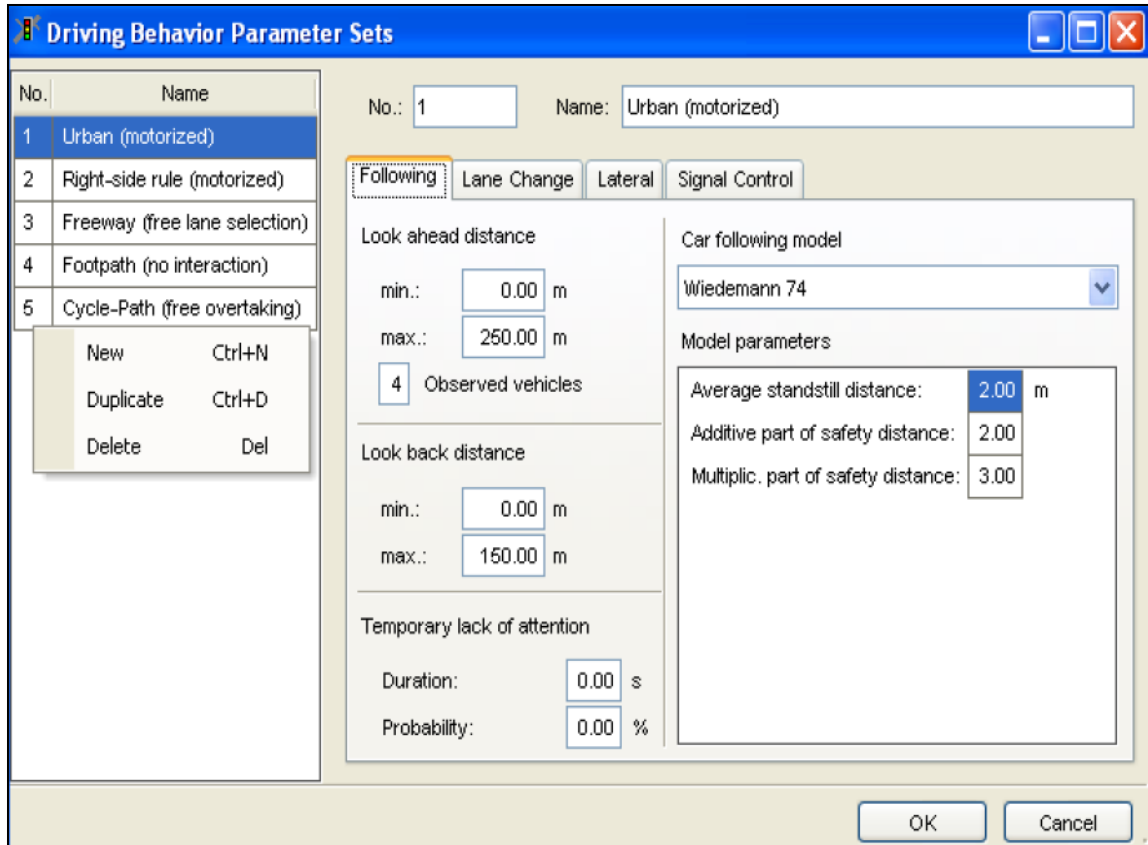


Figure 56: Driving behavior parameter sets for following vehicles in VISSIM (VISSIM 5.20 User Manual 2009)

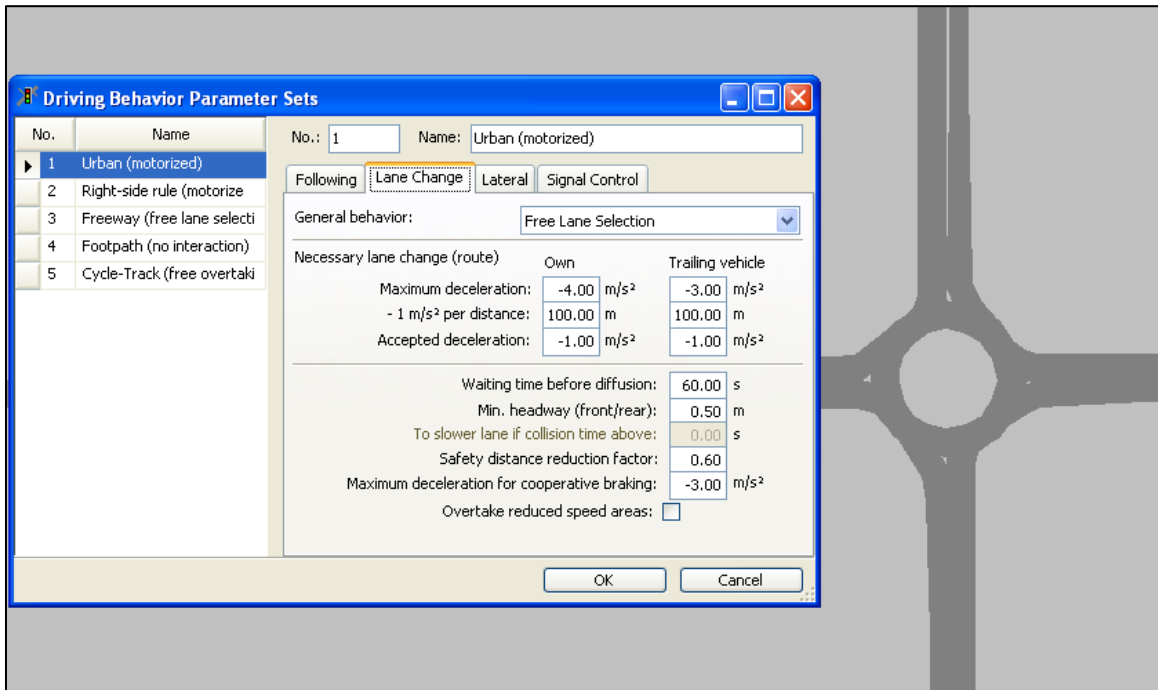


Figure 57: Driving behavior parameter sets for lane change in VISSIM (VISSIM 5.20 User Manual 2009)

- 2- Set link behavior used in VISSIM.
 - a) For car and HGV the urban (motorized) link behavior is used (see Figure 57).
 - b) For pedestrians the footpath (no interaction) is used (see Figure 57).

- 3- Select the geometry of one and two-lane roundabouts.
 - a) The one-lane 35m inscribed diameter has a special geometry based on (Bared & Edara, 2005).

Table 27: The geometry of one lane roundabout

Number of lanes	1
Inscribed diameter	34m
Entry radius	20m
Exit radius	20m
Entry width	4.5 m
Approach width	4 m
Departure width	4 m
Exit width	4.5 m
Circulatory road width	6 m

- b) The two-lane used the default geometric parameters from VISSIM. The following Table shows the coded roundabout with its geometric design.

Table 28: The geometry of two lane roundabout

Number of lanes	2
Inscribed diameter	63 m
Entry radius	23 m
Exit radius	23 m
Entry width	3.5 m
Approach width	3.5 m
Departure width	3.5 m
Exit width	3.5 m
Circulatory road width	3.5 m

- 4- Load a background based on the selected geometry. (The background drawn on a graphic paper to look symmetrical) (See Figure 58).

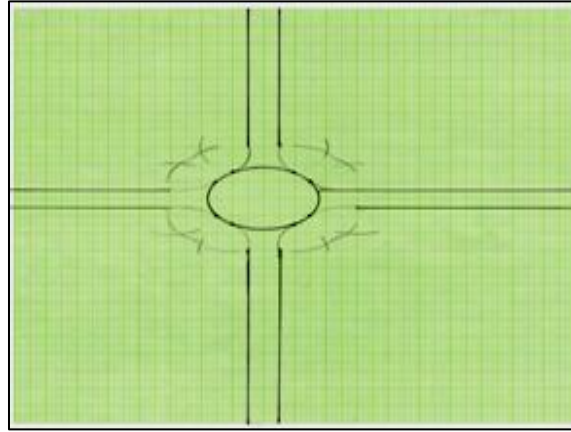


Figure 58: Roundabout back ground

- 5- Scale the background in VISSIM to the selected geometry in meters.

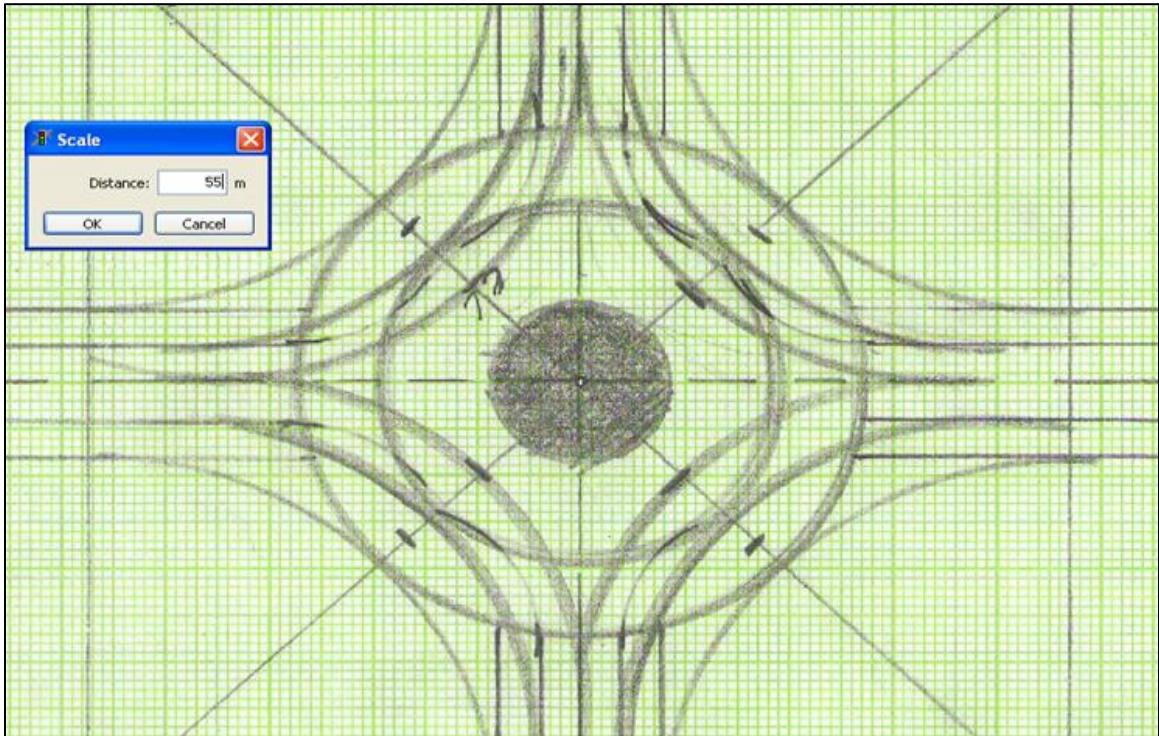


Figure 59: Scaling the roundabout

6- Draw the links and the connectors on the scaled background.

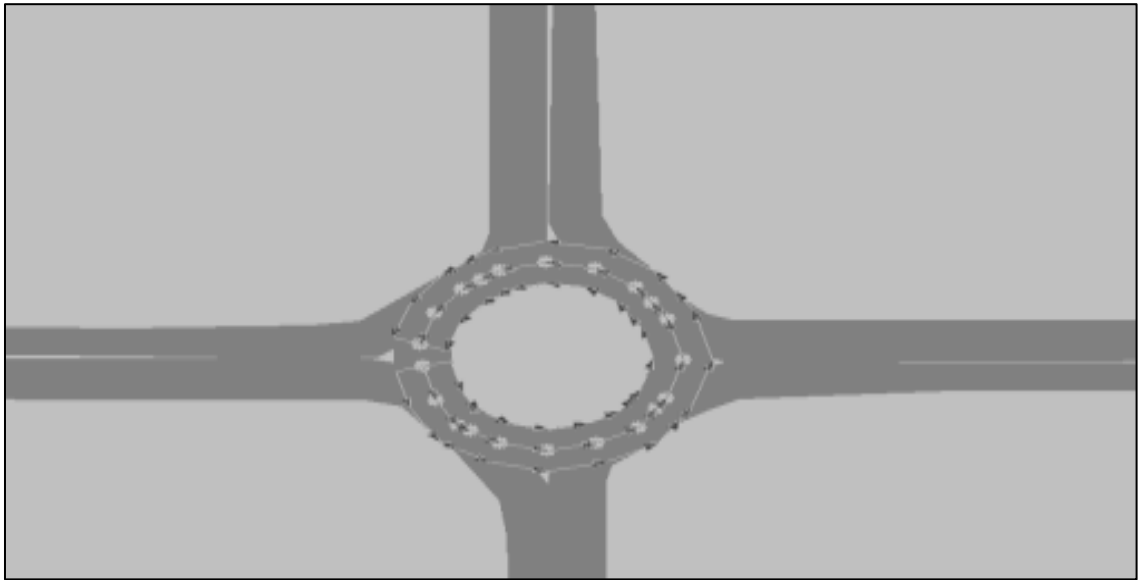


Figure 60: The coded links in VISSIM

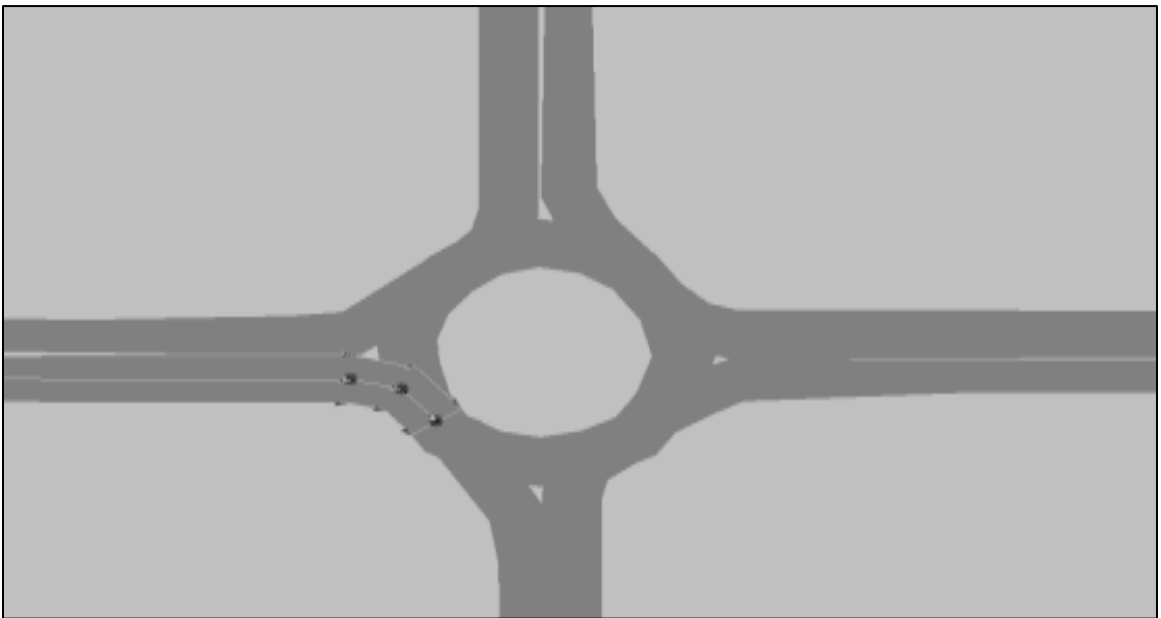
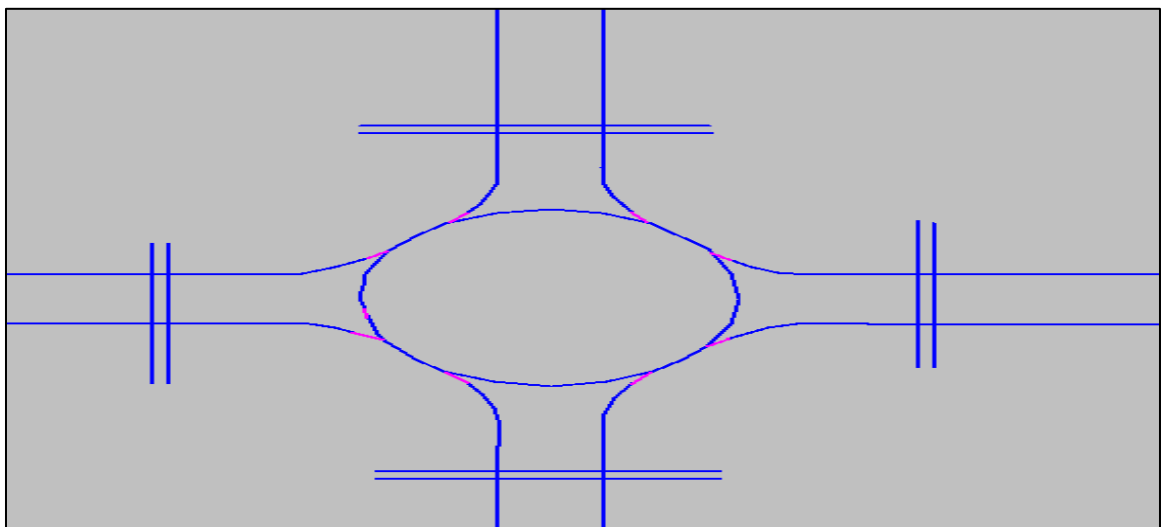
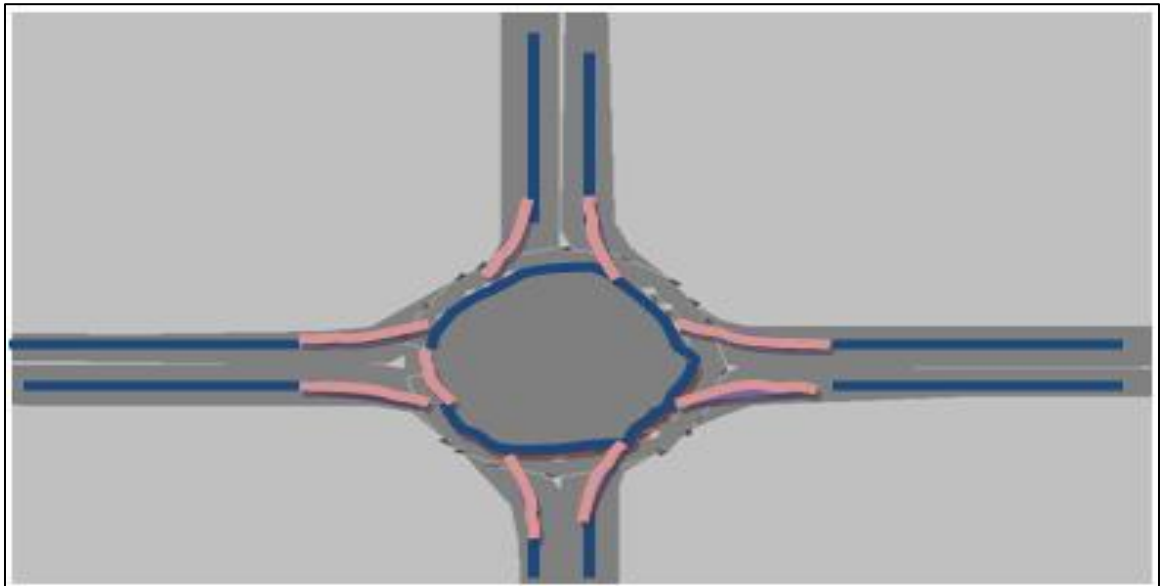


Figure 61: The coded connectors in VISSIM





	Links are in blue color
	Connectors are in pink color

Figure 62: The coded inks and connector location in one-lane roundabout in VISSIM

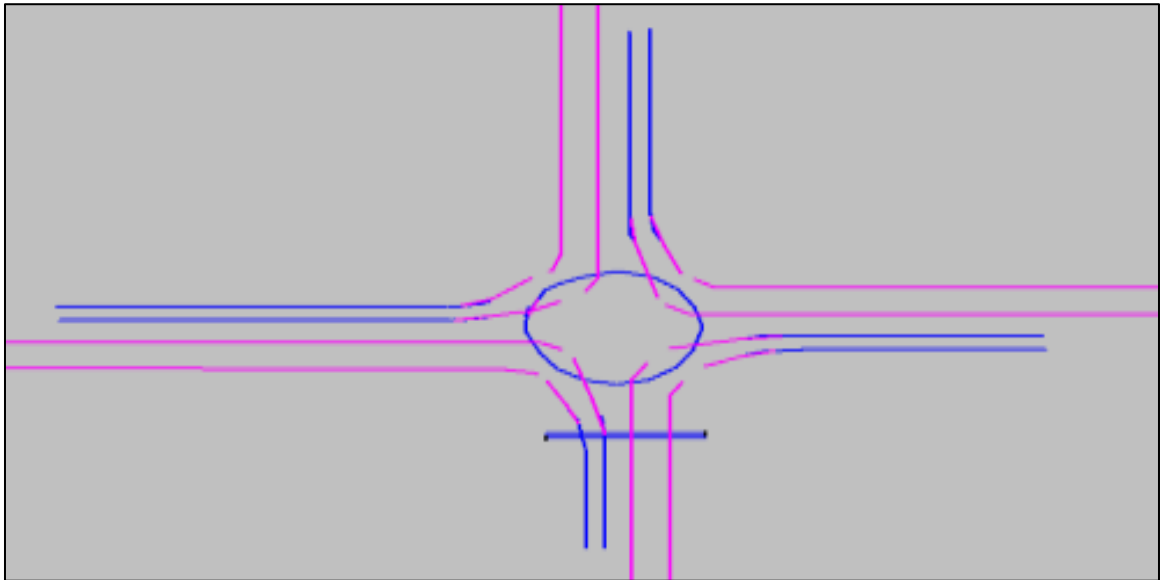


Figure 63: The coded links and connector location in two-lane roundabout in VISSIM

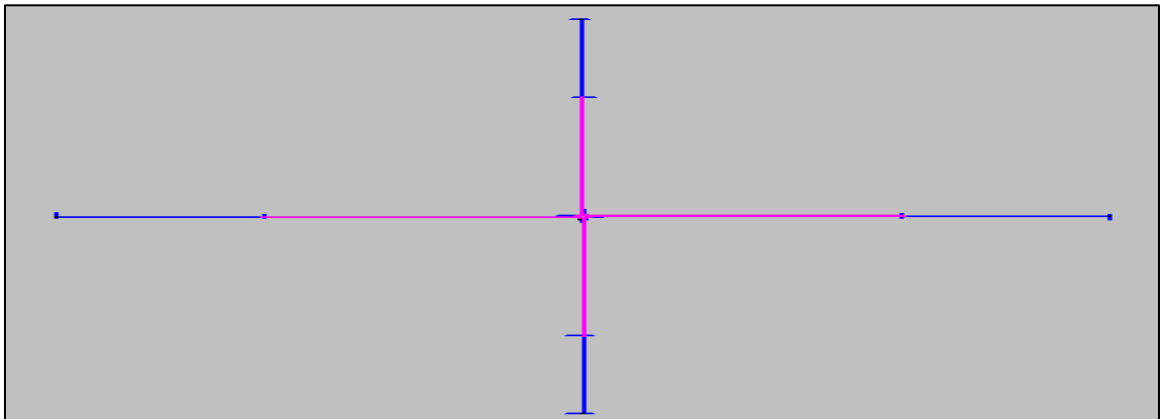


Figure 64: The coded links and connector location in two-lane roundabout in VISSIM

The links have light gray dots or blue lines. The connectors have black dots or purple lines see (Figure 60, 61, 62, 63, and 64). The parameter used in the lane change from link to connectors in a one-lane roundabout is as follows (default values used): emergency stop = 5 m back; lane change = 200 m back. The parameter used in the lane change in the connector in the two-lane roundabout is as follows: emergency stop = 500 m back; lane change = 900 m back. These values are used to make sure that vehicles change to the desired lane early and do not block

the road to change lanes (i.e., allow a large distance to change lanes [900 m] and to stop [500m] from the connector if the driver does not find a gap and will not affect the downstream queue). The pink lines are connectors. The blue lines are the links.

7- Set leg lengths, connectors and links.

- a) The pink lines are connectors.
- b) The blue lines are the links.

The link length is about 1000 m (the blue line). The connector length is 1500 m of the pink lines

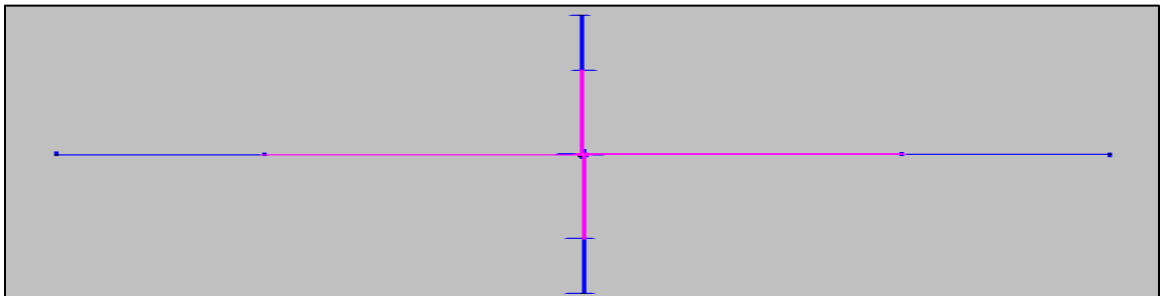


Figure 65: The link and connector lengths

8- Placement of the routing decision.

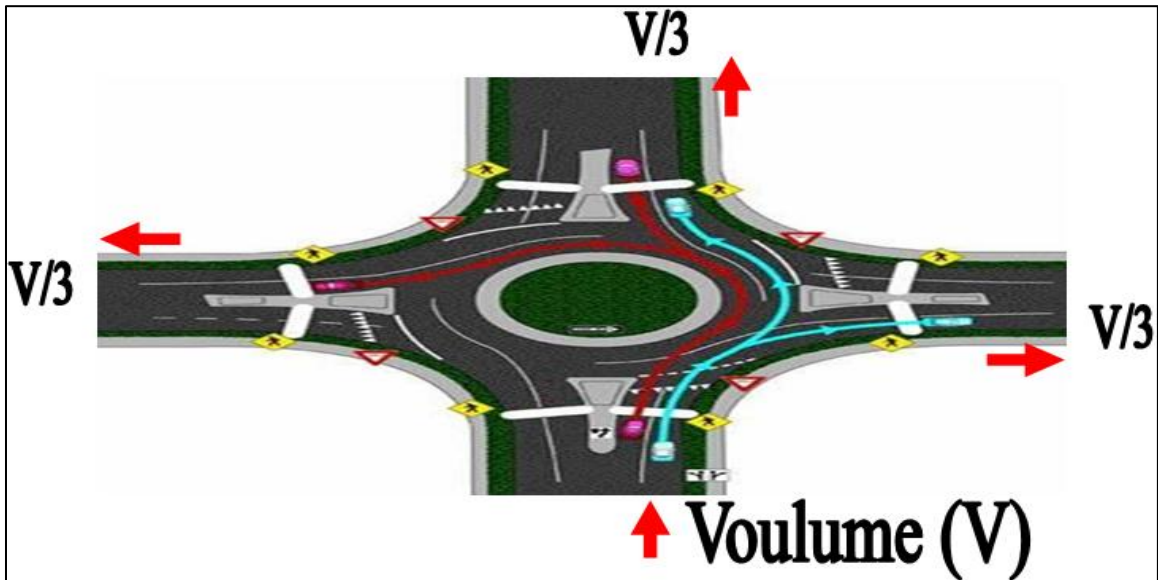


Figure 66: All route decision for two-lane roundabout and for each lane (How to Navigate Modern Roundabouts, 2011)

The flow from each approach is distributed equally to the other three approaches. Assume that no vehicle makes a u-turn as this rarely happens (See Figure 66 and Figure 67).

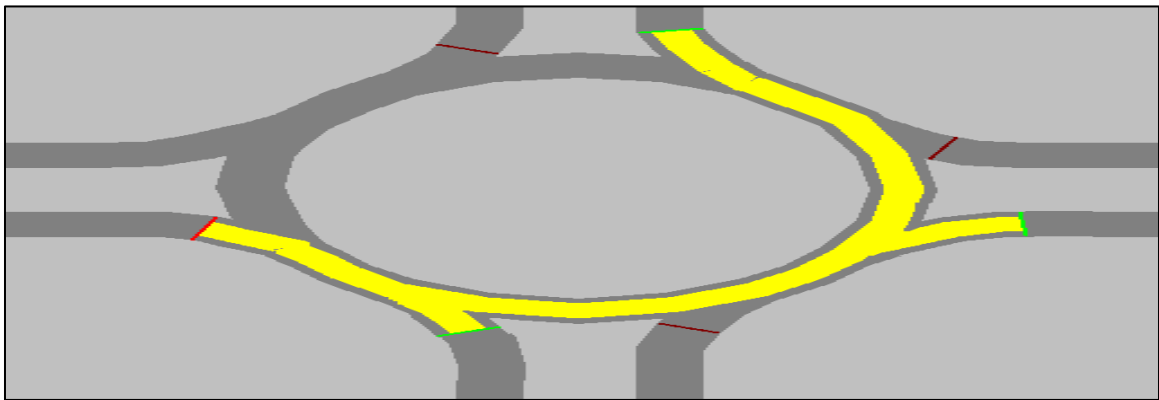


Figure 67: Route decision for one-lane roundabout in VISSIM

- 9- Put the conflicting areas in the conflicting route between entering vehicles and circulating vehicles, and the entrance, exit vehicle lanes and pedestrian crosswalk lane in one- and two-

lane roundabouts. In two lane roundabouts put the conflicting areas in the conflicting route between existing vehicles and circulating vehicles.

Table 29: Conflict area parameters

Conflicting area parameter	Parameter value	Conflicting area parameter	Parameter value
Front gap(s)	0.5	Observed adjustment lane	None
Rear gap(s)	0.5	Anticipate route	0
Safety distance factor	1.5	Avoid blocking	1
Additional stop distance (m)	0		

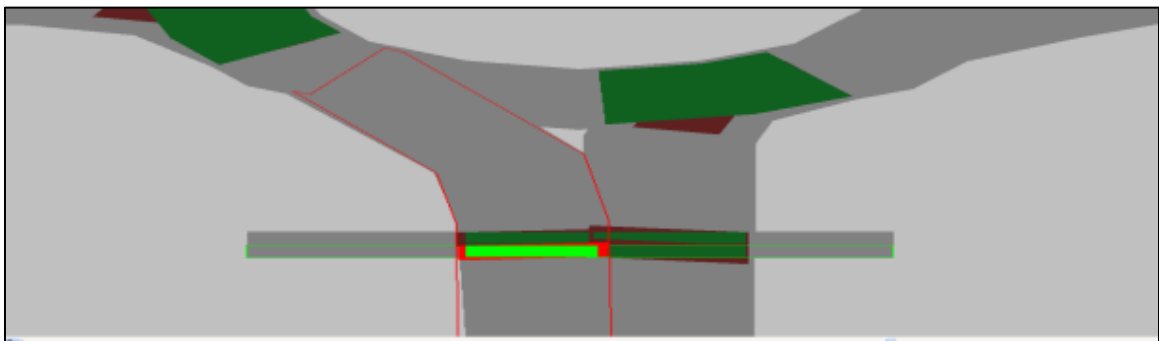


Figure 68: The coded conflict areas for pedestrians and vehicles for one-lane roundabout in VISSIM

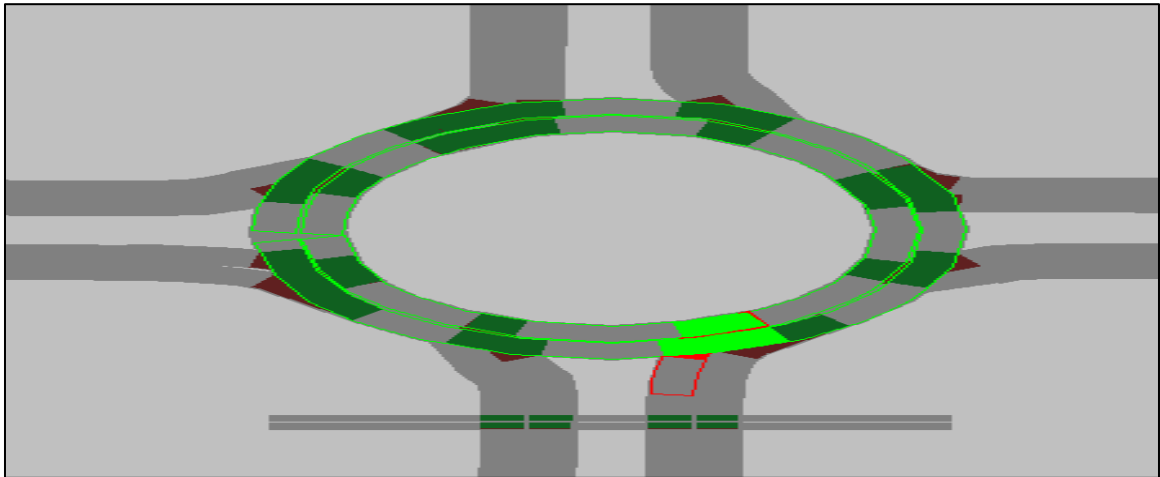


Figure 69: The coded conflicting areas for two-lane roundabout, and for pedestrians in VISSIM

- a) The right-of-way (the green mark) is for vehicles circulating in the roundabout. The approach vehicle yields (the red mark) to the circulating vehicles (See Figure 68 and Figure 69).
 4. In two-lane roundabout, the approach vehicle in the critical lane or the inner lane should yield to both conflicting lanes.
 5. In two-lane roundabout, the approach vehicle in the second lane or the outer lane should yield to the outer conflicting lane only.
 6. In one-lane roundabout, all entering vehicles should yield to all conflicting vehicles.
 7. For two-lane roundabout in the circulating lanes, assume that the right-of-way is to the vehicles circulating the road, not exiting the roundabout. So vehicles exiting the roundabout in the inner circulating lane should yield to vehicles circulating in the roundabout in the outer circulating lane.
 8. In one- and two-lane roundabouts, the right-of-way is always given to pedestrians in the exit and in the entrance vehicle approach.

The meaning of the parameters shown in Table 29 is as follows:

Based on (VISSIM 5.20 User Manual, 2009) front gap is the time that takes the yielding vehicle to enter the roundabout. The time starts when the yielding vehicle begins to enter the roundabout and after the circulating vehicle passes the entry approach and ends after the yielding vehicle enters the roundabout. Rear gap is the time in seconds from the time when the vehicle on the yielding approach passes the conflict area to the time when the vehicle in the main approach has just entered the conflict area in the main approach. Safety distance factor is used for the merging approaches like the entrance to the roundabout and the circulating road. It is a factor multiplied by the safety distance of the vehicle in the major road to estimate minimum headway by the yielding vehicle to enter the major road. Additional stop distance is the distance from the yield line where a yielding vehicle will stop. Observe adjutant lanes feature makes the yielding vehicles notice the vehicle in the main approach that is going to enter the conflict area. Anticipate routes feature makes a percentage of vehicles in the yielding approach notice the vehicles in the major approach that are not entering the conflict area. Avoid blocking feature makes percentage of circulating vehicles not entering the conflict area when there downstream of the conflicting area full with vehicles. Consequently, the circulating vehicles allow entering vehicle to enter the roundabout.

10- Insert approach speed, acceleration and deceleration:

- a) For cars and HGVs, the desired speed is 50km/h; minimum entrance speed is 48 km/h; maximum entrance speed is 58 km/h.
- b) Pedestrian speed: 5km/h; minimum speed is 4 km/h; maximum speed is 6 km/h.
- c) The maximum and desired acceleration and deceleration used default curves.

11- Put the reduced speed area in the circulating road (the green rectangle [see Figure 70]).

For cars and HGVs:

The desired speed = 30 km\h

Minimum speed = 30 km\h

Maximum speed = 35 km\h

Acceleration and Deceleration = 2 m/s^2

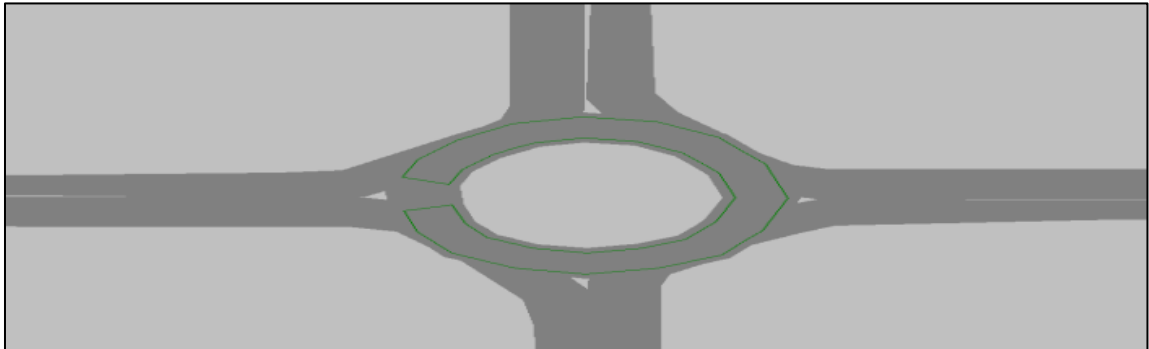


Figure 70: The coded reduced speed area marked in green in VISSIM

12- Insert desired speed decision in the approach (the green mark [See Figure 71]).

The Desired speed decision location is 30 m from the circulating roadway or roundabout.

For Car, and HGV

Vehicle desired speed = 30 km/h

Vehicle minimum speed = 30 km/h

Vehicle maximum speed = 35 km/h

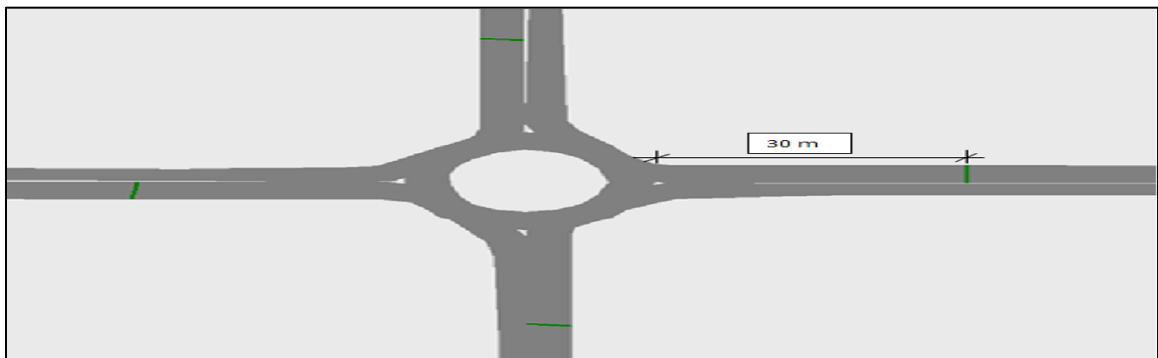


Figure 71: The coded desired speed decision marked in green in VISSIM

13- Insert delay measure (travel time), and data collection points in the approach (a green mark).

- a) The delay measured from 1500 m from the roundabout until the entrance for one-lane and two-lane roundabout. The measure of the delay starts from 1800 seconds to 5400 seconds. The 1800 seconds is a warm-up period.

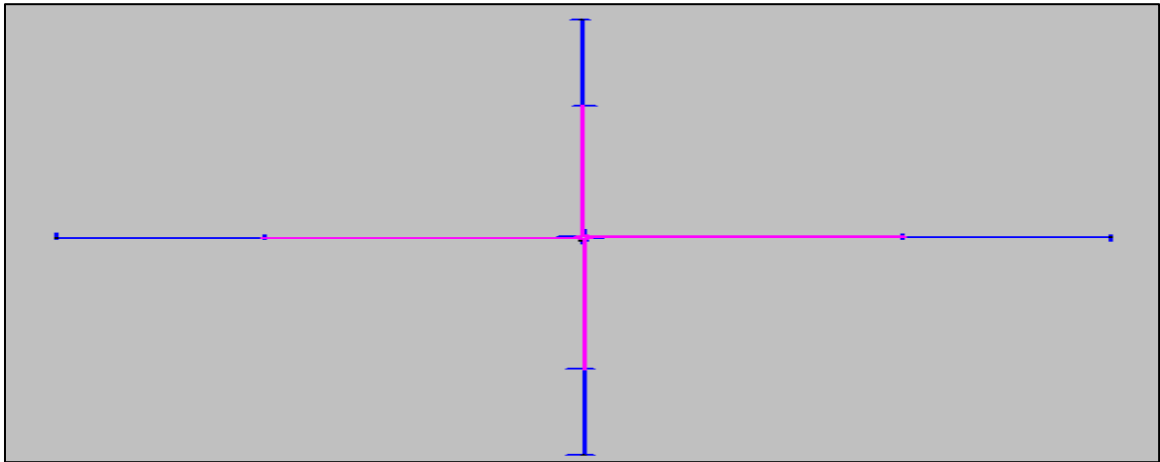


Figure 72: The delay measure start and end

14- Insert vehicle composition.

- a) Truck and car percentages: Truck HGV (heavy good vehicle) is 2%; car is 98%; bus is not included. Vehicle desired speed is 50 km/h; vehicle minimum speed = 48 km/h; vehicle maximum speed = 58 km/h.
- b) Pedestrians percentage (100%): pedestrian desired speed is 5 km/h; pedestrian minimum speed = 4km\h; Pedestrian maximum speed = 6 km/h.

15- Vehicle input traffic volume.

- a) The vehicle generation mark is located at the beginning of the approach far from the roundabout (about 2500 m) for one and two lane roundabouts.
- b) The vehicle and pedestrian volume is inputted in vehicles per hour or pedestrians per hour regardless of the simulation time (5400 minute (hour and a half)).
- c) The pedestrian mark is located at the beginning of the crosswalk in both directions.
- d) Pedestrian volume is located in the major approach only in order not to affect entry volume from the other approaches.

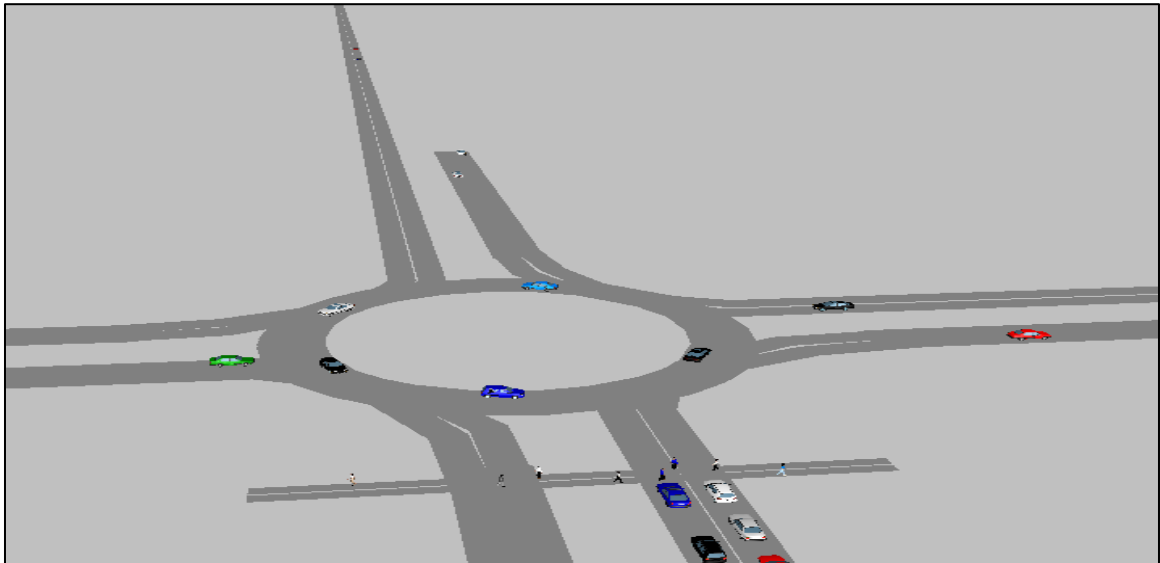


Figure 73: Pedestrian volume generated in the major approach in VISSIM

Coding for Validation:

The codes used for validation is based on the two lane roundabout code with some modifications (adding different flare length based on the different selected three sites). These three codes (based on the three sites) used three roundabout ICDs chosen from The City of Waterloo for the validation purpose. (more detailed about the flare is presented in following appendix [Appendix D]).

Appendix D: Field data collection methodology and coding VISSIM for validation

Video data was collected from three roundabouts in Waterloo. These roundabouts are: University Ave W/ Ira Needles; Erb St. W/ Ira Needles; and Sawmill Rd. / Arthur St. S (HW 85). This appendix illustrates how the field data are collected.

The detailed collected data and VISSIM coding are as follows:

Table 30: Data collection recording condition

Roundabout location	Description of queue length as noticed	Recording period	Number of lanes	Road Condition
University Ave W/ Ira Needles	Low	2 hours (3:00 – 5 PM)	One-lane and flared	Excellent (sunny day and dry road)
Erb St. W/ Ira Needles	Medium	1 hour (2:30 – 3:30 PM)	One-lane and flared	Excellent (cloudy day and a very light snow)
Sawmill Rd. / Arthur St. S (HW 85)	High	1 hour (4:14 – 5:14 PM)	One-lane and flared	Ok (cloudy day and a moderate snow)

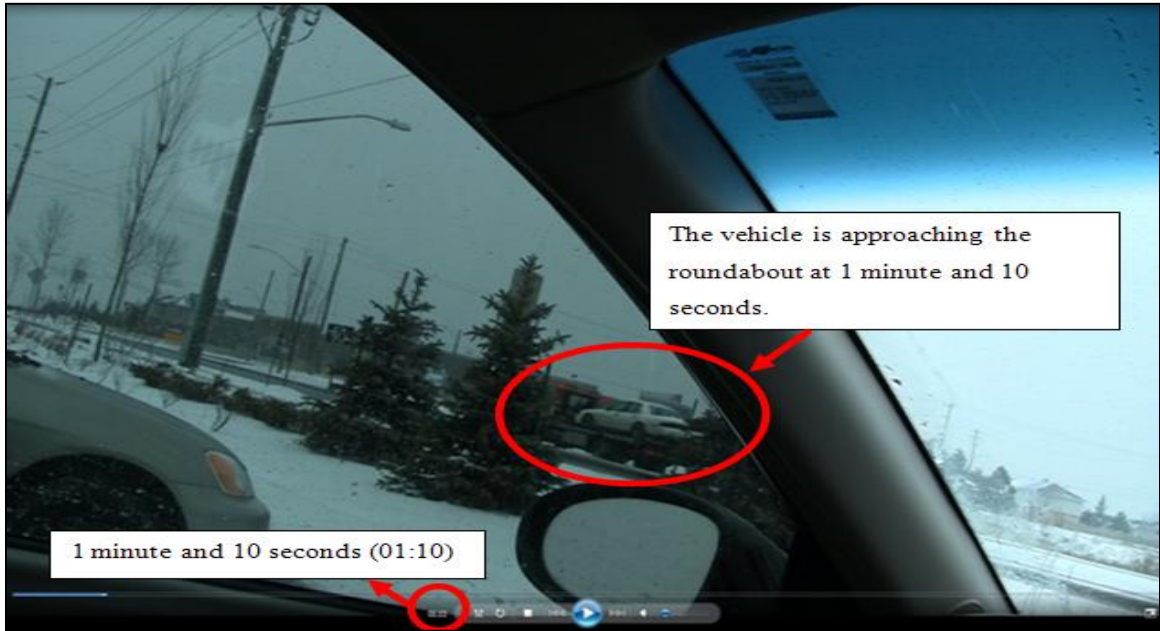


Figure 74: A truck in a roundabout approach

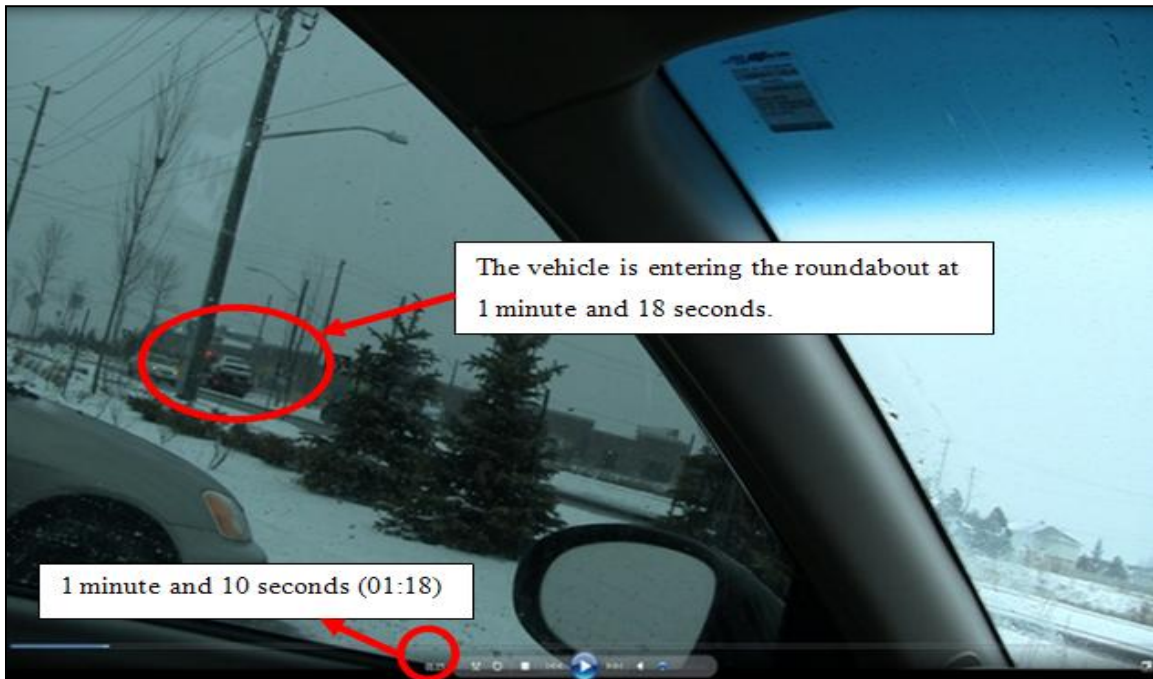


Figure 75: A truck at the yield line or roundabout entry

Average vehicle delay is measured in a video recording as follows:

- 1- Record the time a vehicle approaches the roundabout upstream (Figure 74) and the time the vehicle passed the yield line downstream (Figure 75), and subtract these two times to get vehicle travel time. The average vehicle delay is measured when there is a conflicting volume causing a noticeable reduction in the speed or the stopping of the entering vehicle.

Note:

- a- For the roundabout on Highway 85, all vehicle approaching times and entering times are recorded for the one hour period. So the average vehicle delay is for all vehicles. In other words, the average vehicle delay not only measured when a queue existed but during the whole one-hour period. For the other two sites, vehicle delay is recorded when queue is formed or when entering vehicle reduced its speed to enter the roundabout.
- b- There is a traffic light upstream that causes the vehicles to arrive in platoons (see Figure 76). The traffic light is 3.9 km away from the roundabout.
- c- For University Ave W/ Ira Needles location, the vehicle delay is measured in the first hour.

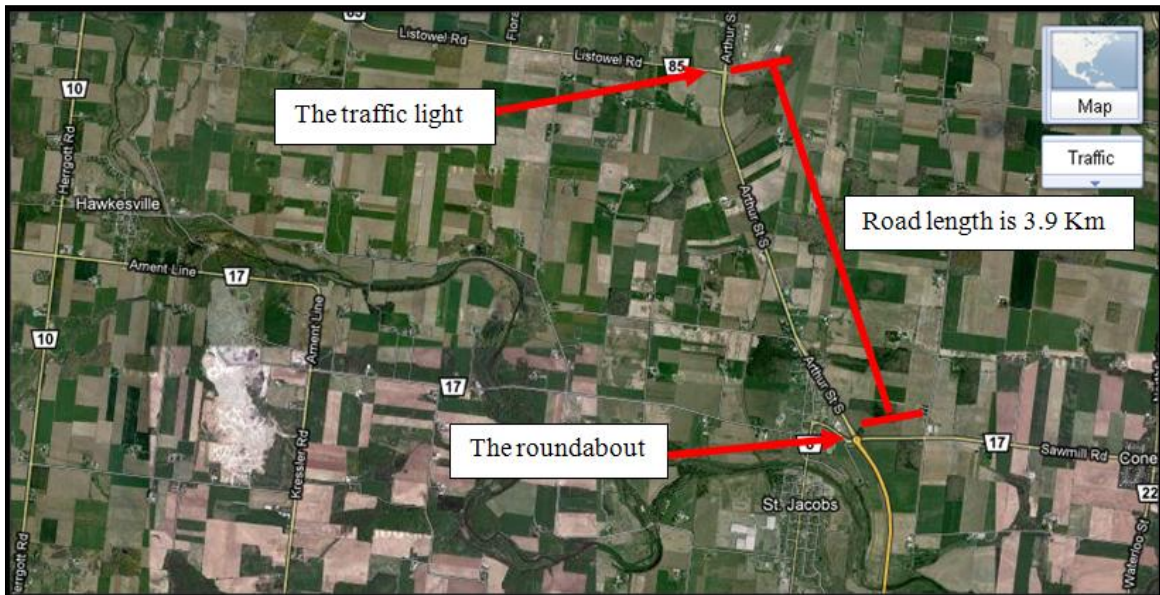


Figure 76: Google satellite picture for Sawmill Rd. / Arthur St. S (HW 85)

- 2- Find the minimum time for a vehicle approaching the roundabout upstream until it passes the yield line downstream. This time should be measured when there is no conflicting volume or any impedance such as pedestrians.
- 3- Subtract step 2 from step 1 to find the single vehicle delay.
- 4- Average step 3 for all vehicles to get the average vehicle delay.

The three roundabouts are coded in VISSIM. The three roundabout Inscribed Circle Diameter (ICD) and flare length are taken from Google map. The following features are considered in coding VISSIM, and the default parameters values in VISSIM are used.

University Ave W/ Ira Needles roundabout



Figure 77: Roundabout in the University Ave W/ Ira Needles as video recorded

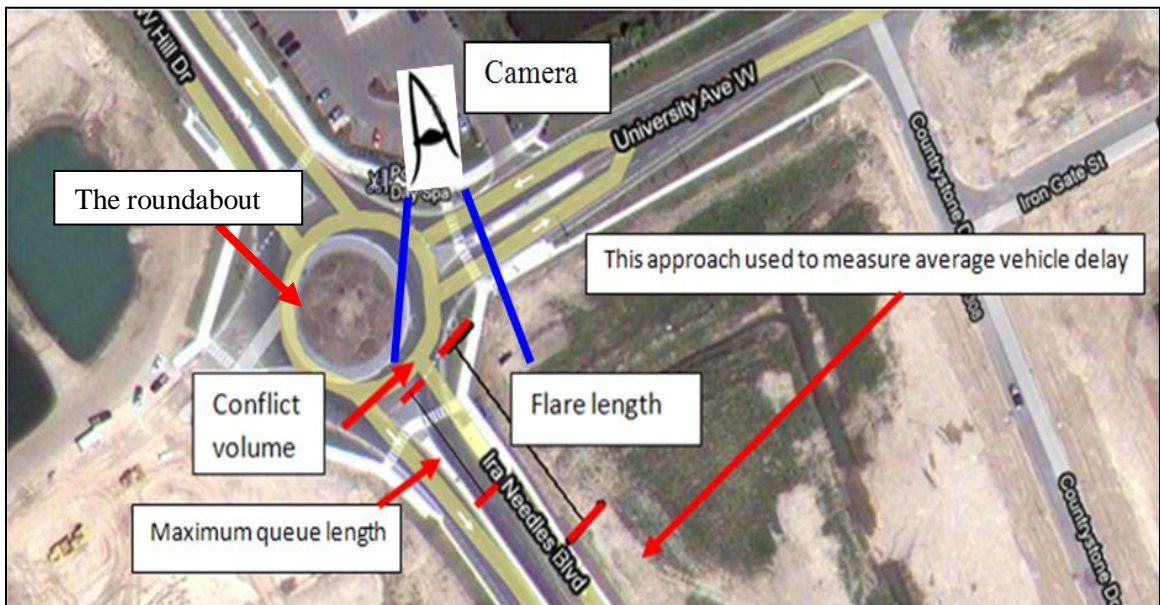


Figure 78: Google satellite picture for University Ave W/ Ira Needles roundabout

Features from field and VISSIM:

Flare length in VISSIM and in site = 63.33m

Maximum queue length or the tail of the queue far way from the yield line = 40.37m.

Two-lane roundabout is used in VISSIM because the flare length of 63.33 m is higher than the maximum queue length of 40.37 m.

Inscribed circle diameter (ICD) in VISSIM and in site = 54 m

The posted speed on the road = 60 km/h

Speed used in VISSIM = 48 – 58 km/h

Entering and circulating speed in VISSIM = 30 – 35 km/h

Entry speed discussion:

For a single lane 35m ICD roundabout with a posted speed of 60.8 km/h, the average approach and entering speed is as follows:

Table 31: Field speed data in kilometers per hour (Anglastro, 2010)

statistical measures	n*	Mean approach speed (km\h)	Standard deviation of approaching speed (km\h)	Minimum approaching speed (km\h)	Maximum approaching speed (km\h)
App spd*	98	54.00	7.49	35.41	70.81
EntSpd*	98	34.87	3.94	28.97	41.84
DiffSpd*	98	19.07	6.90	4.83	37.01
MeanAPPSpd*	98	48.73	7.50	25.75	64.70
MeanEntSpd*	98	29.98	2.98	25.75	35.41
DiffMeanSpd*	98	18.72	6.73	0	34.12

*n: Number of observations, App spd: 85th percentile approach speed, entSpd: 85th percentile entrance speed, DiffSpd: Difference (85th approach speed – 85th entrance speed), MeanAPPSpd: Approach mean speed, MeanEntSpd: Entrance mean speed, DiffMeanSpd: Difference (approach mean speed – entrance mean speed).

Based on the table above the average approach speed (54 km/h) and posted speed (60 km/h), drivers tend to drive below the posted speed when approaching the roundabout. Therefore, coding VISSIM with a speed slightly lower than the posted speed reflects the real world.

The delay measured on the critical lane in the video recording and VISSIM:

Average vehicle delay for the University Ave W/ Ira Needles site using VISSIM equal to 5.38 seconds (the distance road section the delay measured is from 1500m upstream to the yield line); this long distance of 1500 m is considered to be similar to the experimental design used in VISSIM code.

Delay measured from video recording = 5.6 seconds (the distance of the delay measure is from 40.37m upstream to the yield line).

Table 32: Vehicle volume at University Ave W/ Ira Needles

	Entry volume (veh/h) in the critical Lane		Entry volume (veh/h) in the second lane		Conflicting volume in the inner lane (veh/h)		Conflicting volume in the outer lane (veh/h)	
	cars	HGVs*	cars	HGVs	cars	HGVs	cars	HGVs
Total volume of vehicles per hour	493	10	294	11	3	2	117	4
Total percentage of trucks	2.5%				4.7%			

*HGV: Heavy Good Vehicle.

Sample calculation for the percentage of HGVs:

Total number of vehicles in the approach lane per hour (in the critical lane and second lane) =
 $493 + 10 + 294 + 11 = 808$ veh/h

Total number of HGVs in the approach lane per hour (in the inner lane and outer lane) = $10 + 11$
= 21 HGVs/ h

Total percentage of trucks used in the approach lane

$$\begin{aligned} &= \frac{\text{Total number of HGVs in the approach lane per hour (in the critical lane and second lane)}}{\text{Total number of vehicles in the approach lane per hour (in the critical lane and second lane)}} \\ &* 100 = \frac{21}{808} * 100 = 2.5 \% \end{aligned}$$

Total number of vehicles in the conflicting lane per hour (in the inner lane and outer lane) = 120
veh/h

Total number of HGVs in the conflicting lane per hour (in the inner lane and outer lane) = 6
HGVs/ h

Total percentage of trucks used in the conflicting lane

$$\begin{aligned} &= \frac{\text{Total number of HGVs in the conflicting lane per hour (in the inner lane and outer lane)}}{\text{Total number of vehicles in the conflicting lane per hour (in the inner lane and outer lane)}} \\ &* 100 = \frac{6}{126} * 100 = 4.7 \% \end{aligned}$$

Erb St. W/ Ira Needles Roundabout:



Figure 79: Roundabout in the Erb St. W/ Ira Needles as video recorded

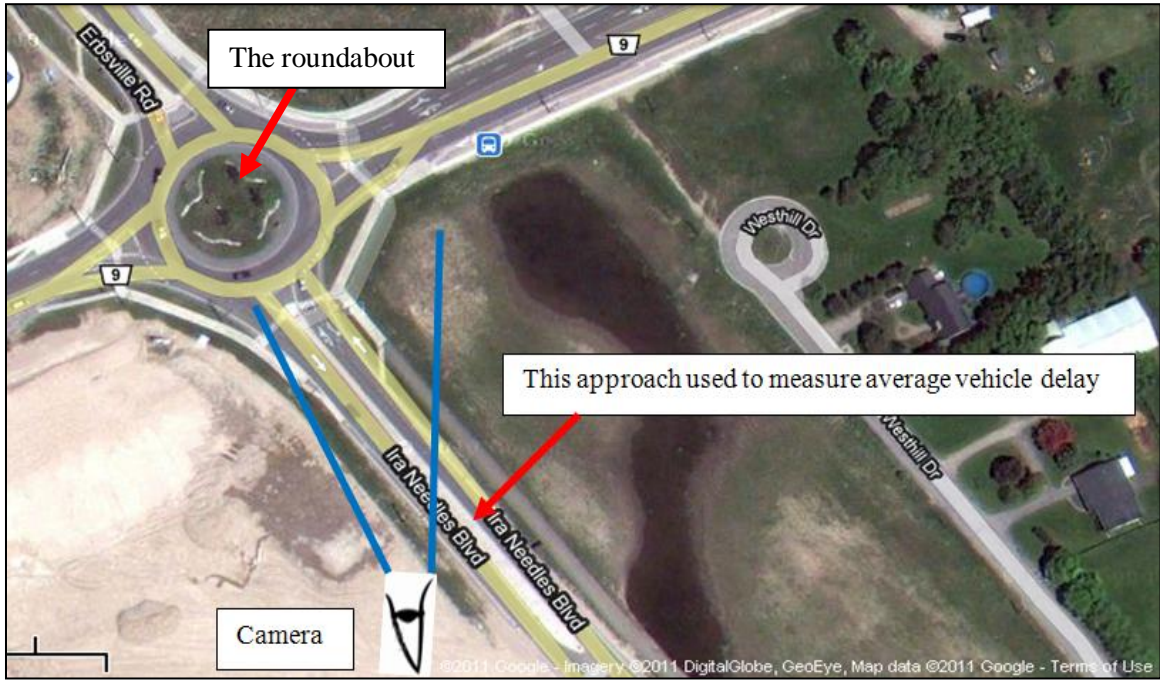


Figure 80: Google satellite picture for Erb St. W/ Ira Needles

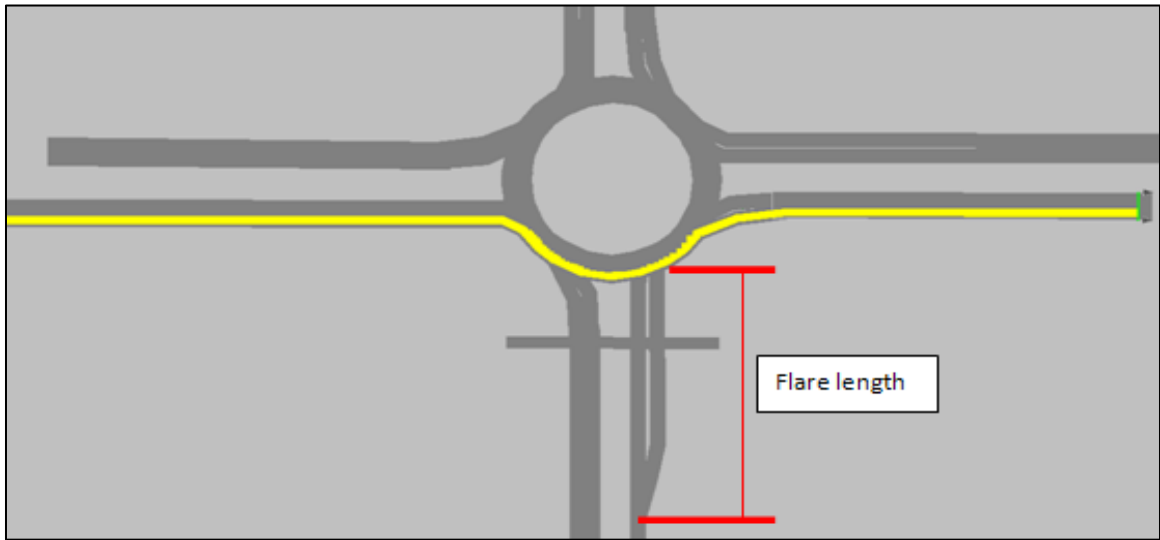


Figure 81: The flare length for Erb St. W/ Ira Needles and Sawmill Rd. / Arthur St. S roundabouts as coded in VISSIM

Features from field and VISSIM:

Flare length in VISSIM and site = 62.42m.

One flared lane roundabout is used in VISSIM because the flare length is lower than the maximum queue length.

Maximum queue length (the tail of the queue) = 90 m.

ICD in site = 55 m.

ICD in VISSIM = 54 m.

The posted speed on the road = 60 km/h

Speed used in VISSIM = 48 – 58 km/h

Entering and circulating speed in VISSIM = 30 - 35km/h

The average vehicle delay is measured on the critical lane in the video recording and VISSIM:

Average vehicle delay from VISSIM = 7.88 seconds (the distance of the delay measure is from 1500m upstream to the yield line similar to the experimental design code).

Delay measured from video recording = 10.23 seconds (the distance of the delay measure is from 90m upstream to the yield line).

Table 33: Vehicle volume at Erb St. W/ Ira Needles

	Entry volume (veh/h) in the critical Lane		Entry volume (veh/h) in the second lane		Conflicting volume in the inner lane (veh/h)		Conflicting volume in the outer lane (veh/h)		Exit volume (veh/h)
	cars	HGVs	cars	HGVs	cars	HGVs	cars	HGVs	cars and HGVs
Total volume of vehicles per hour	372	17	73	19	136	6	268	19	476
Total percentage of trucks	7.3%				5.5%				-

Sawmill Rd. / Arthur St. S (HW 85) Roundabout:



Figure 82: Roundabout in the Sawmill Rd. / Arthur St. S (HW 85) as video recorded

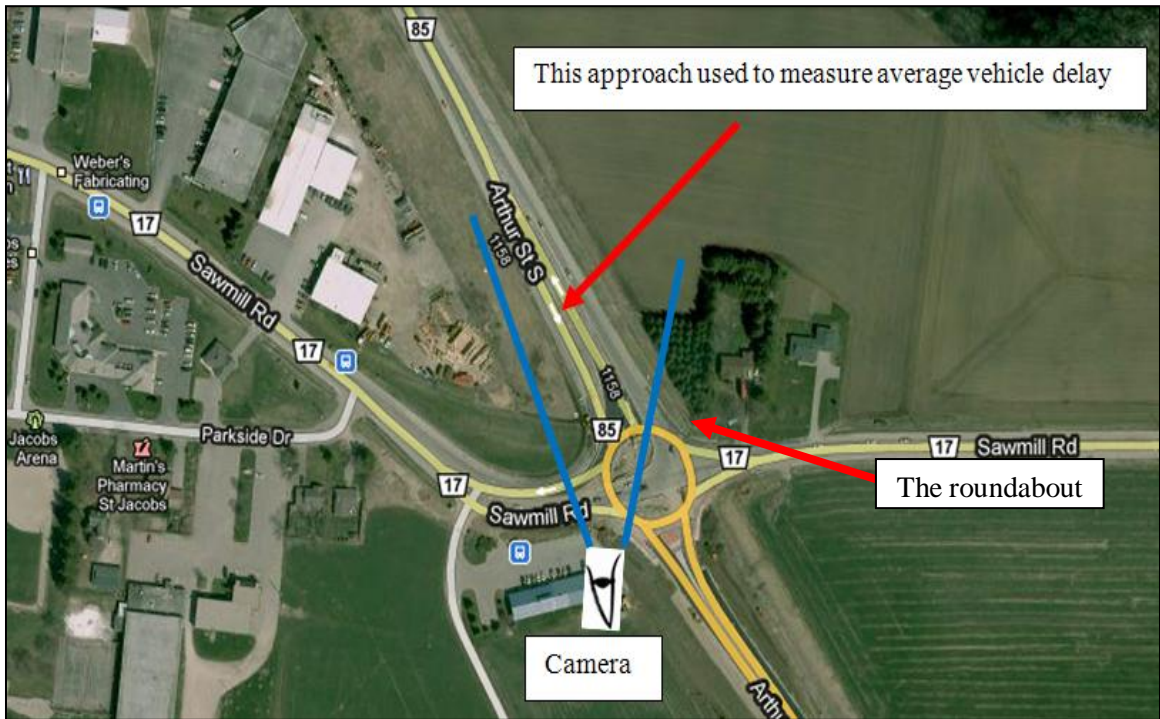


Figure 83: Google satellite picture for Sawmill Rd. / Arthur St. S (HW 85)

Features from field and VISSIM:

Flare length in VISSIM and site= 32m.

One flared lane roundabout is used in VISSIM because the flare length is lower than the maximum queue length.

Maximum queue length (end of the queue tail) = 154 m.

ICD in site = 63 m.

ICD in VISSIM = 60 m.

The posted speed on the road = 80 km/h

Speed used in VISSIM = 75 - 110 km/h

Entering and circulating speed in VISSIM = 30 - 35km/h

The average vehicle delay is measured on the critical lane in the video recording and VISSIM:

Average vehicle delay from VISSIM = 11.93 seconds (the distance of the delay measure is from 1500m upstream to the yield line similar to the experimental design code).

Delay measured from video recording = 8.45 seconds (the distance of the delay measure is from 154m upstream to the yield line); “the average vehicle delay is measured for all vehicles when there is a conflicting flow and when there is no conflicting flow.”

Table 34: Vehicle volume at Sawmill Rd. / Arthur St. S (HW 85)

	Entry volume (veh/h) in the critical Lane		Entry volume (veh/h) in the second lane		Conflicting volume in the inner lane (veh/h)		Conflicting volume in the outer lane (veh/h)		Exit volume in both lanes (veh/h)
	cars	HGVs	cars	HGVs	cars	HGVs	cars	HGVs	cars and HGVs
Total volume of vehicles per hour	568	6	176	15	140	5	37	2	1123
Total percentage of trucks	2.7%				4.2%				-

Error sources:

- 1- Snowy weather and road conditions are not coded in VISSIM.
- 2- Collecting data:
 - a. The collected data accuracy is to seconds.
 - b. Observing the approaching and entering vehicle time is not exactly the same for all vehicles. The yield line does not appear in all the sites. The vehicle entry time to roundabout is recorded when the vehicle increases its speed to enter the roundabout after it reduces it or has stopped at the yield line. In order to record approaching vehicle time, an imaginary line up stream of the yield line at the roundabout entry was set. The locations of vehicles based on the imaginary line when video recording is paused vary each time the video paused. Another imaginary line was set at the yield line to record the time of vehicles entering the roundabout. This variation in recording the approaching and entering time is a source of error. Both the approaching and entering time is estimated as accurately as possible.
 - c. High approaching vehicles and big trucks sometimes block the visibility to observing car type entering the roundabout. Consequently, an error in matching the vehicle type approaching and entering the roundabout might occur.